MIXING OF PHARMACEUTICAL GRANULATIONS

Mahendra R. Patel.

Under the supervision of Professor Jens T. Carstensen.

The blending of spheres of identical sizes leads to the blending equations derived by Hogg et al. (1966) and Lacey (1954). In mixing in a horizontal, rotating cylinder, diffusional movements of particles in the axial direction is the main cause of mixing. In the present study mixing of pharmaceutical granulations having irregular particle shapes and rough surfaces was carried out using a rotating horizontal cylinder mixer. The results of mixing of equal size yellow and white granulations with different proportions followed diffusional mixing kinetics. The rate of mixing was independent of the proportion of the two fractions. Furthermore, mixing rates as a function of particle size indicated that for the size range studied, mixing rate constants decreased linearly with the granulation particle size.

Experiments were carried out for mixing of two monodisperse fractions having different particle sizes, i.e. one size was kept constant and the other was varied systematically to evaluate the effect of particle size difference on mixing kinetics. The results indicate that for this type system diffusional mixing is <u>not</u> followed. The mixing kinetics were dependent on the packing geometry of the two fractions studied. Here percolation was the main reason for mixing. Segregation of particles in the cascading layer was the opposing force for mixing.

Results of mixing studies carried out in a V-blender indicated that mixing can be explained by a diffusional mixing mechanism within each

arm. It was also possible to calculate the amount interchanged between the two arms per revolution during the mixing process. Mixing between different particle size granulations in a V-blender followed similar mixing kinetics as was observed in a horizontal rotating cylinder.

Final equilibrium variance of the mixture where the particle sizes between the two monodisperse fractions differed indicated (for both the horizontal rotating cylinder and the V-blender) they were orders of magnitude higher than theoretically calculated random variances.

Approved John T. Carstensen

Date 10/1-76

MIXING OF PHARMACEUTICAL GRANULATIONS

BY

MAHENDRA PATEL

A thesis submitted in partial fulfillment of the requirements for the degree of

DOCTOR OF PHILOSOPHY

(Pharmacy)

at the

UNIVERSITY OF WISCONSIN

Madison

1976

To my Parents

without whose love and sacrifices this work would not have been possible.

ACKNOWLEDGMENT

I would like to express my deepest gratitude to Professor Jens T. Carstensen for initiating, directing and assisting this research project to a successful conclusion.

A special note of thanks is due Ms. Ping-Ching Chan for her help in the experimental work of this project.

I am deeply indebted to Dr. Michael Zoglio for lending me the V-blender mixing apparatus used for the project.

Finally, the financial support rendered by the Wisconsin Alumni Research Foundation in the form of research assistantship and the support by the Graduate School in form of money used to buy computer time is gratefully acknowledged.

TABLE OF CONTENTS

I. INTRODUCTION

I-1 Background

Although the mixing of solids has been widely used in chemical, pharmaceutical, plastics, glass, metallurgical, cement and food industries, it is only recently that significant efforts have been undertaken to understand the detailed mechanisms of the mixing process.

A number of literature surveys and reviews have been published. The most recent and systematic survey on powder mixing was carried out by Cooke et al. (1976). The review article by Weidenbaum (1958) is a comprehensive survey of much early work, and the evaluation of basic problems written by Bourne (1964) still provides useful reading. The literature survey by Fan et al. (1970) provides among other items a useful table of mixing indices that have been employed to describe mixture quality and a list of detailed studies on mixers and the components being mixed. In the review article by Lloyd et al. (1967) mixing of powders in terms of particle properties and the choice of mixing apparatus is very well summarized.

Review of the literature on the mixing of particulate solids reveals that either experiments could not be designed to check the validity of theories of mixing or experiments in real systems could not be accounted for by a general theory. Consequently the approach has been to carry out experiments on ideal systems in which any of the numerous variables associated with the mixing process can be held constant.

A task of evaluating mixing kinetics of pharmaceutical granulations was undertaken here because it serves as a practical system for tablet and capsule manufacture in pharmaceutical industries. In the first stage experiments were designed to a confined geometry by using a horizontal rotating cylinder so that mixing theories could be evaluated for this apparatus. Similar type of experiments were carried out in a V-blender which is widely used as a mixing apparatus in drug industries. Correlations are sought between results of mixing in these two pieces of equipment in the present study, in order that more information may be gathered regarding mixing processes in the V-blender.

I-2 Fundamentals Regarding the Mixing Process.

In order to examine the fundamentals involved in mixing it is important to distinguish between the mixing process and the degree of mixedness which has been achieved in a particular system at any stage of the process. In any mixing process there are two fundamental mechanisms which must occur for a high degree of mixedness to be achieved: (1) the separate components must be brought together and (2) individual particles must diffuse across boundaries between regions rich in one component into regions rich in another. These two independent mechanisms were referred to by Danckwerts (1953) as "macromixing" and "micromixing" respectively.

A mixing operation can proceed by the macromixing mechanism if aggregates of the separate components are continually broken up by mechanical agitation. However, this will not produce high degrees of mixedness in a finite time unless micromixing can also take place.

The three mechanisms of convection, shear and diffusion were proposed by Lacey (1954) to describe powder mixing. They are analogous to those found in liquid and gas mixing. This analogy is dangerous as no mixing occurs in a particulate system without the input of mechanical work. The mechanisms of mixing must be related to the flow (Lloyd, 1967) properties of materials and the method by which mechanical energy is applied.

Consider an assemblage of particles or a static bed before a mixing process begins. All the particles are subject to a constant force of gravity and they are in some sort of spatial equilibrium with one another. Reynolds (1885) showed that in order to obtain relative particulate movement within such a bed, the volume of the bed must be increased. Subsequent work by Jenkin (1931) and Brown et al. (1947) have amply confirmed that even in the case of a randomly packed bed, no appreciable movement can take place. Brown et al. (1947) found that movement in a bed was produced by a shear movement. For such a movement to take place there must be sufficient space between the particles and this provides the first necessary condition for mixing. Assuming interparticulate movement to be possible, then, in order to produce such movement, suitable forces must be applied to the particles. As shown

by Train (1960) application of pure tensile or compressive forces will serve only to increase or decrease the specific volume of the system without the particles changing relative positions. It follows that shear forces will be necessary to produce interparticulate movement. Radiographic investigations of strained granular materials (Cutress, 1967, Bransby, 1973) have shown that a failure zone is about ten particle diameters thick. This is supported by work of Scott et al. (1976), Bridgewater et al. (1967) and Scott et al. (1975). They used a simple shear apparatus to study interparticulate percolation and mixing of spherical particles due to applied stress on the bed of material.

There have been extensive results reported describing motion of free flowing powders in horizontal rotating cylinders (Lacey, 1954, Weidenbaum et al., 1955, Donald et al., 1962, Roseman et al., 1962, Cahn et al., 1967 and Lloyd et al., 1967). The general description is that for an ideal system where particles have the same size, shape and density, and where they can be distinguished only by some characteristic such as color, radioactivity or trace chemical composition, there is a relationship between particle motion, mixer speed and volume of the fill in the mixer. At low speeds and moderate loads the bed of particles maintains a constant shape and moves with the mixer (Fig. I-1). A thin surface layer flows down in almost flat configuration. The particles in this "cascading" surface layer move in an irregular tumbling motion. The angle of this layer compared to the horizontal plane is equal to the dynamic angle of repose of the particulate system under observation. At moderate speeds the shape of the cascading

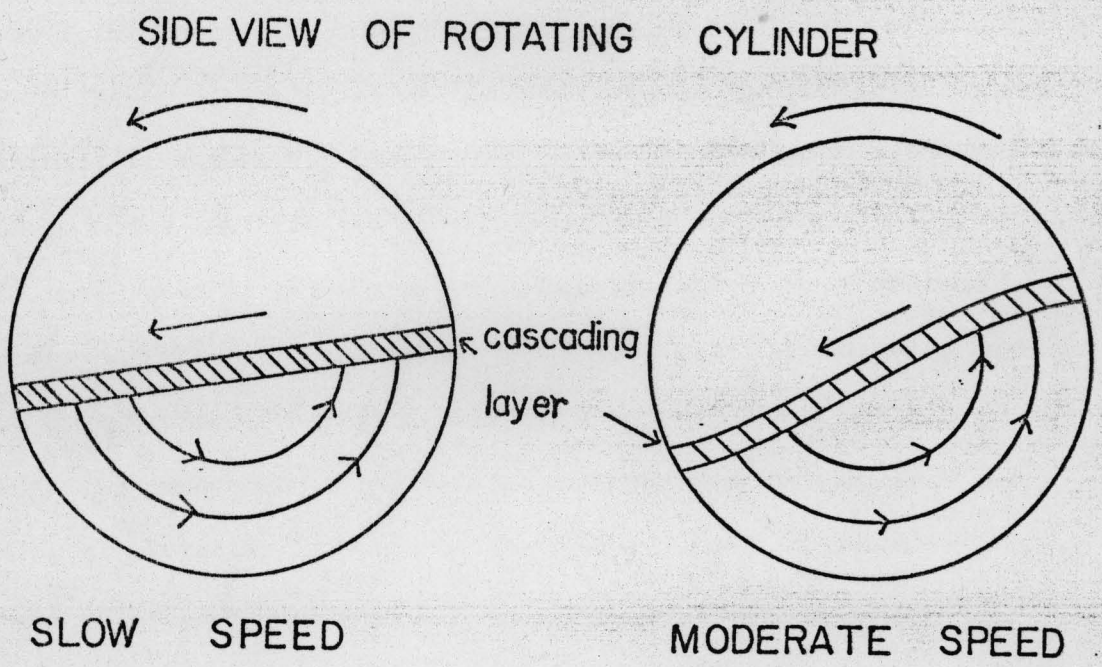

Fig. I-1 Side View of Rotating Cylinder Showing the Motion of Particles.

surface is distorted (Fig. I-1) and causes an increased flow or particles in the layer.

At normal speeds the mixing of particles takes place almost entirely in the cascading layer at the free surface. This cascading layer or mixing zone is actually composed of a number of layers of particles over which a velocity gradient acts and the velocity will decrease from a maximum at the surface to zero at the bottom layer. It was observed that whatever layer of mixing zone (cascading layer) a particle enters, the particle accelerates down the layer towards the center of the mixing zone and then it is retarded at the same rate by the particles in front of it until it enters the static mass with zero downwards velocity. It should be noted that the bed of particles does not necessarily revolve at the same speed as the mixer. Axial diffusion or random movement along the mixer axis is the result of impact collisions between particles on the free surface or grazing collisions between these particles and those in the more compact and more slowly moving layers below. The trapping of particles in voids in the surface layer is the ultimate means by which particles moving from one axial position are brought into the bed from the mixing zone.

Considering the random nature of collisions a solution of Fick's second law of diffusion for mixing of an ideal binary particle system for side by side loading in a horizontal rotating cylinder was presented by Lacey in 1954. Later on Hogg et al. (1966) also presented a detailed solution of Fick's law for this system and adequately verified it by experiment. Theoretical studies by simulation of diffusional mixing of

particulate solids by Monte Carlo techniques was attempted by Cahn et al. (1967). However, at the present stage it is not possible to predict the diffusion coefficient of the particles.

I-3. Plan of Study

One of the purposes of the present study was to consider a more practical system and follow the mixing kinetics via a horizontal rotating cylinder to find out the mixing kinetics of particles having rough surfaces and different shapes. Hence, as a system, wet granulated yellow and white lactose granulation was chosen as a model systm. Use of a V-blender (twin shell blender) as a mixing apparatus is a common practice currently in mixing processes (Adams et al., 1956, Gray, 1957, Harnby, 1967, Hill, 1965, Rumpf et al., 1962, Stange, 1954, Weidenbaum et al., 1963 and Yano et al., 1956). Studies reporting mixing processes carried out in V-blenders are numerous in the literature. Most of these studies were centered on effectiveness of mixing and not on the kinetics of mixing. There is no detailed kinetic theory of mixing followed by experiments in a V-blender reported in the literature to date, except some exploratory attempts by Cahn et al. (1965) and by Weidenbaum et al. (1963). An attempt is made here to formulate a theory describing movement of material in a V-blender and to correlate the kinetic results in a V-blender with those in a horizontal rotating cylinder.

Segregation and percolation are factors that are recognized in literature (Cooke et al., 1976). One of the purposes of the present study was to check whether diffusional mixing kinetics apply to the mixing of two monodisperse fractions with different particle sizes (one from the other). If diffusional kinetics are not followed, it was then the purpose to investigate and elucidate what factors indeed were of importance in such mixing.

Finally, the most commonly used criterion for mixedness is the sample variance of the mixture (Lacey, 1943, Carley-Macauly, 1961, Hearsey, 1975). As blending progresses, the variance approaches some final value, and theoretical values for this final value have been calculated in the past (Lacey, 1943, Stange, 1953,1954,1963,1967, Poole et al., 1964, Johnson, 1972 and Kristensen, 1973). A perusal of actual experimental data in literature cast some doubt on the theoretical formulae cited, and a comparison is made here between the theoretical variance and the experimental variance in the systems tested, and explanations for the discrepancies put forth.

II. EXPERIMENTAL

II-1 Chemicals and Materials

Blending experiments are time consuming (and experimental data are relatively scarce in literature). The reason for this is that each point on a blending curve is a standard deviation, and hence dictates a multitude of assays. Assay difficulties have therefore been minimized in this study by selecting a system which was fairly simple to assay, viz. F.D.&C. Yellow Dye #5, which is a pyrazolone dye of the following structure:

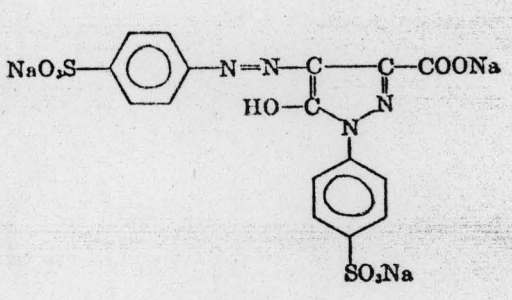

A typical pharmaceutical granulation was used and the system, hence, simulates a practical pharmaceutical system.

II-1-A Materials for Granulations.

Since the experiments consisted of blending two materials, two granulations were made, one white, and one yellow. They differ only in the sense that one contains dye and one does not contain dye. The compositions were as follows:

Table II 1 A-1

Granulation Formulations Used in Blending Studies

Formula	Amount	
	Yellow	White
F.D.C. Yellow No. 5	6 g	None
Cornstarch Powder, U.S.P.(Added Dry)	180 g	180 g
Lactose, U.S.P.	1515 g	1521 g
Cornstarch Powder, U.S.P.(For Paste)	45 g	45 g
Cold Water	100 ml	100 ml
Hot Water	350 ml	350 ml

II-1-B Suppliers

The suppliers of the materials were: Lactose, Yellow Dye and Magnesium Stearate were obtained from Ruger Chemical Inc. Irvington, New Jersey. Cornstarch was obtained from Argo Corn Starch, Coventry, Connecticut. All the materials were used as obtained from supplier.

II-1-C Preparation of Granulation

The 45 g of cornstarch were added to 100 ml of cold distilled water in a 600 cc beaker, and stirred with a glass rod until free of lumps. This suspension was then added to 350 ml of boiling water in a 1000 cc beaker and stirred with a glass rod. This forms a translucent gel. It was covered with aluminum foil and let cool.

The 6 g of dye and 115 g of lactose were premixed in a 500 ml amber glass bottle by shaking. (For the white granulation this step was obviously omitted). This premix was then transferred to a ten liter capacity stainless steel pot for a planetary mixer (Hobart mixer, 1/4 HP Model 1725, manufactured by the Hobart Manufacturing Co., Troy,Ohio). The 180 g of cornstarch and the remaining lactose were then added to the mixer pot, and the dry ingredients mixed for 10 minutes at low speed (50 RPM). The cornstarch paste was then added and the granulation allowed to develop to end point (ca. 5 minutes). The granulation was then passed through a 6 mesh hand screen onto drying trays and dried for six hours at 60°C in a forced air oven (Colton Oven Model 2030E, ARthur Colton Co., Detroit, MI). Approximately 45 kg of yellow granulation and 45 kg of white granulation were prepared and stored in drums prior to milling. The moisture content of the granulations were determined by means of a Cenco moisture balance (Cenco Co., Chicago Ill 60623) and found to be in the range of 3.8 to 4.2% by weight.

35 kg out of the 45 kg of dry granulation produced were milled through a No. 2B screen (2.77 mm screen opening) at a rotational speed of 1700 RPM in a Model M. Fitzmill (The Fitzpatrick Company, Chicago, Ill.). This milled granulation was collected in the drum containing the 10 kg of granulation which was not milled. The purpose of not milling all of the granulation was to retain a certain amount of large (6-10 mesh) granules from the unmilled granulation.

One of the purposes of the study was to study blending rates as a function of particle size, and the granulations were therefore sieved, and separated into the following mesh sizes by using U.S.P. standard sieves (Sargent Sieves, Sargent and Co. Skokie, Ill 60076) on a Cenco Meinzer sieve shaker (Central Scientific Co., Division of Cenco Co., Chicago Ill 60623): 10, 20, 40, 60, 80 and 100 mesh. 500 g samples of granulation were placed on a sequential nest of screens and shaken for fifteen minutes. Previously conducted sieving efficency experiments had shown this time to be adequate to acquire 100% efficiency for mesh sizes coarser than 100 mesh. Each mesh fraction was collected in a labeled bottle, and in this manner adequate quantities of various mesh sizes were obtained so that blending experiments could be performed.

The particle size of a sieve fraction is considered to be the mean of the opening of the confining screens. Mesh sizes are shown in Table II-1-C-1. Since further differentiation in the coarser range was necessary, the 10/20 mesh cut was divided by use of a 14 mesh screen into a 10/14 and a 14/20 mesh fraction.

Table II-1-C-1

Sizes of U.S.P. Mesh in cm.

Mesh Size	Opening (cm)
6	0.357
10	0.200
14	0.156
20	0.084
30	0.059
40	0.042
60	0.025
80	0.0177
100	0.0149

The above 10 mesh fraction was always finer than 6 mesh. Part of the 20/40 mesh fraction was divided into a 20/30 and a 30/40 mesh fraction.

II-1-D Tablet Compression

One kg of each granulation was lubricated with 2% magnesium stearate in a planetary mixer. Tablets were compressed on a single punch tablet machine (Arthur Colton Co., Chicago Ill.) using a set of concave punches. The dimensions of the tablets were: 0.96 cm diameter, thickness at the crown 0.46 cm and thickness at the edge 0.32 cm. Average weight of the tablets was 362 mg with a standard deviation on the average of 2 mg. The average hardness was 14 Strong Cobb units with a standard error of the mean of 0.7 units. The hardness was measured by a Schleuniger Hardness Tester (Vector Corporation, Hiawatha, Iowa).

II-1-E Physical Properties of the Granulations

The particle density of the different size fractions was determined with a pycnometer and using xylene as a pycnometer liquid. For the 6/10 sieve fraction it was also possible to count the particles and arrive at a particle density by weighing them, and assume them to be spherical and of the mean diameter indicated by the size of the 6 and 10 mesh apertures. Apparent densities of all the sieve fractions was measured using a 100 ml graduated cylinder.

II-2 Apparatus Used for Blending Experiments.

One of the most common pieces of blending equipment in the pharmaceutical industry is a so-called V-blender. This consists of two cylinders joined at an angle and rotated about an axis in the plane of the cylinder axes, and forming an equilateral triangle with them. One of the most common blenders is a Patterson-Kelley V-blender (Patterson Kelley Co., East Stroudsburg, Pa.). A small Patterson-Kelley V-blender with the dimensions shown in Fig. II-2-1 were used in this study. A photograph of it is shown in Fig. II-2-2.

A laboratory apparatus simulating an industrial barrel roller was constructed. A photograph of this is shown in Fig. II-2-3 and a dimensional diagram is shown in Fig. II-2-4. This apparatus is a variation of the design by Cahn and Fuerstenau (1968). It consists of a plexiglass cylinder, cut in equal halves along its axis. It is possible to "close" it by clamping on the ends. Material can now be placed in the mixer and it can be closed and placed on a rotating base and rotated for a certain length of time. The top half can then be removed, and the material sampled by a sampling device as shown in Fig. II-2-5. This piece of equipment allows tracing of the blending profile for short as well as for long periods of time under mild blending conditions. This allows analysis of details of the profile, not possible under more rigorous conditions.

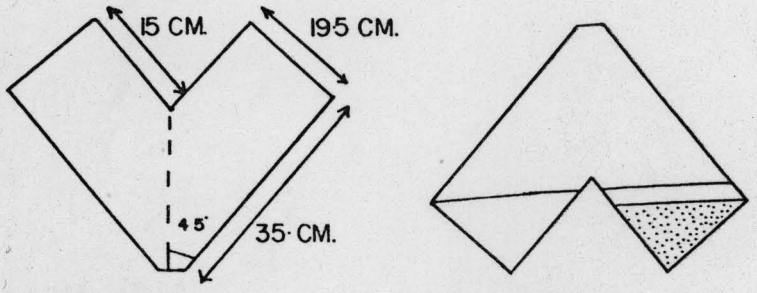

Fig. II-2-1. Schematic Drawing of V-Blender and its Dimensions. The Right Hand Side Shows the Mode of Loading.

Fig. II-2-2. Photograph of V-blender Used

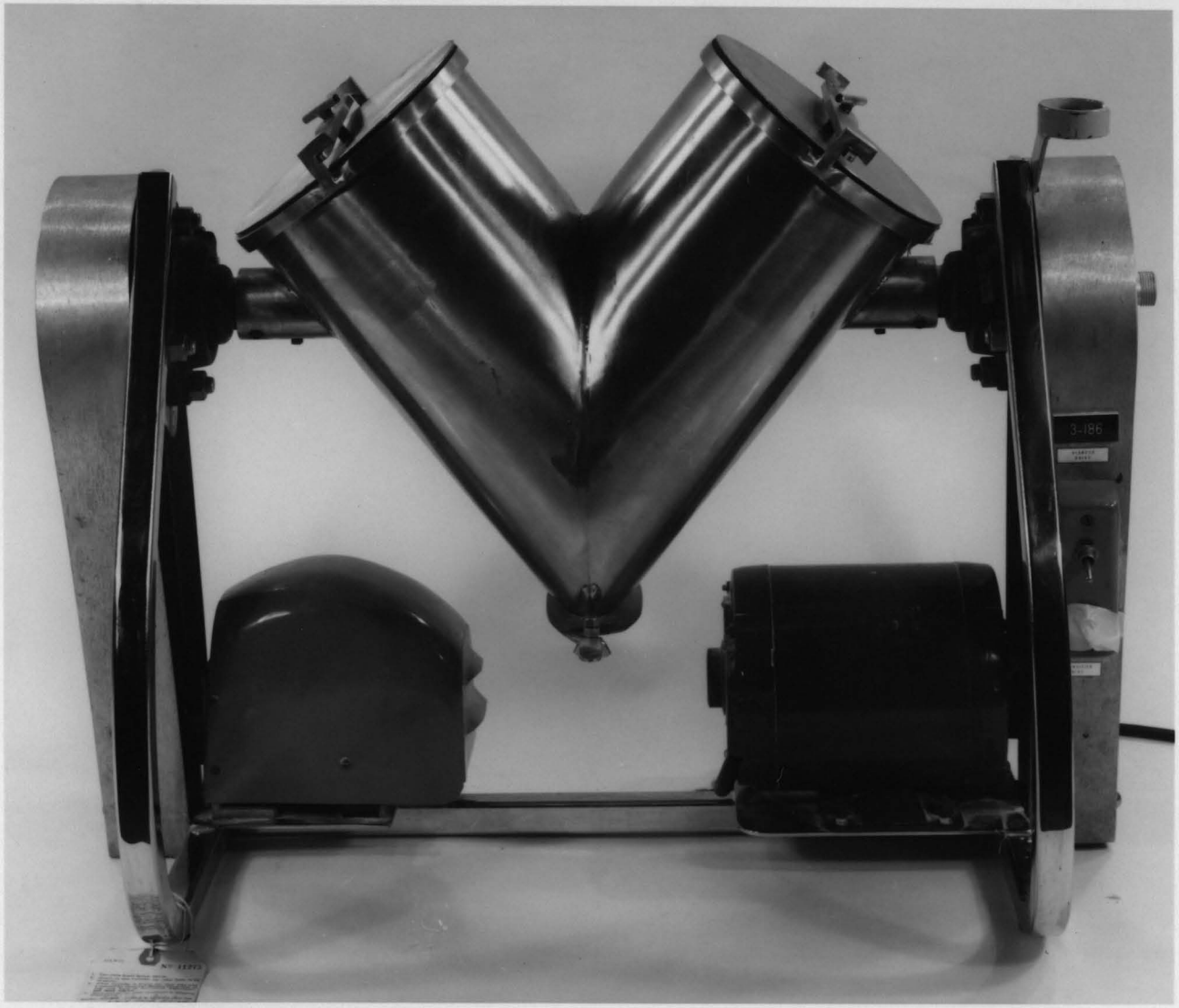
3-186

Fig. II-2-3. Photograph of Horizontal Mixer Set-Up.

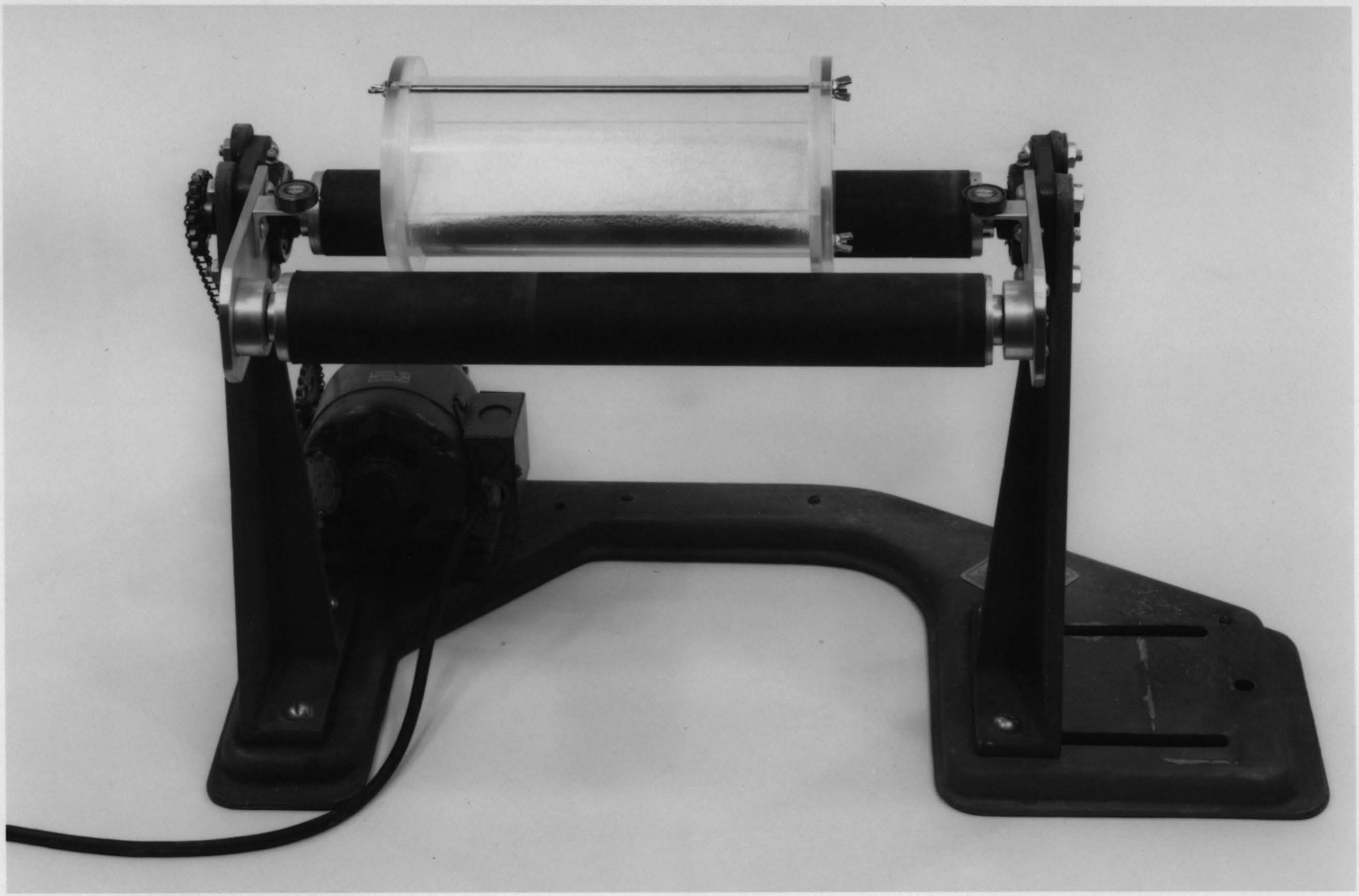

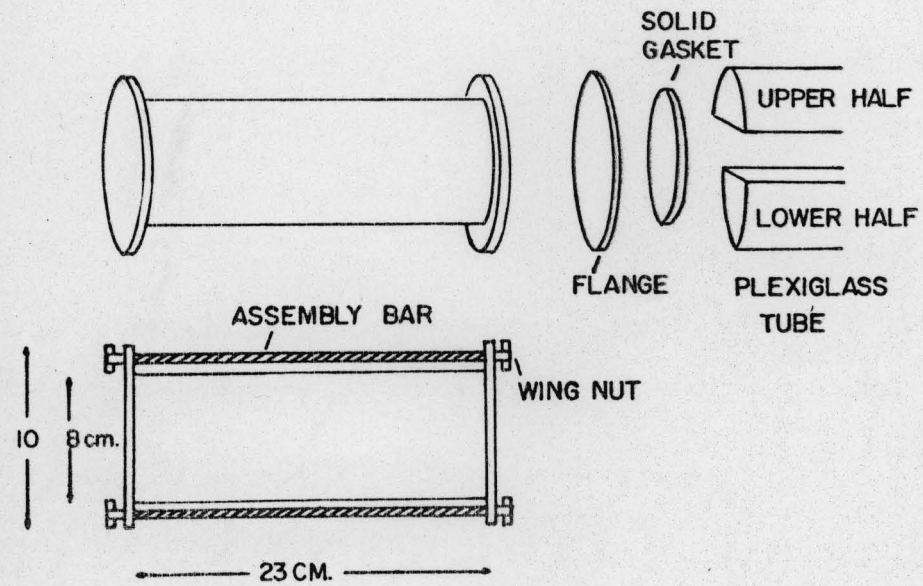

Fig. II-2-4. Schematic Drawing of the Horizontal Mixer Set-Up.

Fig. II-2-5 Schematic Drawing of the Sampling Box Used.

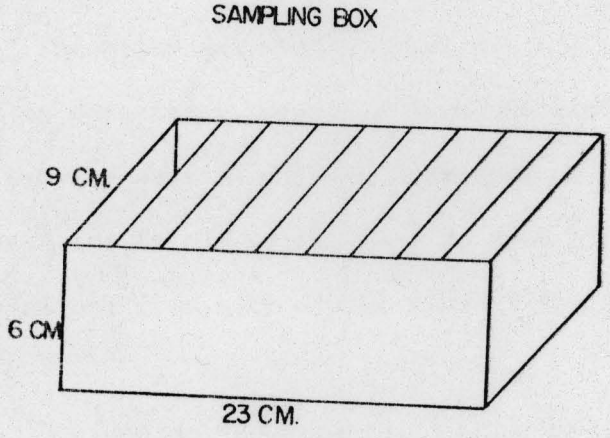

II-2-A Blending Experiments Using a V-Blender.

The V-blender has a fixed rotational speed, viz. 24 RPM. When used for a blending experiment, the mixer was placed with the apex up and 1 kg. of granules were placed in each arm. The left side contained only the abundant component (i.e. 1 kg of it) and the right arm contained all of the sparse component and the remainder of the abundant component. The mixer was then allowed to rotate for the given length of time and then stopped with the apex down. One 25 g sample was taken from the center of the powder surface in each arm. The mixer was then rotated one half revolution and two 25 g samples were taken, one each from the powder surface of each arm. The four samples were assayed as described in Section II-3. In this manner there are four samples taken at each time point, two from the "bottom" and one from each of the tops of the arms.

II-2-B Blending Experiments Using a Horizontal Cylindrical Blender

When using the horizontal blender described in Fig. II-2-3 and 4, the following procedure was used: the lower cylinder was first completely filled with one of the particular size fractions (i.e. either white or yellow). By weighing this, it was established what amount of total mix should be used. An amount corresponding to the desired amount of yellow and white granulation totaling the determined capacity was then weighed out, and the mixer charged

by placing the white granulation in one side and the yellow granulation in the other side in the lower cylinder, and keeping them separate by using a half circular cardboard partition. The interface of the yellow and white granulation is perpendicular to the axis of the cylinder. The cardboard was next removed, and the upper half of the cylinder was positioned above the lower half, and the assembly clamped in place via the end plates. The cylinder was now placed on the base which consisted of two hard rubber cylinders one of which was rotated at 39 RPM by means of a 1/4 HP moter.

At a given time the rotation was stopped and the upper half was removed. The Sample box was placed on it (as shown in Fig. II-2-5) and the assembly inverted, allowing the powder in a particular spot to fall into the box partition at that spot. The nine samples (from the nine compartments) were then removed one by one, and transferred into a 250 ml beaker, and the entire sample assayed for yellow dye as described in Section II-3.

One experiment was performed using the tablets described in Section II-1-D. In this case assays were not performed but the "concentration" determined by counting the number of yellow and white tablets in the sample. A note on how tedious blending ex periments are is in order. To estimate a blending curve of two mesh fraction (8 points) a total of 72 assays are necessary, and for tablets 25,000 total counted tablets are required.

II-2-C Longitudinal Blending

A set of experiments were performed in which the mixer was loaded "the long way". These were all carried out at 50:50 ratio and a cardboard partition was run down the middle of the lower half of the plexiglass cylinder parallel with its axis. Yellow granulation was then placed on one side of the cardboard partition and white granulation was placed on the other side of the partition.

The cylinder was then combined with the top half and secured by means of the ends, and the assembly placed on the motor driven base. The mixing was carried out for 1000 seconds, and then stopped. Six (or in some cases five) partitions were placed in the long direction of the sample box (Fig. II-2-5) and sampling achieved by placing the sample box on top of the bottom cylinder and inverting. The samples obtained in this fashion then are from the far left wall (denoted "1") to the center at the axis of rotation (denoted "3") to the far right wall (denoted "5" or "6").

II-3 Assay Methodology.

II-3-A Spectra of Pure F.D.&C. Yellow No. 5 Dye.

242 mg of dye were dissolved in 100 cc of 0.5 N HCl and diluted with 0.5 N HCl. Eight different dilutions (of the order of a total dilution factor of 1:50,000) were made with 0.5 N HCl. The spectra were determined on a Cary 16 spectrophotometer. The spectra show absorption maxima at 430 nm.

II-3-B Beer's Law Plots of Yellow Granulations

In granulation processes the distribution of dye is not quite uniform, and hence a Beer's law plot is needed for each fraction. Seven samples ranging from two to fifteen grams of yellow granulation were weighed out and extracted with 200 cc of 0.5 N HCl in a 250 cc beaker with magnetic stirring. The material was then filtered through a Whatman #2 filter paper into a 1000 cc volumetric flask. The filter paper and beaker were washed with 500 - 700 cc of 0.5 N HCl and the washings combined with the filtered extract. The solution was adjusted to volume with 0.5 N HCl and diluted with 0.5 N HCl 1:1. The absorbance was then checked at 430 nm on a Cary 16 spectrophotometer. This type determination was carried out for seven samples on each sieve fraction used. In granulation processes the distribution of dye is not quite uniform and hence a Beer's law plot is needed for each fraction.

II-3-C Content Determination in Mixed Mesh Fraction Experiments.

Several experiments were performed in which the white and yellow granulations did not have the same particle size. In this case it is not necessary to assay chemically for yellow dye. Instead, the samples were screened through a sieve which was coarser than the finer of the two granulations and finer than the coarser of the two granulations. This will effect separation of the two, and the relative amounts can be obtained by weighing.

II-3-D Assay Variation

The assay variation was checked by taking second samples of the granulations used for the Beer's law plots and assaying them using the established Beer's law plots.

III. RESULTS

III-1 Densities of Granulations.

The particle densities as determined in Section II-1-E, and the apparent densities of the various sieve fractions are listed in Table III-1-1. The table also lists the mean particle diameter and the calculated number of particles per gram of granulation. The particle density decreases with increasing particle size because of the increasing effect of porosity.

III-2 Results from Blending Studies in the V-Blender.

The results from these studies are listed in Tables III-2-1 through III-2-13. The first column states the point in time (in minutes) and columns 2 through 5 lists the content of yellow granulation in the four samples taken: "1" denotes top of left arm, "2" denotes top of right arm, "3" denotes bottom (right) and "4" denotes bottom (left). The mean ($\bar{X}$), the standard deviation (σ) and the natural logarithm of the variance ($\ln\sigma^2$) are listed in the following columns. Since $\ln\sigma^2$ should be linear in time, as shall be seen in the Discussion Section, the least squares parameters of $\ln\sigma^2$ versus time are listed, viz.: slope (s), intercept (I) and the square of the correlation coefficient (R^2)

To aid in surveying the tables a list of the experimental parameters are listed below, summarizing the tables:

Table III-1-1

Mean Particle Diameters of Various Mesh Fractions:

Mesh Fraction	Mean Diameter (cm)	Particle Density (g/cm^3)	Apparent Density (g/cm^3)	Number of Particles Per Gram
6/10	0.278	1.31[a](1.26)*	0.57	68
10/14	0.178	1.33[a]	0.58	255
14/20	0.121	1.35[a]	0.58	819
10/20	0.142	1.34**	0.58	498
20/30	0.0715	1.43	0.55	3580
20/40	0.0630	1.45	0.55	5020
30/40	0.0510	1.47	0.55	9790
40/60	0.0335	1.49	0.56	33800
60/80	0.0214	1.52	0.53	128000
80/100	0.0163	1.55	0.58	290000

*Calculated density counting and weighing out 1000 particles

[a]Density measured using liquid displacement method (Carstensen, 1973)

** Average of 10/14 and 14/20 mesh values.

Table No. III-2-	Mesh of Yellow Granulation	Fraction of Yellow Granulation	Mesh of White Granulation	Load (kg)
1	20/40	0.5	20/40	2
2	20/40	0.6	20/40	2
3	20/40	0.7	20/40	2
4	20/40	0.8	20/40	2
5	20/40	0.9	20/40	2
6	20/30	0.5	20/30	4
7	20/40	0.5	20/40	2*
8	10/20	0.5	20/30	2
9	40/60	0.5	20/30	2
10	60/80	0.5	20/30	2
11	80/100	0.5	20/30	2
12	40/60	0.5	20/30	4
13	20/40	0.5	20/40	2**

* 1% Magnesium Stearate Added

** Longitudinal Blending

Graphs of ln σ^2 as a function of time are shown after each table. These graphs were generated on a UNIVAC Model 1110 computer, using a GRAPH subroutine in combination with a GRAPHM subroutine, MACC.

III-3 Results from Blending Studies in the Cylindrical Blender.

The results from these studies are listed in Tables III-3-1 through III-3-16. The first column states the time (in minutes) and columns 2 through 10 list the contents of yellow dye in the indicated position of the blender. The mean ($\overline{X}$), the standard deviation (σ) and the natural logarithm of the variance ($\ln\sigma^2$) are listed in the following columns. The least squares fit slope (s), intercept (I) and correlation coefficient squared (R^2) are listed for ln σ^2 as a function of time.

Graphs of ln σ^2 as a function of time (and is some cases graphs of concentration as a function of position) are shown after each table. These graphs were generated on a UNIVAC Model 1110 computer, using a GRAPH subroutine in combination with a GRAPHM subroutine, MACC.

To aid in surveying the tables and graphs, a list of the experimental parameters are listed below , summarizing the tables:

Table No III-3-	Mesh of Yellow Granulation	Fraction of Yellow Granulation	Mesh of White Granulation	Load (g)
1	Tablets	0.5	Tablets	630
2	10/14	0.5	10/14	460
3	14/20	0.5	14/20	460
4	20/30	0.5	20/30	460
5	30/40	0.5	30/40	424
6	40/60	0.5	40/60	450
7	10/14	0.6	10/14	460
8	10/14	0.7	10/14	460
9	10/14	0.8	10/14	460
10	30/40	0.5	30/40	440*
11	20/30	0.5	6/10	440
12	20/30	0.5	10/14	430
13	20/30	0.5	14/20	445
14	20/30	0.5	30/40	445
15	20/30	0.5	40/60	445
16	20/30	0.5	60/80	445

*Lubricated with 4.8% Magnesium Stearate

Table III-2-1: Mixing of 20/40 Mesh Yellow and White Granulations at 2 kg Load in a V-Blender in a Ratio of 50:50

Time (Min)	Percent Yellow Granulation in the Sample Indicated						
	1	2	3	4	$\overline{X}$	σ	$\ln\sigma^2$
1	78.4	11.3	80.3	5.6	43.9	41.0	-1.8
5	59.6	38.5	60.5	31.1	47.5	14.9	-3.8
10	51.3	42.5	51.8	34.6	45.1	8.2	-5.0
15	47.5	44.0	48.9	41.2	45.4	3.5	-6.7
20	46.2	45.0	45.8	43.0	45.0	1.4	-8.5
25	45.3	45.1	44.6	46.5	45.4	0.8	-9.7

$R^2 = 0.996$ $s = -0.32$ $I = -1.81$

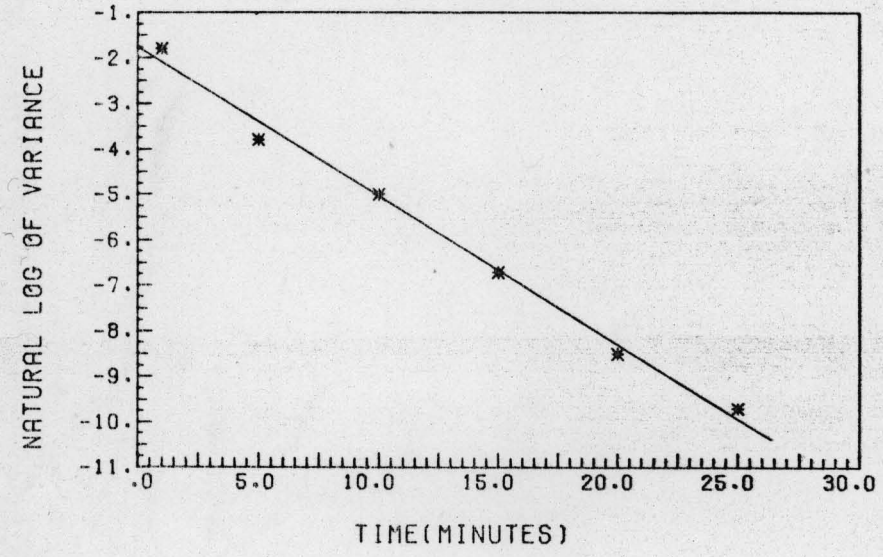

Fig. III-2-1. Blending of 20/40 Mesh Yellow (50%) with White (50%) Granulation in a V-Blender. Results are Plotted According to Eq. IV-10.

Table III-2-2: Mixing of 20/40 Mesh Yellow and White Granulations at 2 kg Load in V-Blender in a Ratio of 60:40

Time	Percent Yellow Granulation in Sample Indicated						
(Min)	1	2	3	4	$\overline{X}$	σ	$\ln\sigma^2$
1	82.1	34.9	95.4	24.7	59.3	34.7	-2.1
5	71.6	49.1	78.1	43.3	60.5	17.0	-3.6
10	65.0	58.1	69.0	53.6	61.4	7.0	-5.4
15	62.5	59.9	65.4	58.4	61.5	3.1	-6.7
20	62.5	60.8	62.8	59.7	61.4	1.4	-8.5
25	61.8	59.5	63.5	59.6	61.1	1.9	-8.0

$R^2 = 0.998$ $s = -0.33$ $I = -1.89$

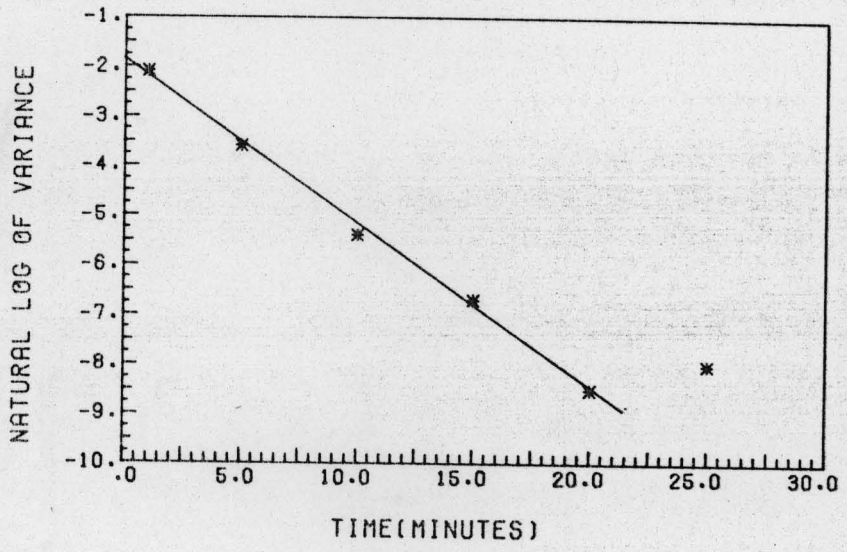

Fig. III-2-2 Blending of 20/40 Mesh Yellow (60%) with White (40%) Granulation in a V-Blender. Results are Plotted According to Eq. IV-10.

Table III-2-3: Mixing of 20/40 Mesh Yellow and White Granulation in a V-Blender at 2 kg Load in a Ratio of 70:30

Time	Percent Yellow Granulation in Sample Indicated						
(Min)	1	2	3	4	$\overline{X}$	σ	$\ln\sigma^2$
1	88.6	42.8	91.8	34.0	64.3	30.2	-2.4
5	74.4	56.2	79.0	53.5	65.8	12.8	-4.1
10	69.6	64.4	71.0	60.0	66.3	5.1	-6.0
15	68.8	70.0	68.0	63.7	67.6	2.8	-7.2
21	67.5	66.9	67.0	66.7	67.0	0.40	-11.3
25	68.2	661.	66.5	65.6	66.6	1.14	-8.9
30	68.1	67.0	66.9	65.2	67.0	1.31	-8.7
35	67.3	67.3	67.4	66.8	67.2	0.11	-11.9

$R^2 = 0.93$ $s = -0.32$ $I = -2.5$

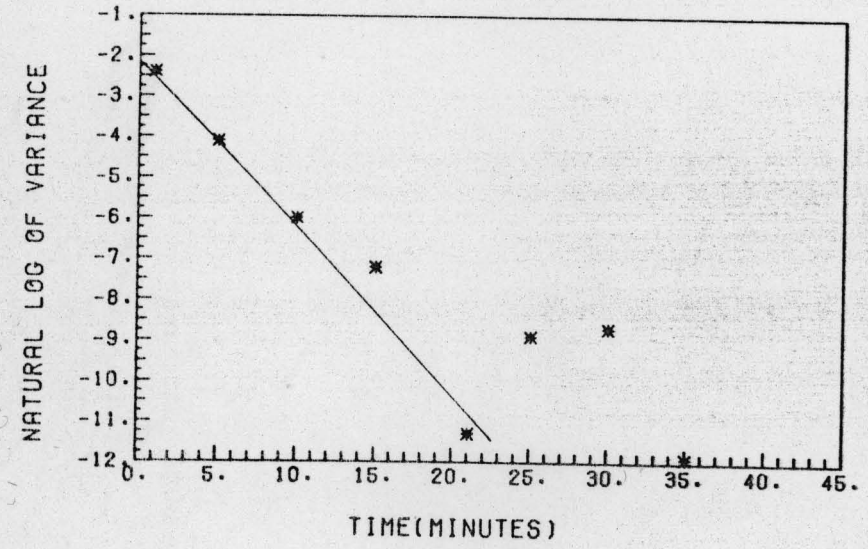

Fig. III-2-3 Blending of 20/40 Mesh Yellow (70%) and White (30%) Granulation in a V-Blender. Results are Plotted According to Eq. IV-10.

Table III-2-4: Mixing of 20/40 Mesh Yellow and White Granulations at 2 kg Load in V-Blender in a Ratio of 80:20

Time	Percent of Yellow Granulation in Sample Indicated						
(Min)	1	2	3	4	$\overline{X}$	σ	σ^2
1	94.9	67.3	100.0	61.3	80.9	19.4	-3.2
5	97.9	76.7	90.3	72.6	81.9	8.6	-4.9
10	84.8	80.1	86.5	79.4	82.7	3.5	-6.7
15	83.7	81.1	82.7	86.2	83.4	2.1	-7.7
20	82.9	81.6	81.7	81.7	82.0	0.60	-10.2
25	82.2	81.6	82.2	81.2	81.8	0.44	-10.8

$R^2 = 0.99$ $s = -0.35$ $I = -2.99$

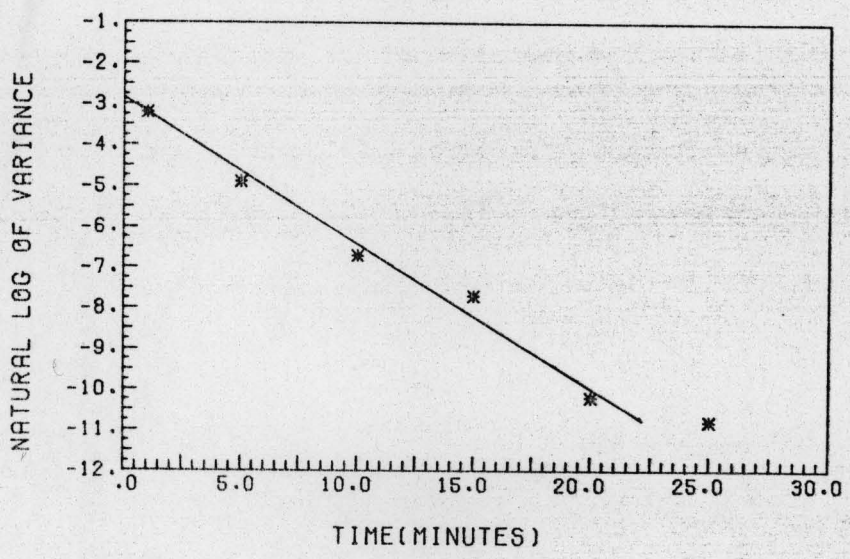

Fig. III-2-4 Blending of 20/40 Mesh Yellow (80%) and White (20%) Granulation in a V-Blender. Results are Plotted According to Eq. IV-10

Table III-2-5 Mixing of 20/40 Mesh Yellow and White Granulations in 2 kg Load in a V-Blender in a 90:10 Ratio.

Time	Percent Yellow Granulation in Sample Indicated						
(Min)	1	2	3	4	$\overline{X}$	σ	$\ln\sigma^2$
1	96.4	85.3	95.2	83.6	90.2	6.5	-5.6
5	92.1	85.9	93.1	87.6	89.7	3.4	-6.7
10	91.5	90.7	91.3	88.2	90.4	1.5	-8.4
15	91.7	88.4	90.7	87.9	89.7	1.8	-8.0
20	90.4	89.9	89.5	89.1	89.7	0.6	-10.3
25	90.2	90.1	90.9	89.7	90.2	0.5	-10.6

$R^2 = 0.96$ $s = -0.21$ $I = -5.6$

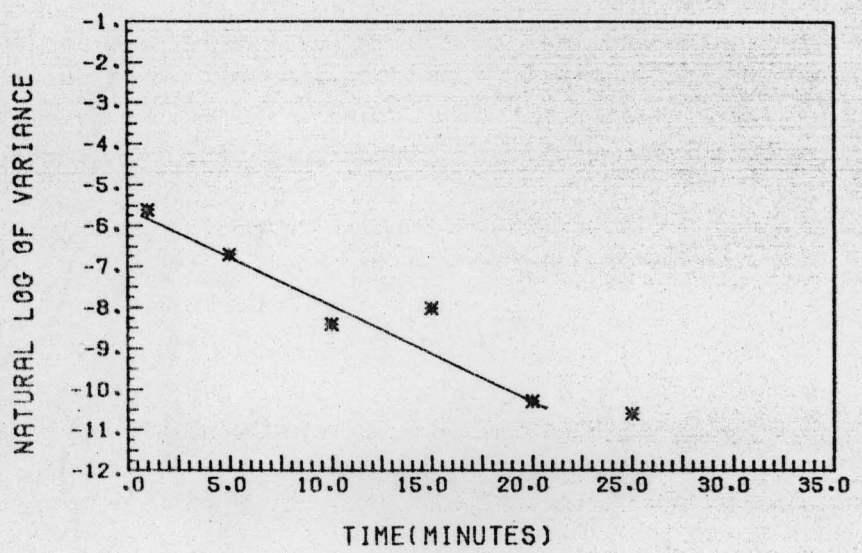

Fig. III-2-5. Blending of 20/40 Mesh Yellow (90%) and White (10%) Granulation in a V-Blender. Results are Plotted According to Eq. IV-10.

Table III-2-6 Mixing of 20/30 Mesh Yellow and White Granulations in 4 kg Load in V-blender in a 50:50 Ratio.

Time	Percent Yellow Granulation in Sample Indicated						
(Min)	1	2	3	4	$\overline{X}$	σ	$\ln\sigma^2$
5	78.6	23.4	92.7	9.0	50.9	40.9	-1.8
10	74.0	49.0	87.8	23.5	58.6	28.4	-2.5
15	69.4	34.4	71.4	29.4	51.5	22.3	-3.0
30	59.3	51.0	63.8	44.3	54.6	8.7	-4.9
45	53.3	48.1	59.0	49.0	52.4	5.0	-6.0
120	53.5	53.1	53.2	52.7	53.1	0.3	-11.6

$R^2 = 0.99$ $s = -0.083$ $I = -1.84$

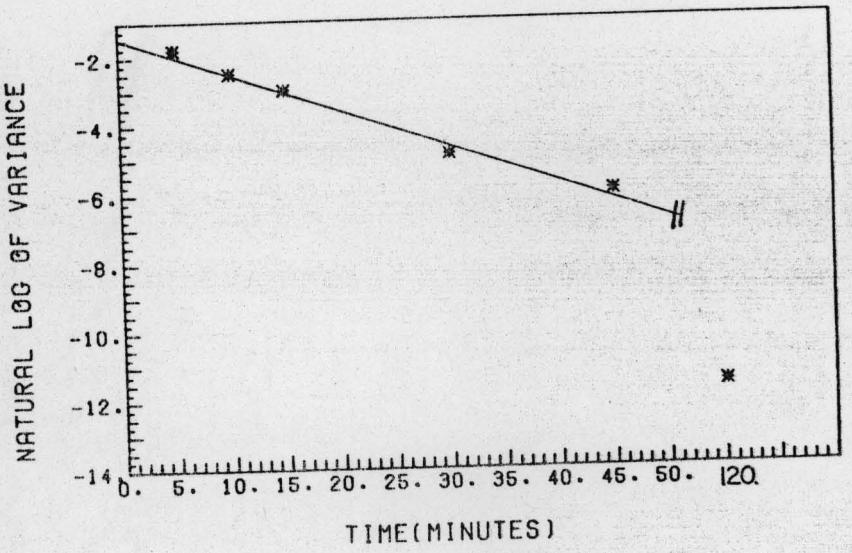

Fig. III-2-6 Blending of 20/30 Mesh Yellow (50%) and White (50%) Granulation in a V-Blender With 4 kg. Load. Results are Plotted According to Eq. IV-10

Table III-2-7: Mixing of 20/40 Mesh Yellow and White Granulation in a V-Blender in 2 kg Load in a 50:50 Ratio with 1% Magnesium Stearate Lubricant Added.

Time (Min)	Percent Yellow Granulation in Sample Indicated				$\overline{X}$	σ	$\ln\sigma^2$
	1	2	3	4			
1	78.4	14.0	89.7	6.2	47.1	43.1	-1.7
5	64.9	39.6	65.6	25.5	48.9	19.7	-3.3
10	56.2	44.6	55.7	38.1	48.6	8.8	-4.9
15	52.3	46.0	51.2	44.5	48.5	3.8	-6.5
20	47.1	49.6	48.8	48.3	48.5	1.1	-9.1
25	49.3	49.5	52.6	50.2	50.4	1.5	-8.4
120	49.6	49.9	48.9	49.5	49.5	0.4	-11.0

$R^2 = 0.99$ $s = -0.38$ $I = -1.27$

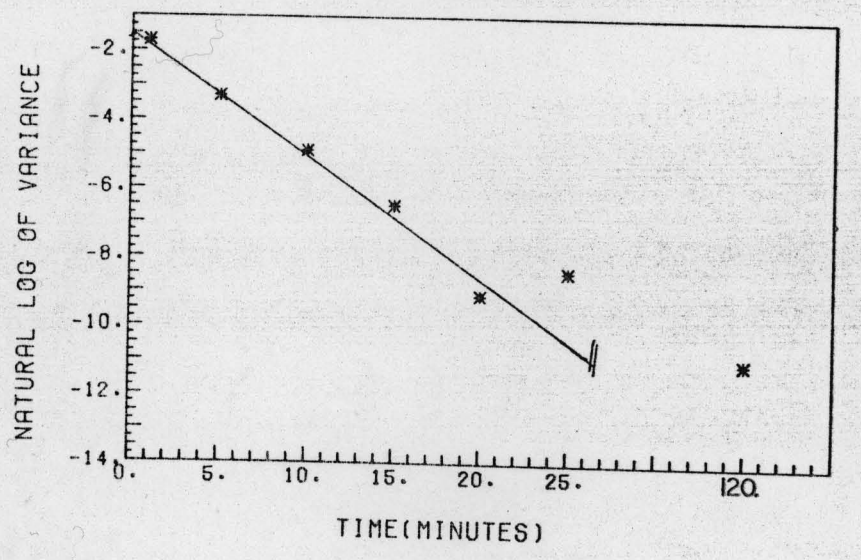

Fig. III-2-7 Blending of 20/40 Mesh Yellow (50%) and White (50%) Granulation Lubricated with 1 Percent Magnesium Stearate in a V-Blender. Results are Plotted According to Eq. IV-10

Table III-2-8 Mixing of 20/30 Mesh White and 10/20 Mesh Yellow Granulations in 2 kg Load in a V-Blender in 50:50 Ratio.

Time	Percent Yellow Granulation in Sample Indicated						
(Min)	1	2	3	4	$\overline{X}$	σ	$\ln\sigma^2$
1	67.5	24.8	70.0	11.0	43.3	29.9	-2.4
5	52.1	41.7	58.9	25.1	44.4	14.7	-3.8
10	56.3	44.3	57.0	42.7	50.1	7.6	-5.2
15	46.3	47.1	49.8	51.1	48.6	2.3	-7.5
20	37.6	44.8	46.5	61.2	47.6	9.9	-4.6
25	35.8	50.3	48.9	59.4	48.6	9.7	-4.7
120	33.9	46.8	48.8	46.1	43.9	6.8	-5.4

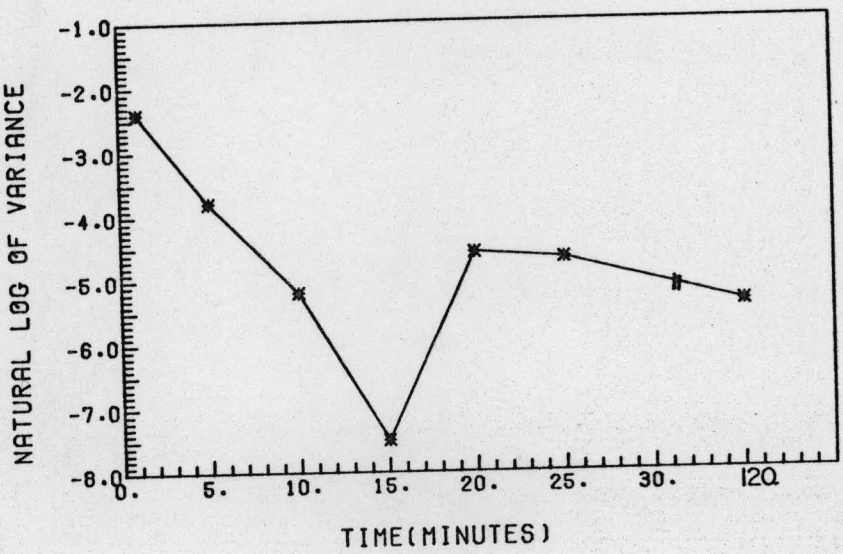

Fig. III-2-8 Blending of 20/30 Mesh White and 10/20 Mesh Yellow Granulation in a V-Blender. Results are Plotted According to Eq. IV-10 in Logarithmic Form.

Table III-2-9 Mixing of 20/30 Mesh White and 40/60 Mesh Yellow Granulation in 2 kg Load in a V-Blender in 50:50 Ratio

Time	Percent Yellow Granulation in Sample Indicated						
(Min)	1	2	3	4	$\bar{X}$	σ	$\ln\sigma^2$
1	76.2	18.3	82.4	17.4	48.6	35.6	-2.1
5	55.8	18.9	73.9	32.3	45.2	24.4	-2.8
10	71.4	22.9	70.9	51.0	54.1	22.8	-3.0
15	53.8	21.5	65.6	33.3	43.5	19.8	-3.2
20	63.2	29.7	76.4	28.4	49.4	24.2	-2.8
25	59.9	26.4	73.3	33.5	48.3	22.1	-3.0
120	59.6	34.3	71.1	13.2	44.5	26.0	-2.7

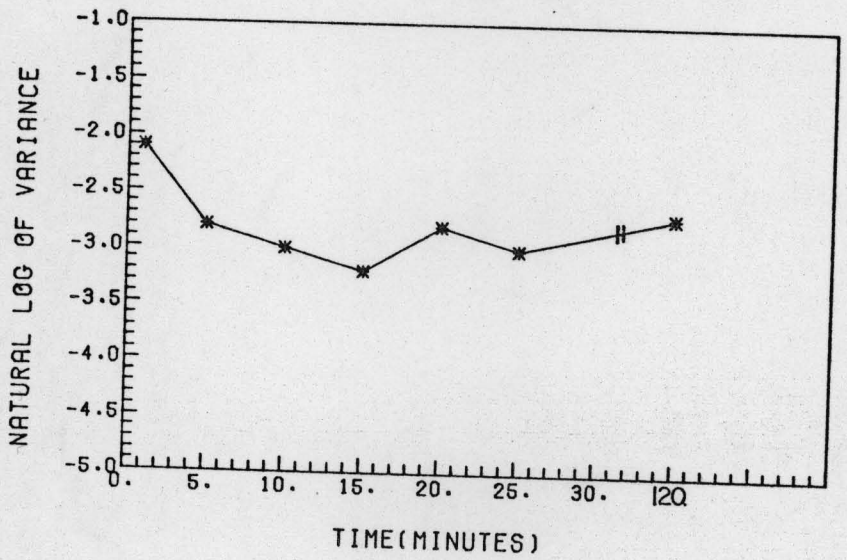

Fig. III-2-9 Blending of 20/30 Mesh White and 40/60 Mesh Yellow Granulation in a V-Blender. Results are Plotted According to Eq. IV-10 in Logarithmic Form.

Table III-2-10 Mixing of 20/30 Mesh White and 60/80 Mesh Yellow Granulations in 2 kg Load in a V-Blender at 50:50 Ratio

Time	Percent Yellow Granulation in Sample Indicated						
(Min)	1	2	3	4	$\overline{X}$	σ	$\ln\sigma^2$
1	60.4	14.2	67.5	13.2	38.0	29.1	-2.5
5	46.9	18.3	55.4	29.4	37.0	16.8	-3.6
10	49.7	27.6	55.5	28.0	40.2	14.5	-3.9
15	49.2	27.5	54.4	25.6	39.2	14.8	-3.8
20	50.7	26.9	52.9	20.6	37.8	16.5	-3.6
25	52.1	24.4	46.7	20.8	36.0	15.7	-3.7
120	42.3	22.0	47.5	16.2	32.0	15.2	-3.8

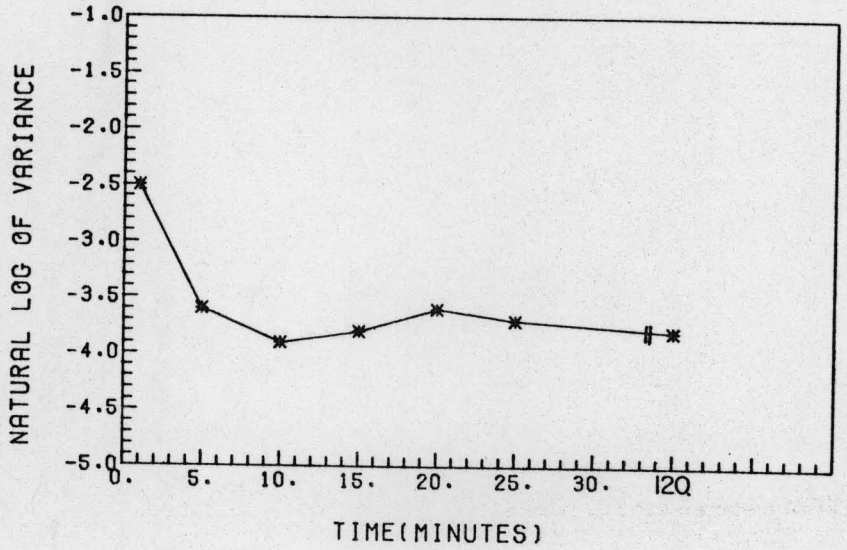

Fig. III-2-10. Blending of 20/30 Mesh White and 60/80 Mesh Yellow Granulation in a V-Blender. Results are Plotted According to Eq. IV-10 in Logarithmic Form

Table III-2-11 Mixing of 20/30 Mesh White and 80/100 Mesh Yellow Granulation in 2 kg Load in V-Blender in 50:50 Ratio

Time	Percent Yellow Granulation in Sample Indicated						
(Min)	1	2	3	4	$\overline{X}$	σ	$\ln\sigma^2$
1	47.8	38.5	55.3	36.3	44.5	8.7	-4.9
5	42.3	44.9	45.0	45.8	44.8	1.7	-8.1
10	45.9	53.9	46.9	45.8	45.6	1.2	-8.8
15	43.0	41.7	45.9	46.6	44.3	2.3	-7.5
25	44.1	42.6	44.4	45.6	44.1	1.2	-8.8
120	48.0	46.4	48.1	45.5	47.0	1.3	-8.7

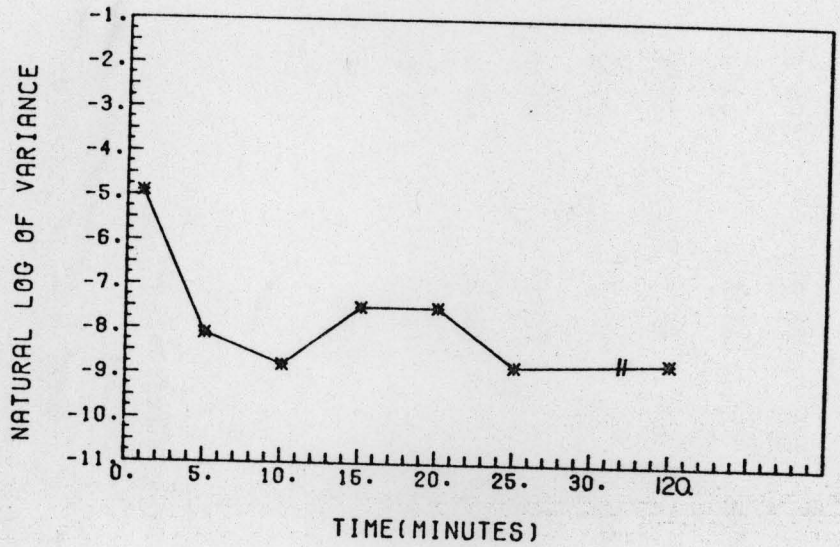

Fig. III-2-11. Blending of 20/30 Mesh White and 80/100 Mesh Yellow Granulation in a V-Blender. Results are Plotted According to Eq. IV-10

Table III-2-12 Mixing of 20/30 Mesh White and 40/60 Mesh Yellow Granulations in 4 kg Load in a V-Blender in 50:50 Ratio

Time	Percent Yellow Granulation in Sample Indicated						
(Min)	1	2	3	4	$\overline{X}$	σ	$\ln\sigma^2$
5	81.2	24.2	87.2	5.1	49.5	41.0	-1.8
10	77.9	30.7	87.2	18.7	53.6	34.0	-2.2
15	83.2	21.0	85.6	15.0	51.2	38.4	-1.9
20	82.7	18.5	85.3	17.4	51.0	38.2	-1.9
30	83.0	19.3	86.0	18.1	51.6	38.0	-1.9
45	79.5	27.7	84.2	19.8	52.8	33.7	-2.2
120	79.6	23.5	84.3	22.0	52.4	34.3	-2.1
240	82.8	64.3	83.1	22.1	50.6	37.5	-2.0

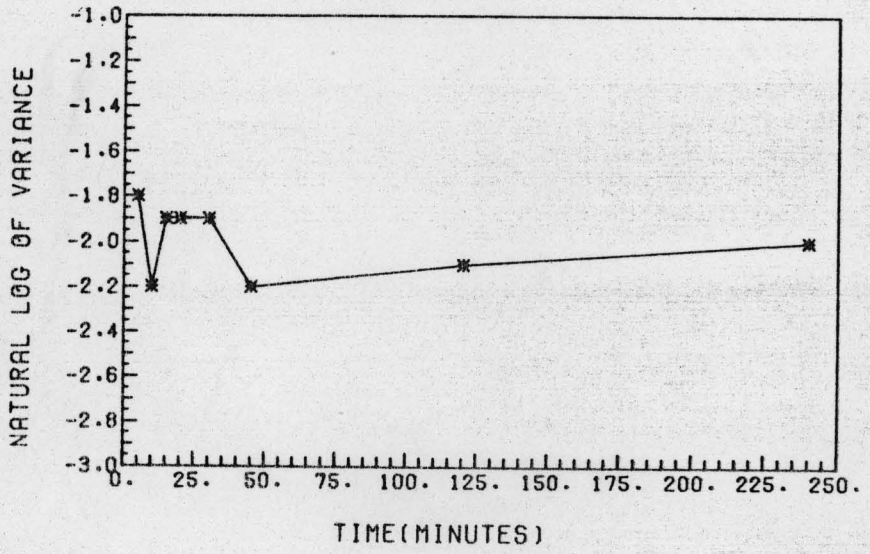

Fig. III-2-12. Blending of 20/30 Mesh White and 40/60 Mesh Yellow Granulation in a V-Blender with 4 kg. Load. Results are Plotted According to Eq. IV-10.

Table III-2-13 Mixing of 20/40 Mesh Yellow and White Granulations in a 2 kg Load in a V-Blender at 50:50 Ratio With Longitudinal Loading.

Time	Percent of Yellow Granulation in Sample						
(Min)	1	2	3	4	$\bar{X}$	σ	$\ln\sigma^2$
1	46.0	55.4	43.4	58.4	50.8	7.2	-5.3
5	47.9	53.2	46.3	53.3	50.2	3.6	-6.6
10	50.2	51.9	48.0	52.7	50.7	2.1	-7.8
15	51.8	51.7	48.8	51.0	50.8	1.4	-8.5
20	50.4	51.7	49.0	51.8	50.7	1.3	-8.6
25	50.6	51.7	48.8	51.6	50.7	1.3	-8.6
120	50.6	52.5	48.9	49.6	50.4	1.5	-8.3

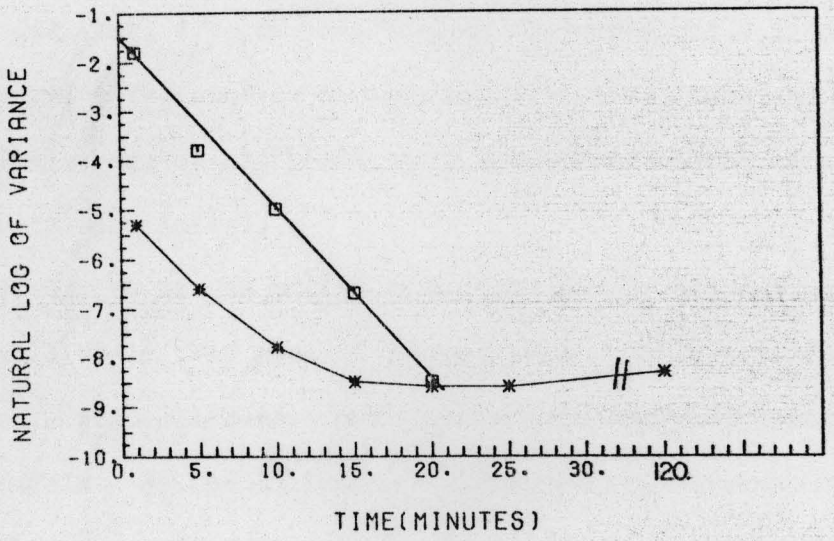

Fig. III-2-13. Blending of 20/40 Mesh Yellow (50%) and White (50%) Granulation in a V-Blender. Results are Plotted According to Eq. IV-10.

* Longitudinal Loading.

□ Axial Loading.

results in line with those predicted from theory. The experiments (II-3-1) employed yellow and white tablets, where effects due to differences in density, particle shape (between particles) or surface roughness could be ruled out. It should be noted that the shapes of the particles are not spherical (and hence deviate from previously studied model systems). The dimensions of the convex tablets were: 0.69 cm diameter, 0.46 cm thickness at the crown and 0.32 cm thickness at the edge. (The studies by Cahn et al. (1966), Cahn and Fuerstenau (1967,1968), Hogg et al. (1966,1968) and Fisher (1963) were restricted to spherical particles).

The results of the mixing of tablets in 1:1 proportion are shown in Table III-3-1. The plot of percent yellow tablets versus distance is shown in Fig. III-3-1A. The results were analyzed using diffusional mixing models. As the analyses of the compositions were carried out by counting the yellow and white tablets in the specific compartments, it was possible to carry out the experiments after small periods of mixing.

Table III-3-1: Axial Mixing of Yellow and White Tablets in a 50:50 Ratio in Rotating Cylinder.

Time	Percent of Yellow Tablets in Compartment Number Given									$\bar{X}$	σ	$\ln\sigma^2$
(Sec.)	1	2	3	4	5	6	7	8	9			
50	0.25	2.4	7.9	23.9	47.8	61.3	92.3	97.6	100	48.2	41.6	-1.75
100	4.3	6.9	14.9	30.4	50.2	66.2	83.7	90.6	97.5	49.4	36.8	-2.00
150	5.3	11.3	18.2	32.9	46.5	68.6	81.0	88.9	94.5	49.7	34.6	-2.12
200	12.0	18.3	24.9	33.3	49.2	64.9	71.8	81.4	88.0	49.3	28.5	-2.51
300	19.4	22.4	30.0	37.6	47.8	59.3	70.1	78.9	83.3	49.9	24.2	-2.84
400	30.1	33.5	36.2	43.0	47.4	55.8	61.5	74.5	71.2	50.4	16.3	-3.63
600	37.8	38.8	40.2	45.1	52.2	53.5	58.5	61.7	65.4	50.4	10.3	-4.54
900	50.1	43.0	43.6	42.6	48.3	55.7	52.5	61.1	51.3	49.8	6.2	-5.55

$R^2 = 0.994$ $s = -4.6\ 10^{-3}$ $I = -1.55$

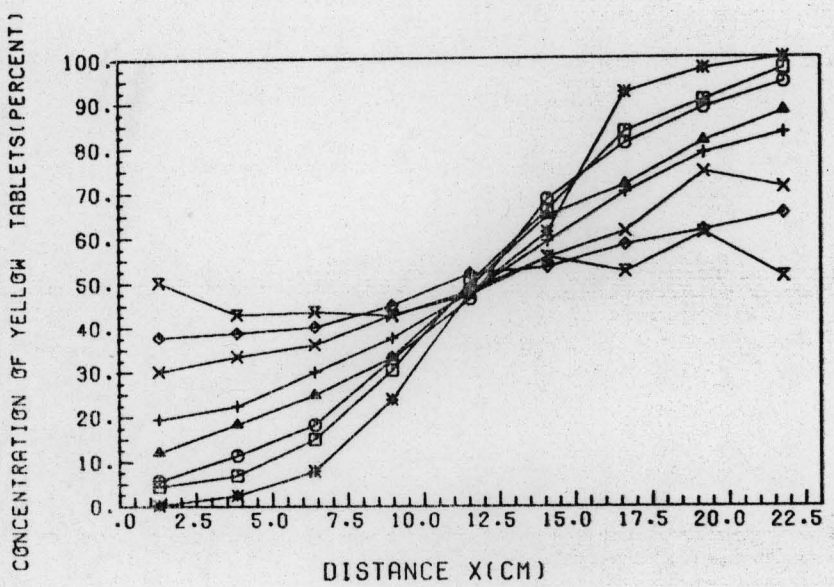

Fig. III-3-1A. Percent Yellow Tablets Versus Distance in a Horizontal, Rotating Cylinder.

Table III-3-2: Axial Mixing of Yellow and White Granulation in 50:50 Ratio in Rotating Cylinder

(Both 10/14 Mesh)

Time	Percent of Yellow Granulation in Compartment Number Given											
(Min)	1	2	3	4	5	6	7	8	9	$\bar{X}$	σ	$\ln\sigma^2$
6.7	100	97.9	89.9	74.4	47.3	21.4	7.2	1.6	0.0	48.8	42.5	-1.7
13.3	91.2	87.5	76.4	63.2	50.1	35.7	20.6	11.9	8.3	49.4	32.1	-2.3
26.7	74.7	80.8	69.4	62.4	51.2	40.1	29.2	24.7	21.1	50.4	22.6	-3.0
40.0	78.5	75.2	66.3	58.7	48.5	38.4	30.0	26.8	24.0	49.6	21.0	-3.1
58.3	76.9	74.1	66.3	57.3	49.5	38.5	31.1	25.5	23.6	49.2	20.6	-3.2
90.0	62.6	63.3	56.5	53.2	48.8	43.6	39.6	36.6	34.8	48.8	10.8	-4.4
106.7	60.2	61.3	57.2	54.9	50.0	46.5	42.9	39.5	36.1	49.8	9.2	-4.8
130.0	55.7	55.7	55.3	53.0	51.1	49.1	45.6	42.0	40.1	49.7	6.0	-5.6

$R^2 = 0.984$ $s = -2.84\ 10^{-2}$ $I = -1.84$

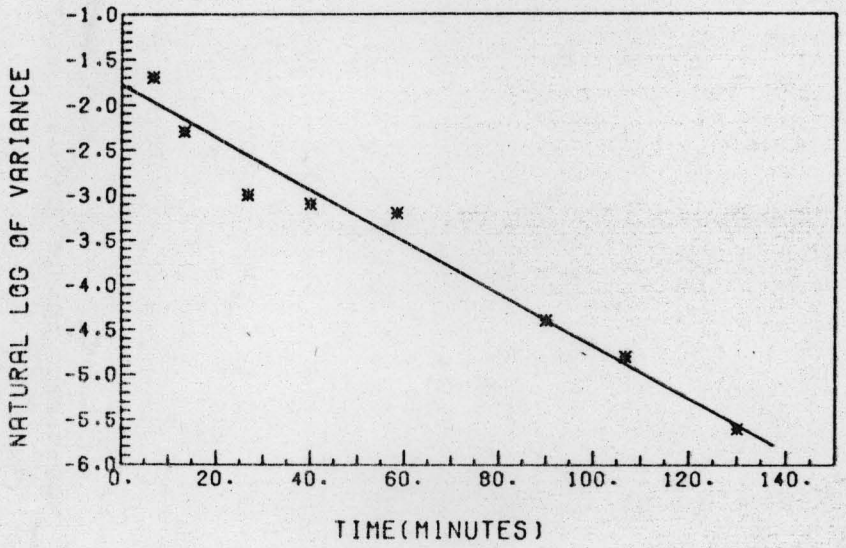

Fig. III-3-1. Blending of Monodisperse Fractions of Identical Diameter According to Eq. IV-10. Horizontal Blender. 10/14 Mesh Granules.

Table III-3-3: Axial Mixing of Yellow and White Granulation (14/20 Mesh) in 50:50 Ratio in Cylinder.

Time	Percent of Yellow Granulation in Compartment Number Given											
(Min)	1	2	3	4	5	6	7	8	9	$\bar{X}$	σ	$\ln\sigma^2$
8.3	100.0	100.0	97.7	81.8	47.7	15.9	3.7	0.0	0.0	49.6	45.5	-1.6
16.7	100.0	98.1	90.4	75.2	51.8	26.4	9.3	1.9	0.0	50.3	42.0	-1.7
33.3	92.8	93.4	82.5	68.5	50.7	32.4	17.9	8.8	5.8	50.3	35.5	-2.1
66.7	85.5	84.2	73.2	62.2	49.2	36.6	23.7	18.7	14.9	49.8	27.8	-2.6
100.0	75.0	76.6	66.7	57.6	48.8	39.4	31.9	27.4	22.2	49.5	20.6	-3.2
133.3	65.5	69.3	60.9	57.1	49.8	42.9	36.7	32.0	23.8	48.7	15.8	-3.7
166.7	64.4	67.2	60.5	55.6	50.2	44.1	40.2	32.3	32.0	49.6	13.3	-4.0
200.0	60.4	63.0	58.6	54.4	50.2	44.4	40.8	40.1	35.4	49.7	10.0	-4.6

$R^2 = 0.997$ $s = -1.55\ 10^{-2}$ $I = -1.53$

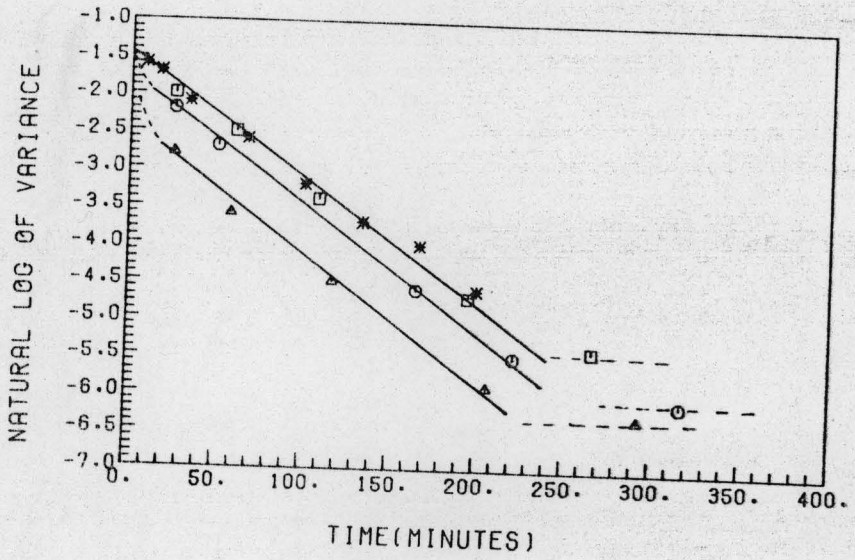

Fig. III-3-2. Blending of Monodisperse Fractions of Identical Diameter According to Eq. IV-10. 14/20 Mesh Granules in Horizontal Mixer. * 50% Yellow. □ 60% Yellow. ○ 70% Yellow. △ 80% Yellow Component.

Table III-3-4: Axial Mixing of Yellow and White 20/30 Mesh Granulation in 50:50 Ratio in Cylinder

Time	Percent of Yellow Granulation in Compartment Number Given											
(Min)	1	2	3	4	5	6	7	8	9	$\bar{X}$	σ	$\ln\sigma^2$
25.0	95.7	100.0	93.8	76.5	48.9	23.9	8.4	2.6	0.0	50.0	42.4	-1.7
50.0	83.7	94.7	82.2	67.2	48.8	31.3	16.2	9.4	8.4	49.1	34.2	-2.1
83.3	79.6	90.0	80.4	67.2	52.0	36.6	20.6	13.4	7.9	49.7	31.3	-2.3
133.3	74.4	87.3	77.4	62.9	49.3	35.6	27.3	22.6	14.0	50.1	26.6	-2.6
183.3	74.3	81.0	73.2	62.0	50.5	39.0	30.6	25.3	19.1	50.6	23.2	-2.9
233.3	62.4	76.2	70.4	59.8	50.8	43.5	29.3	23.2	20.8	48.5	20.5	-3.2
285.0	62.0	76.9	65.2	59.6	49.0	43.9	37.5	32.3	14.9	49.0	19.1	-3.3
333.3	55.4	65.6	62.3	57.1	52.3	47.4	43.6	40.7	33.0	50.8	10.6	-4.5

$R^2 = 0.96$ $s = -0.74\ 10^{-2}$ $I = -1.59$

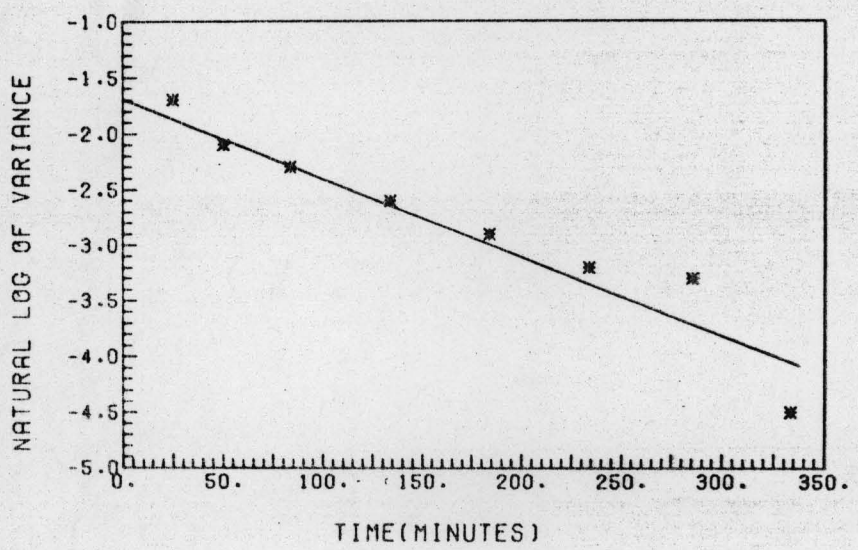

Fig. III-3-3. Blending of Monodisperse Fractions of Identical Diameter in Horizontal Mixer. Data are Plotted According to Eq. IV-10. 20/30 Mesh Granules.

Table III-3-5 Axial Mixing of Yellow and White 30/40 Mesh Granulation in 50:50 Ratio in Cylinder

Time	Percent of Yellow Granulation in Compartment Number Given											
(Min)	1	2	3	4	5	6	7	8	9	$\overline{X}$	σ	$\ln\sigma^2$
50.0	99.6	99.6	90.8	74.1	49.8	25.6	9.4	3.5	1.3	50.4	41.7	-1.7
100.0	91.3	94.0	86.2	71.2	51.7	31.2	15.8	7.1	3.3	50.2	37.0	-2.0
166.7	92.1	88.8	74.4	63.8	48.0	33.4	21.4	13.3	12.6	49.8	31.4	-2.3
250.0	84.0	82.1	72.3	61.6	48.6	36.2	26.1	20.3	19.9	50.1	25.9	-2.7
333.3	72.2	77.5	71.2	61.0	51.6	41.9	32.5	26.3	19.6	50.4	21.4	-3.1
416.7	74.9	72.1	66.3	57.9	49.7	41.1	34.3	30.3	29.5	50.7	17.9	-3.4
500.0	69.9	67.1	63.5	57.0	50.3	45.2	39.5	36.6	39.4	52.1	12.8	-4.1
593.3	55.0	63.5	62.0	56.8	51.0	45.4	42.6	42.5	42.4	51.2	8.5	-4.9

$R^2 = 0.99$ $s = -0.55\ 10^{-2}$ $I = -1.36$

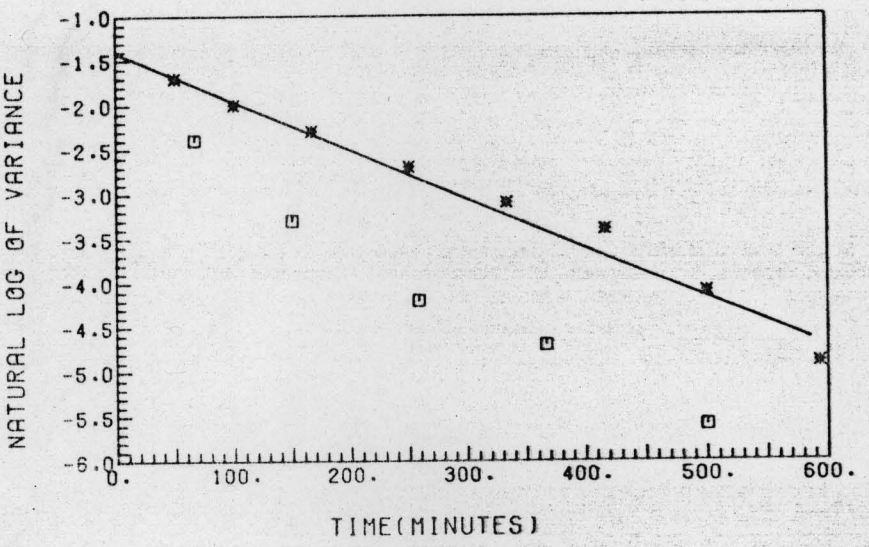

Fig. III-3-4. Blending of Monodisperse Fractions of Identical Diameter According to Eq. IV-10. 30/40 Mesh Granules in a Horizontal Mixer. Lower Line with One Percent Magnesium Stearate.

Table III-3-6: Axial Mixing of Yellow and White 40/60 Mesh Granulation in 50:50 Ratio in Cylinder

Time	Percent of Yellow Granulation in Compartment Number Given											
(Min)	1	2	3	4	5	6	7	8	9	$\overline{X}$	σ	$\ln\sigma^2$
66.7	94.3	88.7	79.4	64.3	46.7	30.3	18.2	9.6	6.7	48.7	34.3	-2.1
133.3	90.8	92.6	84.3	71.2	51.2	39.2	21.3*	-	12.3	57.8	31.6	-2.3
218.7	78.5	78.7	71.3	61.7	50.4	38.6	28.7	21.7	18.3	49.8	24.0	-2.9
300.0	62.6	66.9	63.9	58.4	50.5	21.7	18.9	33.5	32.3	45.4	18.9	-3.3
400.0	63.3	63.1	61.0	56.4	51.5	46.3	42.4	39.3	38.5	51.3	10.1	-4.6
500.0	60.2	60.9	59.4	56.2	52.3	50.3	47.9	47.8	44.1	53.2	6.2	-5.6
600.0	61.4	61.7	59.2	56.9	54.4	51.2	48.9	47.6	6.3	49.7	17.1	-3.5
700.0	59.3	59.4	56.9	56.1	52.9	49.8	50.1	6.1	49.2	48.9	16.5	-3.6

$R^2 = 0.98$ $s = -0.82\ 10^{-2}$ $I = -1.24$

*From Compartments 7 and 8

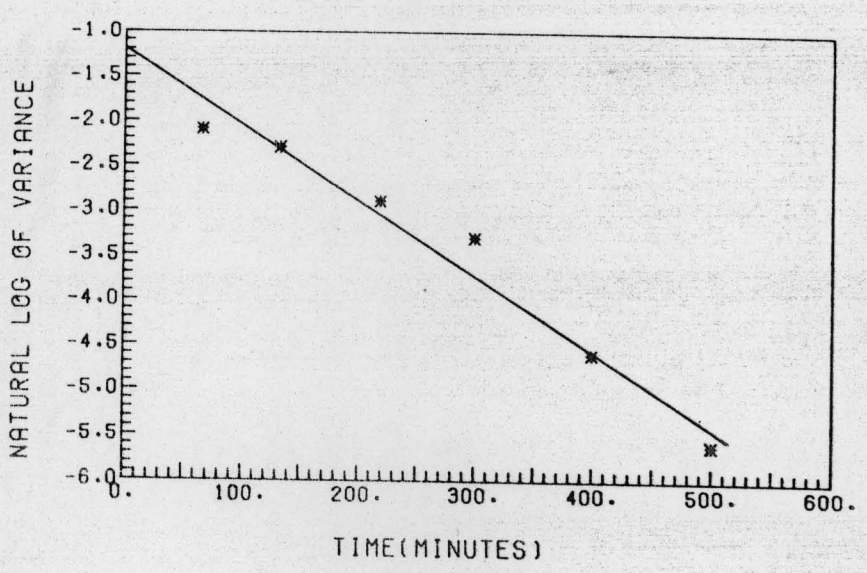

Fig. III-3-5. Blending of Monodisperse Fractions of Identical Diameter According to Eq. IV-10. 40/60 Mesh Granules in a Horizontal Mixer.

Table III-3-7 Axial Mixing of Yellow and White 14/20 Mesh Granulation in 60:40 Ratio in Cylinder

Time	Percent of Yellow Granulation in Compartment Number Given											
(Min)	1	2	3	4	5	6	7	8	9	$\bar{X}$	σ	$\ln\sigma^2$
25.0	97.9	98.0	92.3	83.9	66.3	45.2	26.5	11.9	6.0	58.7	37.2	-2.0
60.0	93.6	92.6	83.9	74.2	62.5	49.0	36.6	26.5	19.7	59.8	28.3	-2.5
108.3	83.3	82.9	76.0	68.0	59.1	51.0	44.1	39.2	35.4	59.9	18.6	-3.4
195.0	72.6	73.0	67.1	64.1	58.6	54.9	52.8	50.7	46.7	60.1	9.6	-4.7
266.7	66.4	68.7	65.4	62.4	59.3	57.7	48.2	55.1	52.6	59.5	6.8	-5.4

$R^2 = 0.99$ $s = -1.6\ 10^{-2}$ $I = -1.59$

Table III-3-8: Axial Mixing of Yellow and White 14/20 Mesh Granulation in 70:30 Ratio in Cylinder.

Time	Percent of Yellow Granulation in Compartment Number Given											
(Min)	1	2	3	4	5	6	7	8	9	$\bar{X}$	σ	$\ln\sigma^2$
25.0	100.0	100.0	94.7	91.1	80.8	65.8	44.8	27.2	14.6	68.8	32.6	-2.2
50.0	95.4	95.6	90.1	83.3	73.5	60.7	47.3	36.2	30.5	68.1	25.4	-2.7
165.0	82.2	81.6	78.1	73.8	69.2	64.4	61.3	59.3	56.0	69.5	9.9	-4.6
221.7	77.0	76.2	74.7	71.4	68.3	66.3	63.9	61.7	60.1	68.8	6.3	-5.5
316.7	72.1	75.0	73.5	71.9	71.3	68.4	67.6	60.3	65.0	69.5	4.6	-6.1

$R^2 = 0.999$ $s = -1.66\ 10^{-2}$ $I = -1.83$

Table III-3-9: Axial Mixing of Yellow and White 14/20 Mesh Granulation in 80:20 Ratio in Cylinder

Time	Percent of Yellow Granulation in Compartment Given											
(Min)	1	2	3	4	5	6	7	8	9	$\overline{X}$	σ	$\ln\sigma^2$
25.0	100.0	100.0	98.8	97.7	90.3	78.6	63.7	49.0	35.6	79.3	24.4	-2.8
58.3	100.0	97.3	94.3	90.0	83.6	75.1	66.8	60.7	53.7	80.1	16.9	-3.6
116.7	92.7	93.0	89.4	84.0	80.1	75.3	71.4	69.6	65.2	80.1	10.4	-4.5
206.7	84.2	88.1	85.2	82.3	79.4	76.3	75.7	76.1	72.2	79.9	5.3	-5.9
293.3	78.8	82.6	73.0	80.1	78.9	79.3	76.2	78.5	67.8	77.1	4.4	-6.3

$R^2 = 0.997$ $s = -1.66\ 10^{-2}$ $I = -2.51$

Table III-3-10: Axial Mixing of Yellow and White 30/40 Mesh Granulation in 50:50 Ratio in Horizontal Cylinder, With 4.8% of Magnesium Stearate Added.

Time	Percent of Yellow Granulation in Compartment Given											
(Min)	1	2	3	4	5	6	7	8	9	$\bar{X}$	σ	$\ln\sigma^2$
66.7	87.1	81.8	60.3	57.9	44.8	29.8	18.3	10.3	7.5	44.2	29.7	-2.4
150.0	71.3	68.9	61.1	53.3	45.4	35.3	26.2	22.4	22.3	45.1	19.6	-3.3
258.3	60.9	58.7	55.0	50.7	46.5	39.7	34.2	29.8	28.5	44.9	12.4	-4.2
366.7	50.0	53.0	52.1	49.1	45.8	28.2	37.5	31.8	33.2	42.3	9.6	-4.7
500.0	53.7	52.3	49.9	48.4	46.1	43.3	40.5	37.6	38.5	45.6	5.9	-5.6

$R^2 = 0.99$ $s = -0.7\ 10^{-2}$ $I = -2.12$

Table III-3-11 Axial Mixing of 20/30 Mesh* Yellow Granulation with 6/10 Mesh White Granulation in 50:50 Ratio in Rotating Cylinder

Time	Percent of Yellow Granulation in Compartment Given											
(Min)	1	2	3	4	5	6	7	8	9	$\bar{X}$	σ	$\ln\sigma^2$
8.3	100.0	99.0	90.5	63.6	36.9	21.2	11.0	7.8	5.9	48.4	40.2	-1.8
23.3	64.8	92.0	75.9	68.6	43.8	35.0	26.6	24.0	12.1	49.2	27.2	-2.6
41.7	59.0	92.9	76.9	57.1	43.8	35.8	28.6	25.2	13.3	48.1	27.8	-2.7
66.7	40.1	92.6	80.8	61.3	45.8	36.4	32.4	29.9	15.8	48.1	25.8	-2.7
100.0	27.7	70.8	77.8	73.4	54.2	42.8	38.9	33.5	16.1	48.4	21.9	-3.0
133.3	30.2	64.2	66.6	52.5	45.1	47.5	58.7	55.1	21.1	49.0	15.1	-3.8
183.3	18.3	38.8	42.4	45.8	52.5	59.1	69.7	72.4	36.0	48.3	17.2	-3.5
233.3	31.4	68.2	56.4	55.8	63.3	49.1	44.8	47.2	21.6	48.6	14.8	-3.8

* 20/30 Mesh Yellow Granulation Initially Loaded on the Left Hand Side of the Cylinder.

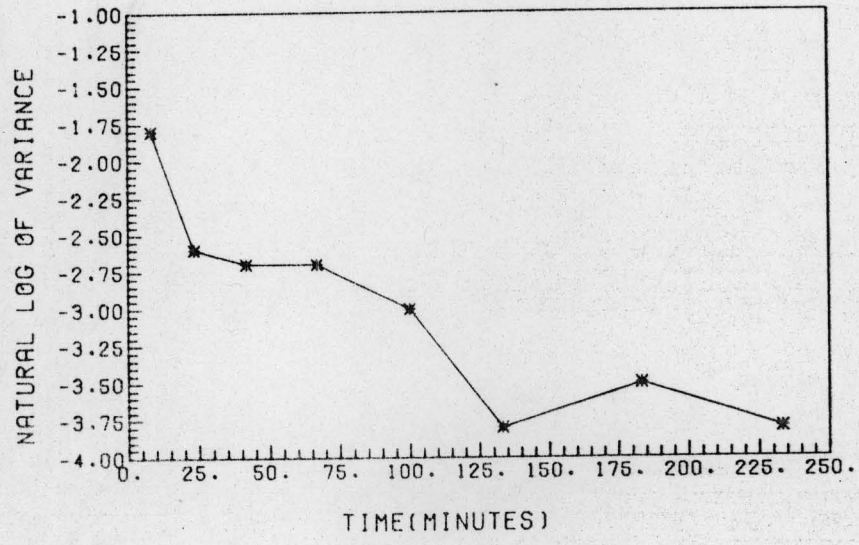

Fig. III-3-6. Blending of 20/30 Mesh Yellow and 6/10 Mesh White Granulation in a Horizontal, Rotating Cylinder. Results Are Plotted According to Eq. IV-10

Table III-3-12 Axial Mixing of 20/30 Mesh Yellow Granulation with 10/14 Mesh White Granulation in 50:50 Ratio in Rotating Cylinder

Time	Percent of Yellow Granulation in Compartment Given											
(Min)	1	2	3	4	5	6	7	8	9	$\bar{X}$	σ	$\ln\sigma^2$
10.0	99.2	95.4	86.9	73.9	48.0	19.9	6.3	3.5	3.4	48.5	41.2	-1.8
21.7	91.3	95.1	84.4	72.4	52.2	26.0	8.8	6.2	6.0	49.2	38.0	-1.9
33.3	70.2	93.1	82.6	73.6	60.2	33.4	12.4	10.8	8.6	49.4	33.4	-2.2
50.0	64.5	94.7	83.2	73.3	59.2	38.5	16.4	9.7	7.6	49.7	32.8	-2.2
116.7	84.6	97.8	88.3	71.1	47.9	20.3	9.0	11.3	9.7	52.5	36.8	-2.0
200.0	70.8	97.2	83.8	72.4	55.3	27.4	11.1	11.8	9.7	48.8	34.3	-2.1
291.7	74.3	97.6	87.8	73.4	49.9	20.3	12.1	14.9	10.7	49.0	35.2	-2.1
533.3	77.0	98.9	90.5	77.7	42.2	16.3	11.7	18.0	11.1	49.3	36.6	-2.0

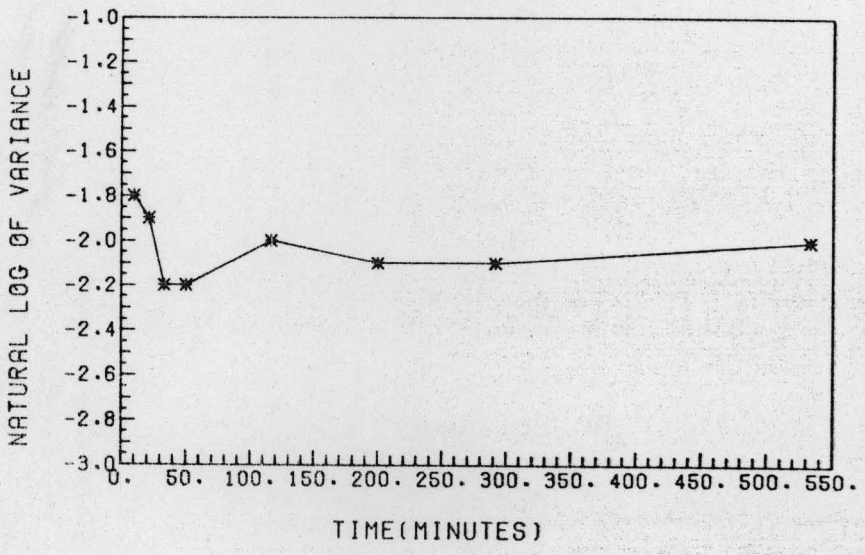

Fig. III-3-7. Blending of 20/30 Mesh Yellow and 10/14 Mesh White Granulation in a Horizontal, Rotating Cylinder. Results Are Plotted According to Eq. IV-10.

Table III-3-13: Axial Mixing of 20/30 Mesh Yellow Granulation with 14/20 Mesh White Granulation in 50:50 Ratio in Rotating Cylinder

Time	Percent of Yellow Granulation in Compartment Given											
(Min)	1	2	3	4	5	6	7	8	9	$\overline{X}$	σ	$\ln\sigma^2$
33.3	100.0	100.0	96.4	69.9	33.3	13.9	5.3	2.5	1.6	47.0	44.2	-1.6
100.0	100.0	100.0	92.4	63.4	34.8	19.5	11.7	9.9	7.0	48.7	40.4	-1.8
191.7	98.2	98.6	81.4	54.3	33.8	19.7	13.3	15.5	12.9	47.5	36.6	-2.0
333.3	87.8	94.4	57.1	50.5	32.1	22.8	21.3	26.8	14.5	45.3	29.4	-2.4
583.3	68.7	90.2	89.0	61.0	39.0	27.8	23.0	20.7	10.6	47.8	30.2	-2.4
833.3	62.2	92.5	79.6	65.2	46.4	26.7	21.3	24.5	13.2	48.0	28.3	-2.5

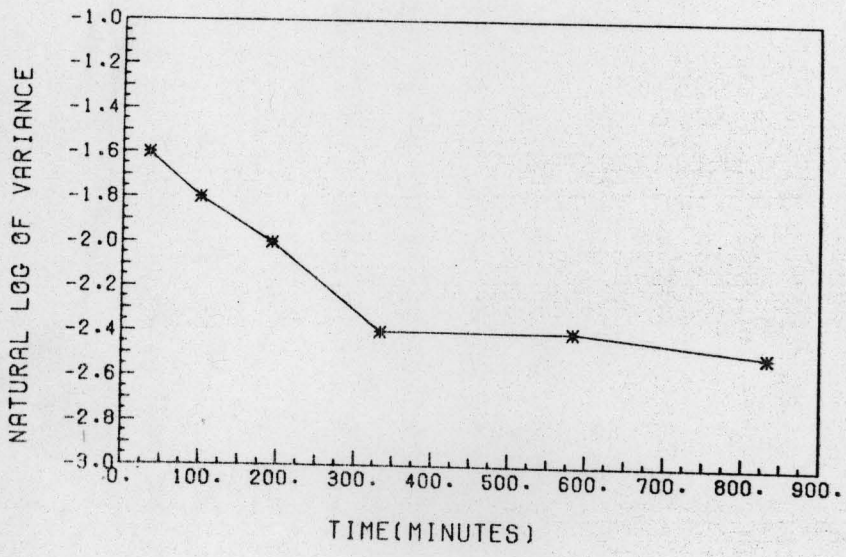

Fig. III-3-8. Blending of 20/30 Mesh Yellow and 14/20 Mesh White Granulation in a V-Blender. Results Are Plotted According to Eq. IV-10. Ratio is 50:50.

Table III-3-14: Axial Mixing of 20/30 Mesh Yellow Granulation with 30/40 Mesh White Granulation in 50:50 Ratio in Rotating Cylinder

Time	Percent of Yellow Granulation in Compartment Given											
(Min)	1	2	3	4	5	6	7	8	9	$\bar{X}$	σ	$\ln\sigma^2$
88.3	1.0	1.0	4.3	24.2	46.9	70.9	92.9	98.0	98.6	48.6	42.5	-1.7
166.7	2.9	2.0	6.4	32.2	49.6	63.7	83.7	97.7	98.6	48.5	39.8	-1.8
350.0	2.4	1.4	4.0	13.4	50.9	88.6	93.2	93.8	95.0	49.2	43.8	-1.6
583.3	4.1	2.2	4.4	12.4	52.6	90.5	94.3	93.1	96.1	50.0	44.0	-1.6
833.3	8.7	4.6	9.0	25.2	51.1	70.4	86.7	91.6	94.6	49.1	38.0	-1.9

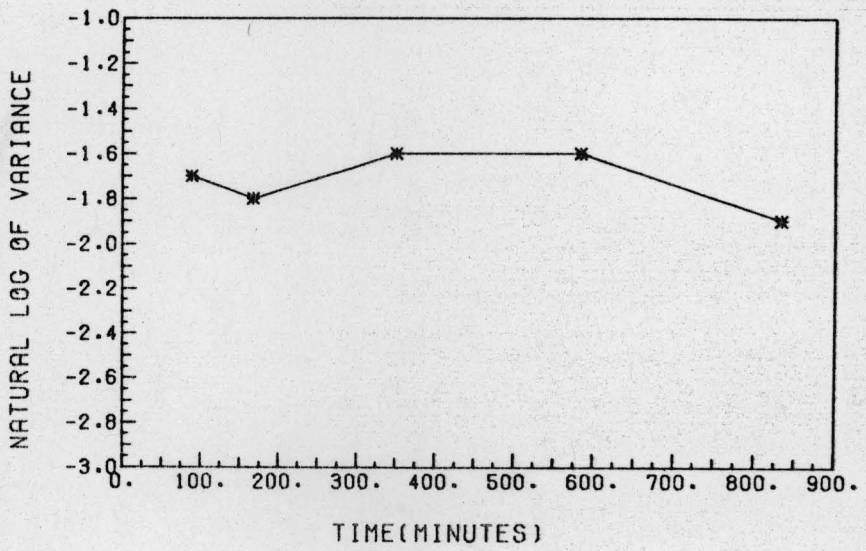

Fig. III-3-9. Blending of 20/30 Mesh Yellow and 30/40 Mesh White Granulation in a Horizontal, Rotating Cylinder in 50:50 Ratio. Results Are Plotted According to Eq. IV-10.

Table III-3-15: Axial Mising of 20/30 Mesh Yellow Granulation with 40/60 Mesh White Granulation in 50:50 Ratio in Rotating Cylinder

Time	Percent of Yellow Granulation in Compartment Given											
(Min)	1	2	3	4	5	6	7	8	9	$\overline{X}$	σ	$\ln\sigma^2$
25.0	0.0	0.0	0.0	7.9	68.5	82.6	86.5	90.7	96.6	48.1	44.4	-1.62
50.0	0.0	0.0	0.0	6.6	73.4	81.0	86.8	91.9	95.3	48.3	44.8	-1.61
166.7	0.0	0.0	0.0	1.6	65.8	87.9	89.3	91.6	94.0	47.8	45.7	-1.57
333.3	0.0	0.0	0.0	8.0	76.3	83.0	84.5	90.2	95.1	48.6	44.5	-1.62
500.0	0.0	0.0	1.0	55.9	79.2	75.2	68.6	64.9	97.6	49.2	38.3	-1.92
833.3	0.4	1.2	41.1	63.0	72.3	76.3	75.3	56.8	38.6	47.2	29.6	-2.43

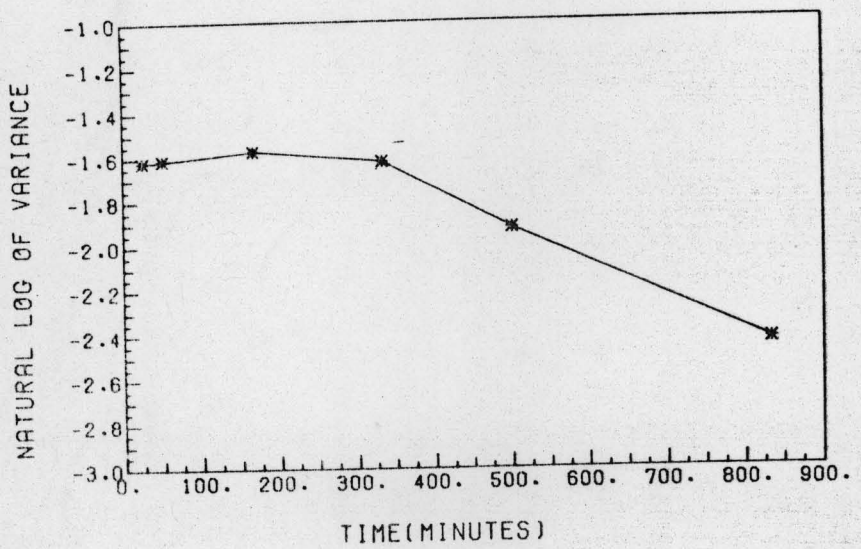

Fig. III-3-10. Blending of 20/30 Mesh Yellow and 40/60 Mesh White Granulation in a Horizontal Rotating Cylinder. The Results are Plotted According to Eq. IV-10.

Table III-3-16: Axial Mixing of 20/30 Mesh Yellow Granulation with 60/80 Mesh White Granulation in a Rotating Cylinder.

Time	Percent of Yellow Granulation in Compartment Given											
(Min)	1	2	3	4	5	6	7	8	9	$\overline{X}$	σ	$\ln\sigma^2$
33.3	9.7	5.4	33.8	52.0	59.4	63.8	64.2	61.1	87.7	48.6	27.1	-2.61
83.3	12.4	18.3	50.1	55.0	55.7	58.2	58.9	54.8	86.3	50.0	22.3	-3.00
166.7	12.9	17.6	48.3	53.1	53.1	55.9	56.4	52.6	87.8	48.6	22.2	-3.01
333.3	17.2	8.5	34.2	54.2	57.9	60.5	60.0	58.6	87.4	48.7	24.5	-2.81
583.3	14.4	16.8	48.8	54.5	56.0	58.2	58.8	53.3	80.9	49.1	21.0	-3.12
833.3	14.2	8.4	44.6	54.6	57.1	59.1	59.7	55.6	84.6	48.7	23.7	-2.88

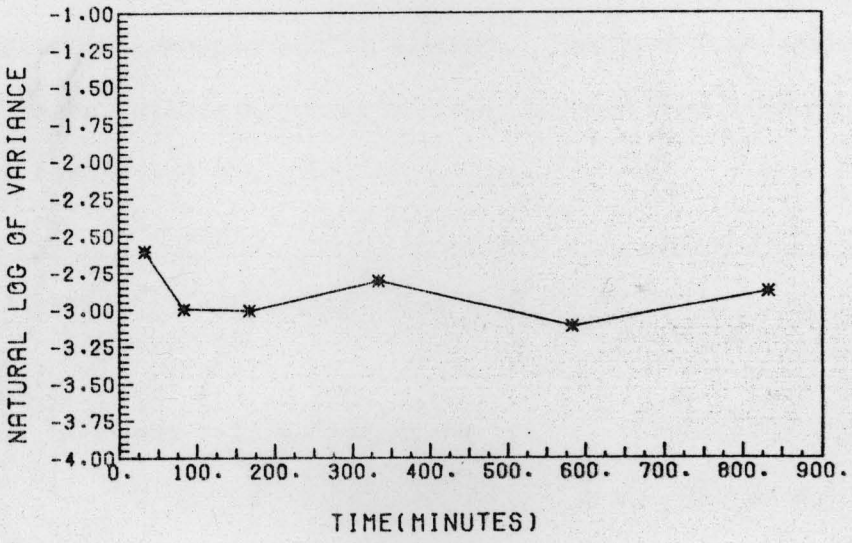

Fig. III-2-11. Blending of 20/30 Mesh Yellow and 60/80 Mesh White Granulation in a Horizontal,Rotating Cylinder in a 50:50 Ratio. Results Are Plotted According to Eq. IV-10.

III-4 Longitudinal Blending.

The results from these experiments are shown in Table III-4-1. The first column shows the mesh size of the granulations, and the next six columns show the content of yellow granulation in the longitudinal compartment indicated. The last four columns show the mean, standard deviation (σ), natural logarithm of the variance ($\ln\sigma^2$) and the load.

Table III-4-1: Longitudinal Mixing at 50:50 Ratio

Mesh	Percent Yellow Granulation in									Load
Size	1	2	3	4	5	6	$\overline{X}$	σ	$\ln\sigma^2$	(g)
10/14	42.0	48.3	41.9	48.2	49.0	44.2	45.6	3.3	-6.8	460
14/20	49.3	49.3	48.9	48.4	47.4	46.5	48.3	1.1	-9.0	464
20/30	47.2	48.0	48.4	49.7	5o.6	43.2	48.0	2.8	-7.1	460
30/40	50.4	49.1	46.9	48.1	51.2	35.6	47.0	5.7	-5.7	424
40/60		46.9	46.8	46.4	41.7	46.2	45.6	2.2	-7.6	450

III-5 Assay Variation

The results from the study of assay variation are shown in Table III-5-1:

Table III-5-1: Analysis of Yellow Granulation Using the Established Beer's Law Plots.

Mesh Size	Slope of Calibration Chart (mg)*	Amount (g) in Sample	Amount (g) from Analysis	Percent Difference
10/14	7.12	17.3	17.6	1.7
		35.3	35.6	0.8
14/20	6.61	22.1	22.2	0.5
		40.8	40.9	0.3
20/30	6.7	19.6	19.8	0.5
		42.1	42.5	1.0
30/40	6.55	16.4	16.5	0.6
		33.9	33.9	0.0
40/60	6.16	15.5	15.7	1.3
		32.2	32.1	0.3

*Slope from the plot of amount of yellow granulation (mg) versus absorbance. Absorbance values are for 1:2000 dilution.

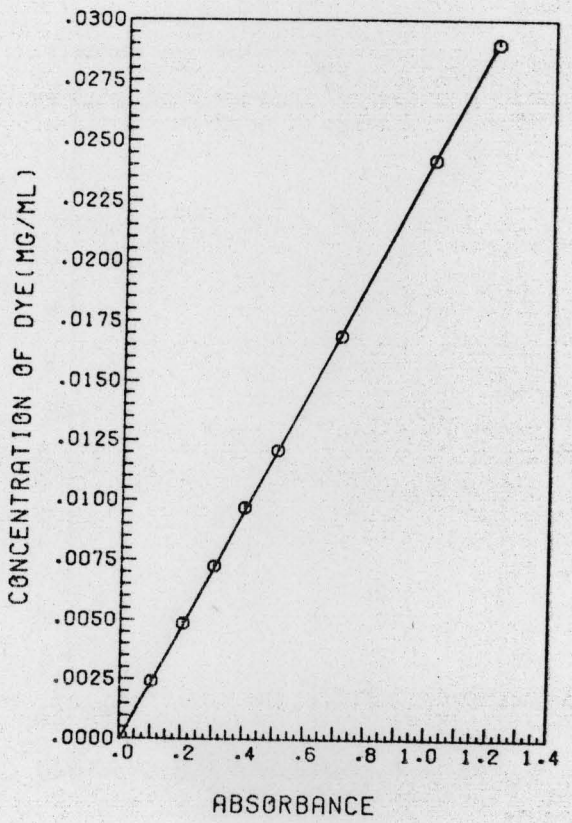

Fig. III-5-1. Beer's Law Plot for F.D.and C.Yellow Dye No. 5. Absorbance Values are for a 1:2000 Dilution.

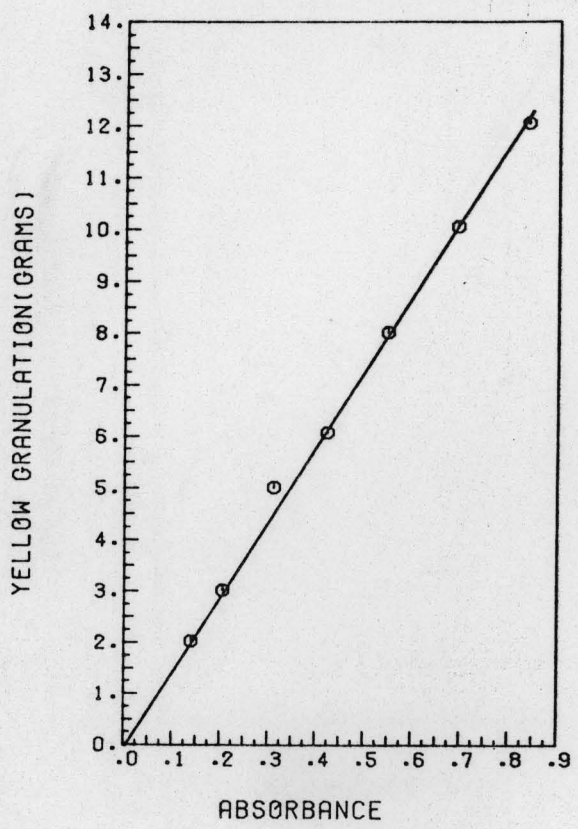

Fig. III-5-2. Calibration Chart for 10/14 Mesh Yellow Granulation. Absorbance Values are for a 1:2000 Dilution.

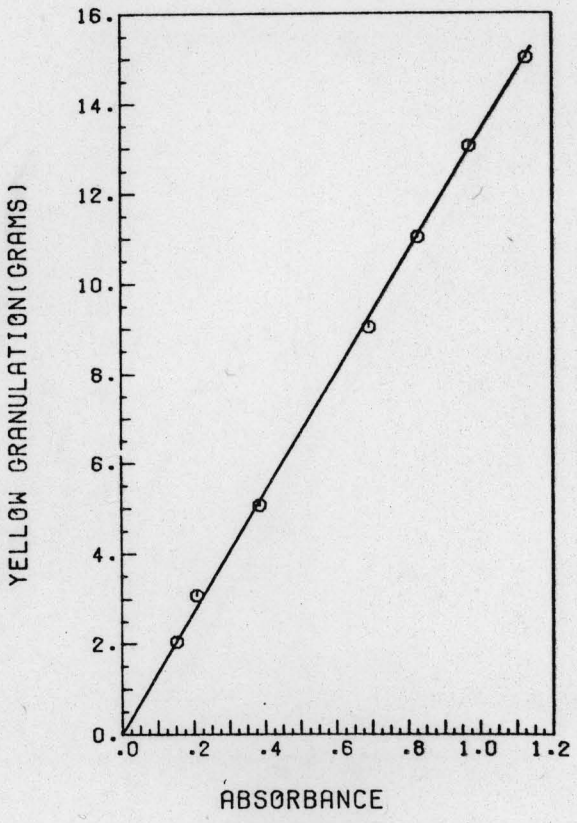

Fig. III-5-3. Calibration Chart for a 14/20 Mesh Yellow Granulation. Absorbance Values Obtained after 1:2000 Dilution.

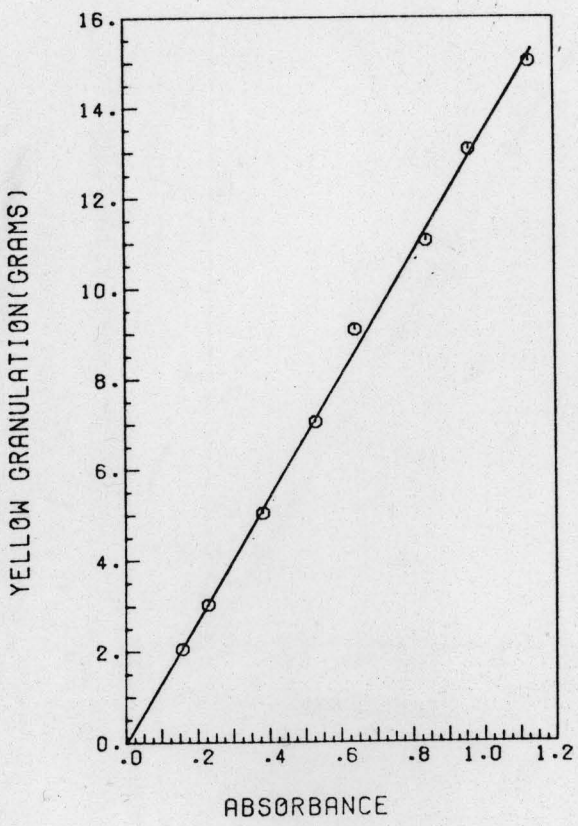

Fig. III-5-4 Calibration Chart for 20/30 Mesh Yellow Granulation.

Absorbance Values Refer to a 1:2000 Dilution

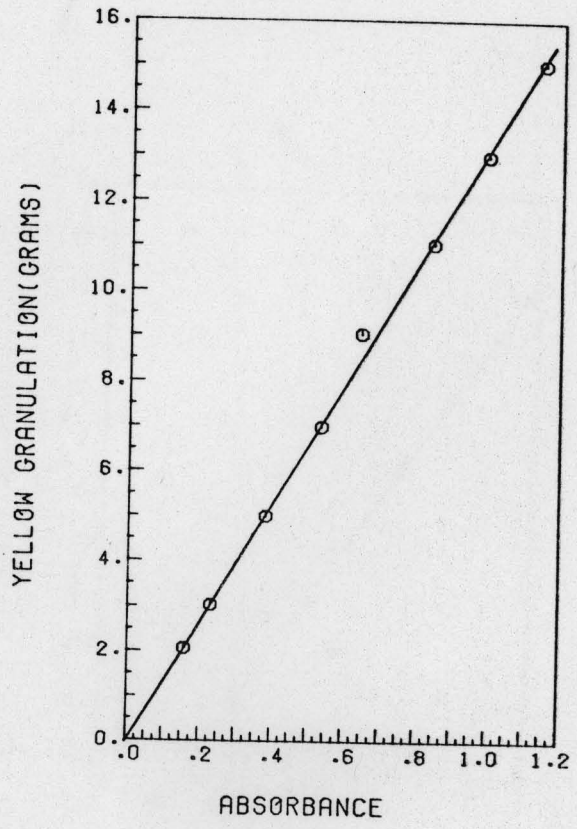

Fig. III-5-5 Calibration Chart for 20/30 Mesh Yellow Granulation. Absorbance Values Refer to a 1:2000 Dilution.

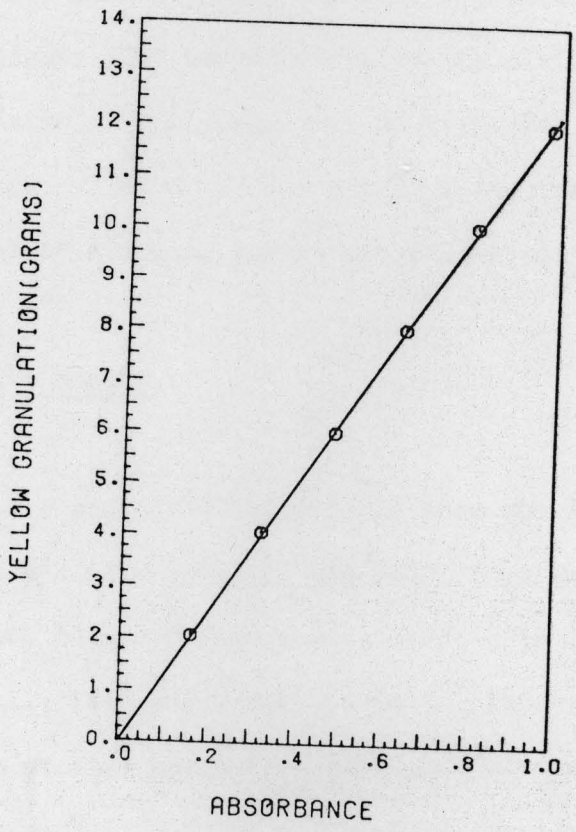

Fig. III-5-6. Calibration Chart for 40/60 Mesh Yellow Granulation. Absorbance Values Refer to 1:2000 Dilution.

IV. DISCUSSION

The theory of mixing of solids was developed first by Lacey (1954). He classified solids mixing processes into three categories, viz. (a) convective mixing, where transfer is considered of groups of adjacent particles from one location in the mixture to another, (b) diffusive mixing, which deals with distribution of particles over a freshly developed surface and (c) shear mixing, which deals with the establishment of slipping planes within the mixture.

IV-1 Diffusive Mixing.

A considerable amount of theoretical work has been done on the model of diffusive mixing (Hogg et al. 1967, Hogg et al., 1968, Cahn et al., 1966, Cahn and Fuerstenau, 1967, Cahn and Fuerstenau, 1968, Otake et al., 1961 and Fisher, 1963). Experimentally these models have been studied by loading particles differing only in color into a horizontal cylinder mixer which rotates about its axis. In the mixer, the behavior of the particles rolling down the freshly developed surface is similar to ordinary molecular diffusion. Each particle has an equal chance of deflecting to either side on each collision with another particle. Thus, within the mixing plane, particles exhibit random movement. Lacey (1954) applied the classical diffusion theory to describe the mixing process. Fick's diffusion equation was applied in the form:

$$\partial C/\partial t = D \cdot \partial^2 C/\partial x^2 \qquad \text{(Eq. IV-1)}$$

where C is concentration of colored spheres in the mixture, t is time, x is distance in the direction of diffusion (axial) and D is the (axial) diffusion coefficient. It should be noted that experiments were carried out using spheres. Fig. IV-1 shows coordinate nomenclature.

For simplicity Lacey (1954) considered the simplest case of a horizontal cylinder rotating about its axis. Since radial diffusion is extremely fast, the rate of mixing is controlled by axial diffusion. Hence the mixing process can be considered as a one dimensional diffusion process, and Eq. IV-1 can be applied in the form shown. Lacey (1954) used the following initial and boundary conditions:

$$\begin{aligned} &t = 0,\ C = 1 \quad 0 \leqq x \leqq \overline{C}_f L \\ &t = 0,\ C = 0 \quad \overline{C}_f L \leqq x \leqq L \\ &t = t,\ \partial C/\partial x = 0,\ x = 0,\ x = L \end{aligned} \qquad \text{(Eq. IV-2)}$$

where $\overline{C}_f$ is the concentration of the colored particles in the bulk mixture (average fraction concentration) and L is the length of the mixer. Eq. 1 can be solved with the initial and boundary conditions in Eq. IV-2 to give the following expression:

$$C = \overline{C}_f + (2/\pi)\sum_{n=1}^{\infty} (1/n) \exp[-n^2\pi^2 Dt/L^2] \sin(n\pi\overline{C}_f) \cos[n\pi x/L] \qquad \text{(Eq.IV-3)}$$

(There appears to be a printing error in Lacey's article, in that the term (1/n) appears as 1/C. The final derivations by Lacey, however, are correct.). n in the above equation is an integer running index.

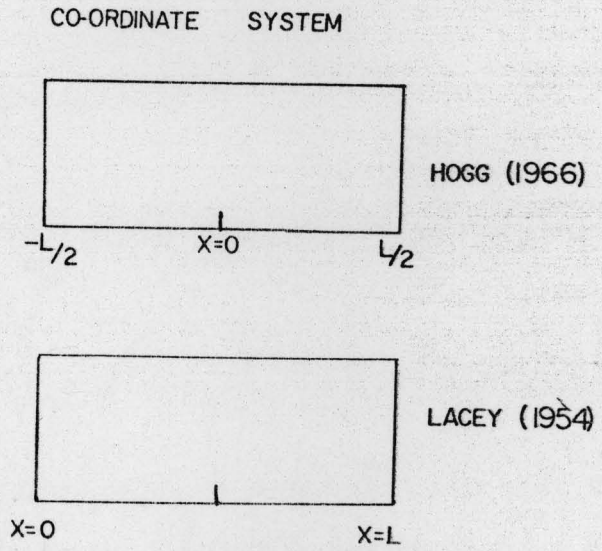

Fig. IV-1 Coordinate System Nomenclature.

Hogg et al. (1966) and Cahn et al. (1966) solved Eq. 1 with the following initial and boundary conditions:

$$C = 1 \qquad -L/2 \leq x \leq 0$$

$$C = 0 \qquad 0 \leq x \leq +L/2 \qquad \text{(Eq. IV-4)}$$

$$\partial C/\partial x = 0 \quad \text{for } x = -L/2 \text{ and } x = +L/2$$

and arrived at the solution

$$C = 0.5 - (2/\pi)\sum_{n=1}^{\infty} [1/(2n-1)]\cdot\exp[-(2n-1)^2\pi^2 Dt/L^2]\cdot\sin[(2n-1)\pi x/L] \qquad \text{(Eq. IV-5)}$$

for $\overline{C}_f = 0.5$

For large values of t, or more exactingly when $Dt/L^2 > 0.1$, higher terms in n become negligible and Eq. 3 and 5 can be approximated by:

$$C = \overline{C}_f + (2/\pi)\cdot\exp[-\pi^2 Dt/L^2]\cdot\sin[\pi\overline{C}_f]\cdot\cos[\pi x/L] \qquad \text{(Eq. IV-6)}$$

and $$C = 0.5 - (2/\pi)\cdot\exp[-\pi^2 Dt/L^2]\cdot\sin(\pi x/L) \qquad \text{(Eq. IV-7)}$$

The variance of the mixture at any time is given by:

$$\sigma^2 = \int_0^L [(C-\overline{C}_f)^2/L]\, dx \qquad \text{(Eq. IV-8)}$$

Eq. 6 and 7 inserted in Eq. 8 give:

$$\sigma^2 = (2/\pi^2)\cdot\sin(\overline{C}_f\pi)\cdot\exp[-2\pi^2 Dt/L^2] \qquad \text{(Eq. IV-9)}$$

and $$\sigma^2 = (2/\pi^2)\cdot\exp[-2\pi^2 Dt/L^2] \qquad \text{(Eq. IV-10)}$$

Hogg et al. (1966) solved Eq. 1 for small times of mixing by considering diffusion in an infinite cylinder. The solution to the system is:

$$C = 0.5 \cdot \left(1 - \text{erf}[x/(2 \cdot \sqrt{Dt})]\right) \qquad \text{(Eq. IV-11)}$$

The variance for short periods of time is then given by:

$$\sigma^2 = (0.25) \cdot [1-(4\sqrt{2Dt/\pi}/L)] \qquad \text{(Eq. IV-12)}$$

IV-2 Mixing of Particles of Defined Geometric Shape.

A review of the literature concerning the mixing of particulate solids reveals that either experiments could not be designed to check the validity of theories of mixing, or experiments in real systems could not be accounted for by a general theory. For instance in the publications by Cahn et al. (1966), Cahn and Fuerstenau (1967,1968) and by Hogg et al. (1966,1968) dealing with diffusional mixing, only ideal systems were considered. In two component systems, both the components were essentially identical, so that effects due to differences due to density, particle shape or surface roughness would not influence the kinetics of mixing.

The eventual goal of this study involves blending of particles with surface roughness and with non-spherical geometry. However, to test the workability of the system, experiments were carried out with particles of defined shape, to establish that the system would give

results in accordance with theory (for smooth regular particles). This was the reason for carrying out the experiments using yellow and white tablets (Section II-3-1). It should be noted that although the tablets are smooth, they are not of as regular a shape as investigated in the past (e.g. by Cahn et al. (1966), Cahn and Fuerstenau (1967,1968),Hogg et al. (1966,1968) and Fisher (1963)), in experiments that supported the diffusive theory of mixing. As shall be seen below, not only do the experiments carried out with tablets show that the system used was a workable system, but it also shows that particles that are smooth but off-spherical will obey the diffusive mixing equations.

The dimensions of the convex tablets were: 0.96 cm diameter, 0.46 cm thickness at the crown and 0.32 cm thickness at the edge. The results of the mixing of tablets (1:1 proportion) are shown in Table III-3-1. The plot of percent yellow tablets versus distance is shown in Fig. III-3-1A. The results were analyzed via Eq. IV-11 which holds for times sufficiently small to insure that particles in the left half have not reached the right wall and vice versa. This is true e.g. for a mixing time of 150 seconds, and this set of data are therefore amenable to plotting according to Eq. IV-11. This equation is best followed experimentally by plotting C (in percent) on normal probability paper. A straight line should result; this is indeed the case with the data in this study (up to 400 sec) as shown in Fig. IV-1A. In this figure the right ordinate is transformed from percentage to normal standard deviate (C_n). The slope of a C_n versus x plot has been shown by Hogg et al. (1966) to be

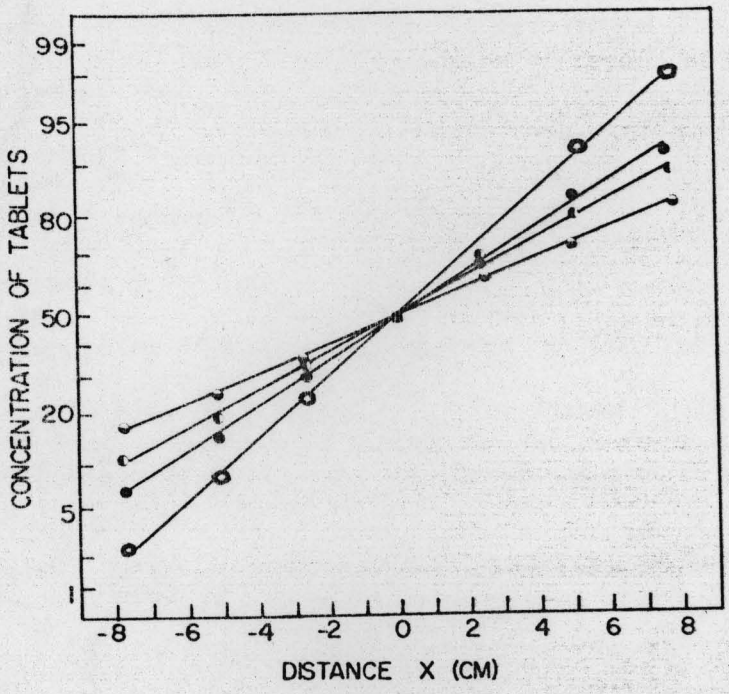

Fig. IV-1A Blending of Tablets in a Horizontal Blender. Results Plotted According to Eq. IV-11. ○ 50 sec.; ◍ 100 sec; ◑ 150 sec; and ◒ 200 sec.

$$\text{Slope}(C_n \text{ vs. } \underline{x}) = 1/\sqrt{2Dt} \qquad \text{(Eq. IV-13)}$$

The D-values obtained in this fashion are denoted D_x and are shown in Table IV-1.

There are in each experimental point (curve) 9 assays. The mean and standard deviation of these can be calculated and the calculated variance should (according to Hogg et al.,1966) adhere to Eq. IV-12. If the variance (of a 1:1 mixture) is plotted versus the reciprocal of the square root of time, then a straight line should ensue with slope and intercept values given by:

$$\text{Slope}(\sigma^2 \text{ versus} \sqrt{t}) = -\sqrt{(2D/\pi)}/L \qquad \text{(Eq. IV-14)}$$

$$\text{Intercept} = x(1-x) \qquad \text{(Eq. IV-15)}$$

The latter point dictates an intercept of 0.25 for a 1:1 mixture. Fig. IV-2 shows a plot of σ^2 versus $\sqrt{t}$. The linearity is good (correlation coefficient of 0.996) and the least squares fit is

$$\sigma^2 = -0.0113\sqrt{t} + 0.252 \qquad \text{(Eq. IV-16)}$$

The 95% confidence limits on the intercept is 0.249-0.255, and hence the value is in good agreement with theory. The diffusion coefficient calculated from Eq. IV-14 (denoted D_t in Table IV-1) is of the same order of magnitude as those calculated from Eq. IV-13.

For longer periods of mixing the concentration versus distance profile for a particular time point will be described by Eq. IV-6. A plot of concentration versus $\cos(\pi x/L)$ should be linear with an intercept of 0.5 (50% of yellow) and a slope of:

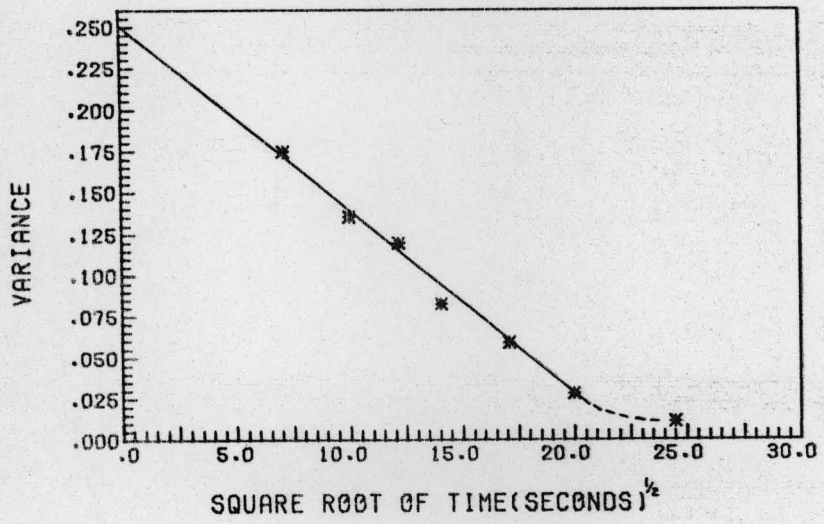

Fig. IV-2. Blending of Tablets in a Horizontal Blender. The Results are Plotted According to Eq. IV-12

Table IV-1

Diffusion Coefficients of Tablets Calculated from Eq. IV-13

Time (Sec)	Slope (cm^{-1})	Diffusion Coefficient (cm^2/sec)
50	0.26	0.14
100	0.20	0.13
150	0.17	0.12
200	0.13	0.14
	Average	0.13± 0.01

$$\text{Slope (C versus } \cos\{\pi x/L\}) = -(2/\pi)\exp(-\pi^2 Dt/L^2) \quad \text{(Eq. IV-17)}$$

As seen in Fig. IV-3, longer time value data plotted in this fashion are indeed linear. For instance the results at 600 sec give a least squares fit (correlation coefficient of 0.993) of:

$$C = 0.504 - 0.137 \cos(\pi x/L) \quad \text{(Eq. IV-18)}$$

The theoretical intercept value (0.5) is bracketed by the 95% confidence limits in Eq. IV-18 (0.496 - 0.512), and hence the data confirm both theory and soundness of experimental design. The diffusion coefficients obtained from Eq. IV-17 are of the same order of magnitude as D_x and D_t, and are listed in Table IV-1.

Finally for long mixing times (when $Dt/L^2 > 0.1$) a plot of $\ln\sigma^2$ versus t should give a straight line (Eq. IV-10) with slopes and intercepts given by:

$$\text{Slope}(\ln\{\sigma^2\} \text{ versus } t) = -2\pi^2 D/L^2 \quad \text{(Eq. IV-19)}$$

and $$\text{Intercept} = \ln(2/\pi^2) = -1.595 \quad \text{(Eq. IV-20)}$$

Data plotted in this fashion are shown in Fig. IV-4; the linearity is good (correlation coefficient of 0.996) and the least squares fit equation is

$$\ln\sigma^2 = -0.0046 \cdot t - 1.54 \quad \text{(Eq. IV-21)}$$

The value of the intercept is 1.52-1.56 with 95% confidence and hence does not differ greatly from the theoretical value given in Eq.

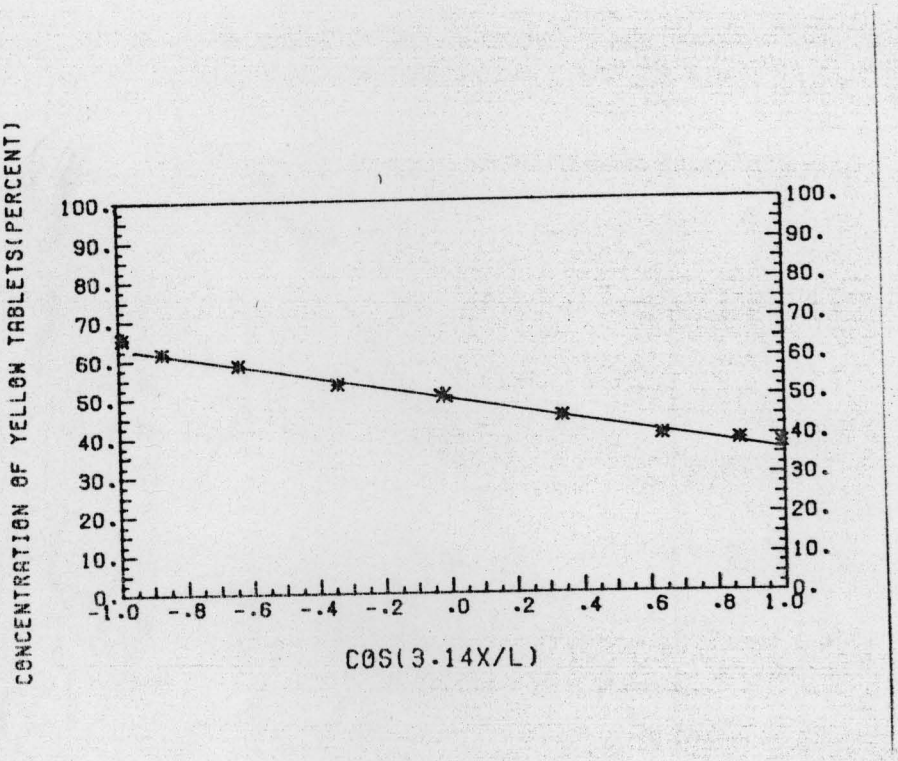

Fig. IV-3 Blending of Tablets in a Horizontal Blender. Results are Plotted According to Eq. IV-18.

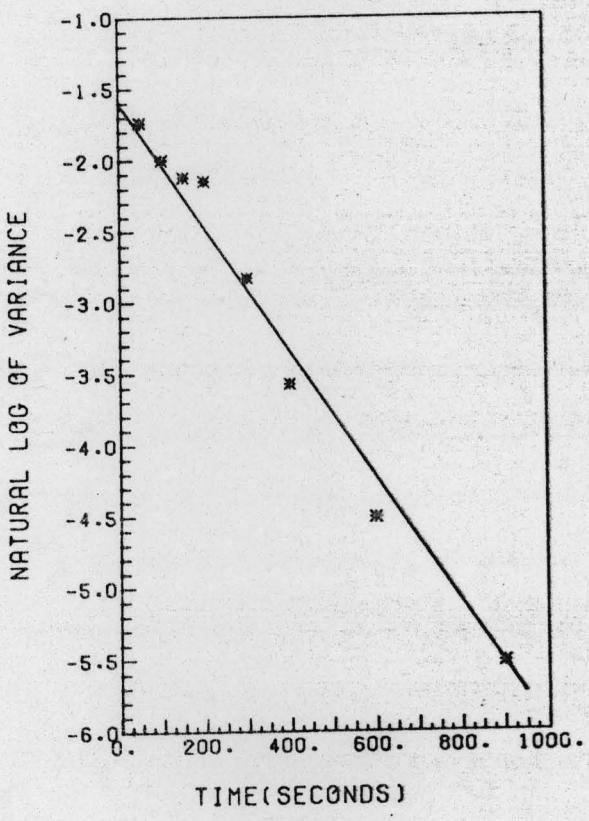

Fig. IV-4. Blending of Tablets in a Horizontal Blender. Results Plotted According to Eq. IV-10 (Eq. IV-21)

IV-20. The diffusion coefficients D_L obtained from the slopes of these plots are listed in Table IV-1, and are of the same order of magnitude as the other D-values. The examples given in the test above, for instance give:

$D_x = 0.13\ cm^2/sec$ (C_n versus x)

$D_t = 0.11\ cm^2/sec$ (σ^2 versus $\sqrt{t}$)

$D_c = 0.14\ cm^2/sec$ (C versus $\cos\{\pi x/L\}$)

$D_L = 0.12\ cm^2/sec.$ ($\ln\sigma^2$ versus t)

From the above it may therefore be concluded that (a) the theoretical diffusion equations apply to off spherical particles that are smooth and (b) the experimental design (horizontal cylinder mixer) gives results in accordance with those of other investigators. Any deviation from such patterns in the results to follow can therefore not be attributed to experimental equipment or design.

IV-3 Mixing of Monodisperse Granulations - Effect of Particle Size on Mixing Rate.

In the earlier section it was shown that the theoretical diffusion equations apply to off-spherical particles that are smooth. The purpose of the study reported in this section was to explore systems of non-spherical geometry with surface roughness. A pharmaceutical granulation was chosed as a model system. This, of course, is a relevant and practical point, since granulations of the type chosen are used extensively in the manufacture of tablets. These are usually obtained by compressing granules, and since these frequently are mixtures of granules (or powders) the dosage form uniformity depends on the degree of mixing. These granulations are usually polydisperse, but to study the problem with the least number of variables at first, mixing of white and yellow granulations each consisting of a narrow mesh fraction was studied initially. The results of mixing of yellow and white granulation (10/14 mesh) are shown in Table III-3-2. The results for sufficiently small time values could not be obtained because of sampling and analytical limitations. For longer times the concentration versus distance profile for a particular time point will be described by Eq. IV-6. A plot of concentration versus $\cos(\pi x/L)$ should be linear with an intercept of 0.5 (50% yellow) and a slope given by Eq. IV-17.

As seen in Table IV-3-1, longer time value data treated according to Eq. IV-6 for each time point value shows that observed intercept values are close to 50 percent and diffusion coefficients calculated at each time point using the slope value and Eq. IV-17 are all of the same order of magnitude. Examplewise the mean and standard deviation of diffusion coefficients for eight time point values are 1.1 cm^2/min and 0.03 cm^2/min. In similar fashion the results for 14/20 mesh, 20/30 mesh, 30/40 mesh and 40/60 mesh fractions show that for all these mesh size fractions (Table IV -3-2 to 5), mixing is described by diffusional mixing, i.e. by Eq. IV-6. Furthermore for long mixing times a plot of $\ln\sigma^2$ versus t should give a straight line according to Eq. IV-10, for all these experiments (regardless of particle size). Data plotted in this fashion are shown in Fig. III-3-1 to III-3-5. A summary of the results regarding slope, intercept value and correlation coefficients are shown in Table IV-3-6. The results in Table IV-3-6 indicate that for monodisperse granulation particles with rough surface and off spherical shape, diffusional mixing applies. An interesting point to note from Table IV-3-6 is that with decreasing particle size of granulation, the mixing rate is also decreased. A plot of mixing rate constants (min^{-1}) versus mean diameter (cm) is shown in Fig. IV-5. The explanation to this is probably to be found in the findings by Carstensen and Chan (1976) that for larger particles flow and packings are governed by packing geometries, but that cohesion starts affecting flow at lower particle sizes.

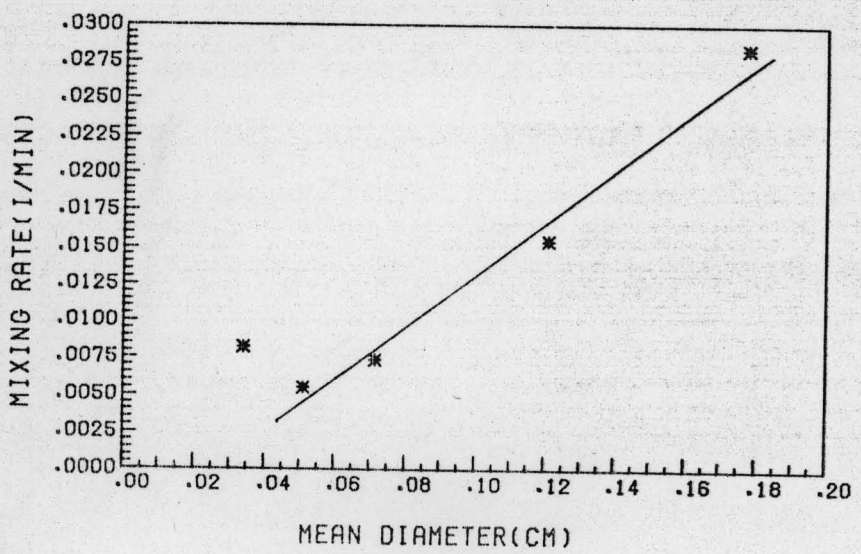

Fig. IV-5 Mixing Rate Versus Mean Diameter of Granulation Mixed in a Horizontal, Rotating Cylinder in 50:50 Ratio.

Table IV-3-1

Values of Diffusion Coefficient Calculated at Each Time Point for Mixing of 10/14 Mesh Yellow and White Granulation in a Rotating Cylinder. Data From Table III-3-2.

Time (Min)	Slope*	Intercept	Diffusion Coefficient (cm^2/min)
6.7	56.1	48.9	1.0
13.3	42.7	49.4	1.6
26.7	29.9	50.4	1.5
40.0	27.9	49.6	1.1
58.3	27.4	49.2	0.85
90.0	14.3	48.8	0.90
106.7	12.1	49.8	0.84
130.0	7.7	49.7	0.9
		Average	1.1 ± 0.03

*Slope and Intercept Values Refer to the Plot of Percent Yellow Granulation Versus cos[πx/L]

Table IV-3-2

Values of Diffusion Coefficient Calculated at Each Time Point for Mixing of 14/20 Mesh Yellow and White Granulations in a Rotating Cylinder. Data are from Table III-3-3

Time (Min)	Slope*	Intercept*	Diffusion Coefficient (cm^2/min)
33.3	47.1	50.3	0.49
66.7	37.0	49.8	0.44
100.0	27.3	49.5	0.45
133.3	20.8	48.7	0.45
166.7	19.4	48.5	0.38
200.0	13.1	49.7	0.42
		Average	0.44 ± 0.04

*Slope and Intercept Values refer to the Plot of Percent Yellow Granulation Versus cos[πx/L]

Table IV-3-3

Values of Diffusion Coefficient Calculated at Each Time Point for Mixing of 20/30 Mesh Yellow and White Granulation in a Rotating Cylinder. Data are from Table III-3-4.

Time (Min)	Slope*	Intercept*	Diffusion Coefficient (cm^2/min)
25.0	55.7	50.0	0.29
50.0	44.9	49.1	0.37
83.3	41.2	49.7	0.28
133.3	34.8	50.0	0.24
183.3	30.5	50.6	0.22
233.3	26.3	48.6	0.20
285.0	24.0	49.0	0.19
333.3	13.1	50.8	0.25

Average: 0.25 ± 0.06

*Slope and intercept values refer to the plot of percent yellow granulation versus $\cos[\pi x/L]$

Table IV-3-4

Values of Diffusion Coefficients Calculated at Each Time Point for Mixing of 30/40 Mesh Yellow and White Granulation in a Rotating Cylinder. Data are From Table III-3-5.

Time(Min)	Slope*	Intercept*	Diffusion Coefficient (cm^2/min).
50.0	55.1	50.4	0.16
100.0	48.9	50.2	0.14
166.7	41.7	49.8	0.14
250.0	34.4	50.1	0.13
333.3	28.3	50.4	0.13
416.7	23.8	50.7	0.13
500.0	16.8	52.1	0.14
593.3	10.4	51.2	0.16
		Average:	0.14 ± 0.01

*Slope and intercept values refer to the plot of percent yellow granulation versus $\cos[\pi x/L]$

Table IV-3-5

Values of Diffusion Coefficients Calculated at Each Time Point for Mixing of 40/60 Mesh Yellow and White Granulation in a Rotating Cylinder. Data are from Table III-3-6.

Time (Min)	Slope*	Intercept*	Diffusion Coefficient(cm^2/min)
66.7	45.6	48.7	0.27
133.3	42.3	53.9	0.17
218.7	31.9	49.8	0.17
300.0	22.1	45.4	0.19
400.0	13.4	51.3	0.21
500.0	8.1	53.2	0.22
		Average	0.21 ± 0.04

*Slope and intercept values refer to the plot of percent yellow granulation versus cos[πx/L]

Table IV-3-6

Parameters From the Mixing Rate Equations as a Function of Particle Size in Rotating Cylinder Mixing. Ratio of White to Yellow Granulation is 50:50.

	Mesh Size of the Granulations				
	10/14	14/20	20/30	30/40	40/60
Slope (min^{-1})*	-0.028	-0.016	-0.0074	-0.0055	-0.0082
Intercept*	-1.84	-1.53	-1.59	-1.36	-1.24
Mean Diameter (cm)	0.178	0.121	0.072	0.051	0.017
Correlation Coefficient	-0.984	-0.997	-0.960	-0.992	-0.984

*Slope and intercept values refer to the plot of $\ln\sigma^2$ versus time

IV-4 Mixing of Monodisperse Granulations - Effect of Composition of Yellow and White Granulation on Mixing Rate.

In a practical situation of mixing it is important to arrive at a general theory of mixing which applies to all possible combinations of initial compositions in a system where two or more components are considered for blending. For diffusional mixing of solids, Fisher (1963) and Hogg et al. (1968) considered only one case where one component was present in trace quantities. For axial loading geometry and by making an assumption that the trace component occupies no volume, the solution to Fick's first law was obtained to be (Crank, 1956):

$$C = \bar{C}_f L/(\sqrt{\pi Dt}) \cdot \exp\{-x^2/(4Dt)\} \qquad \text{(Eq. IV-22)}$$

for early stages of mixing only. Hogg et al. (1968) plotted the natural logarithm of concentration versus distance squared to check the validity of the theory and found it to be satisfactory. However, experimental proof of the diffusional mixing theory where different initial combinations of amount are considered, has not been reported in literature. If one considers the mixing theory of Lacey (1954) as expressed in Eq. IV-9, one can see that this theory can be applied to the mixing of two components having varying amounts of initial compositions. In this equation (and in Eq. IV-22) $\bar{C}_f$ is the average bulk concentration of the colored particles. The important fact to remember is that Eq. 9 applies to time values which are sufficiently large so that the transients have decayed, i.e. the condition

$$Dt/L^2 > 0.1 \qquad \text{(Eq. IV-23)}$$

applies. Considering this constraint, the limiting factors are the length of the cylinder and the magnitude of the diffusion coefficent. The horizontal rotating cylinder designed in the present study had a diameter to length ratio of 0.35 compared to the cylinder designed by Hogg et al. (1968) which had a ratio of 0.25. As described in Section III-3-2, experiments using 14/20 mesh yellow and white granulations of equal proportions were carried out. In this study three more combinations of initial compositions of yellow and white granulations (60:40, 70:30 and 80:20 ratios) were considered. The results from these experiments, if they follow diffusional mixing, should adhere to Eq. IV-6 for large values of t. Results of experiments with 60 percent yellow and 40 percent white 14/20 mesh granulation treated according to Eq. IV-6 are shown in Table IV-4-1. It is seen that all the intercept values are close to 60 percent and the diffusion coefficients calculated at each time point are of the same order of magnitude. The average diffusion coefficient and the normal error of the mean for the five time points were 0.45 cm^2/min and 0.03 cm^2/min. Similar results were obtained for the experiments carried out using 70:30 and 80:20 ratios of 14/20 mesh yellow and white granulations, and the results are shown in Tables IV-4-2 and IV-4-3.

If the results are treated according to Eq. IV-9, then for a plot of $\ln\sigma^2$ versus time, the theoretical intercept value will be:

$$\text{Intercept } (\ln\sigma^2 \text{ versus } t) = \ln(2/\pi^2) + \ln[\sin C_f\pi] \qquad \text{(Eq. IV-24)}$$

Table IV-4-1

Values of Diffusion Coefficients Calculated at Each Time Point for Mixing of 14/20 Mesh Yellow and White Granulations in 60:40 Ratio in a Rotating Cylinder. Data are From Table III-3-7

Time (Min)	Slope*	Intercept*	Diffusion Coefficient (cm^2/min)
25.0	48.9	58.7	0.46
60.0	37.4	59.8	0.43
108.3	24.7	59.9	0.44
195.0	12.7	60.1	0.43
266.7	8.4	59.5	0.51
		Average:	0.45 ± 0.03

*Slope and intercept values refer to the plot of percent yellow granulation versus $\cos[\pi x/L]$

Table IV-4-2

Values of Diffusion Coefficient Calculated at Each Time Point for Mixing of 14/20 Mesh Yellow and White Granulations in 70:30 Ratio in a Rotating Cylinder (Data are from Table III-3-8)

Time (min)	Slope*	Intercept*	Diffusion Coefficient (cm^2/min)
25.0	41.6	68.8	0.46
50.0	33.4	68.1	0.47
165.0	13.1	69.5	0.46
221.7	8.4	68.8	0.44
316.7	5.5	69.4	0.38
		Average	0.44 ± 0.04

*Slope and intercept values refer to the plot of percent yellow granulation versus $\cos\pi x/L$

Table IV-4-3

Values of Diffusion Coefficient Calculated at Each Time Point for Mixing of 14/20 Mesh Yellow and White Granulation in a 80:20 Ratio in a Rotating Cylinder. Data are from Table III-3-9

Time (Min)	Slope*	Intercept*	Diffusion Coefficient (cm^2/min)
25.0	30.3	79.3	0.46
58.3	22.2	80.2	0.48
116.7	13.7	80.1	0.46
206.7	6.7	79.9	0.45
293.3	2.9	77.1	0.47
		Average	0.47 ± 0.01

*Slope and intercept values refer to the plot of percent yellow granulation versus cos[πx/L]

and the slope will be:

$$\text{Slope}(\ln\sigma^2 \text{ versus } t) = -2\pi^2 D/L^2 \qquad \text{(Eq. IV-25)}$$

Data plotted in this fashion are shown in Fig. III-3-2 the least squares fit parameters for slope, intercept and correlation coefficient are listed in Table IV-4-4. One can see that there is a fairly good fit fore this particular model. The theoretical intercept values are also close to the observed intercept values for all the cases with different initial composition of yellow and white granulations.

One more important point in this study was that the mixing rates for all different compositions (Table IV-4-4) are independent of composition as expected from Eq. IV-24. The calculated diffusion coefficients for the experiments carried out with tablets and granulations are summarized in Table IV-4-5. The conclusions from these results are that the diffusion coefficient is independent of composition for mixing of monodisperse granulations which are off-spherical and have rough surfaces.

Table IV-4-4

Parameters from Mixing Rate Equations of 14/20 Mesh Yellow and White Granulations with Different Initial Compositions. Axial Loading in Half Filled Rotating Cylinder.

Percent Yellow	50.0	60.0	70.0	80.0
Percent White	50.0	40.0	30.0	20.0
Slope (min^{-1})	-0.016	-0.016	-0.017	-0.017
Intercept	-1.53	-1.59	-1.83	-2.51
Predicted Intercept	-1.6	-1.7	-2.0	-2.7
Correlation Coefficient	-0.997	-0.996	-0.999	-0.997

Table IV-4-5

Diffusion Coefficients of Granulations of Different Size in a Rotating Cylinder.

Mesh Size	Percent Yellow Granulation	Diffusion Coefficients (cm^2/min)	
		From $\ln\sigma^2$ Versus Time	From Concentration Versus $\cos[\pi x/L]$
Tablets	50	7.4	6.6
10/14	50	0.76	1.1
14/20	50	0.43	0.44
14/20	60	0.43	0.45
14/20	70	0.46	0.44
14/20	80	0.46	0.47
20/30	50	0.20	0.25
30/40	50	0.15	0.14
40/60	50	0.22	0.21

IV-5 Mixing of Granulations with Different Particle Size in a Horizontal Rotating Cylinder.

Mixing of two components having different particle size has been the subject of study by some investigators in the past. Coulson et al. (1948) studied the mixing of coal and salt with different particle sizes in an inclined rotating cylinder. They found that if fine particles (salt) were placed at the bottom of the drum and coarse particles of material (coal) on the top, no mixing occurred. When the position of the sizes was reversed, the larger being on the bottom, then mixing did occur for a short time, but segregation developed as the coarse particles rose to the top of the bed. The reason for this difficulty of producing or maintaining a mix with particles of different sizes was attributed to small particles being able to fall through the void spaces between the large ones. Rippie et al. (1964,1967), Faiman et al. (1965), and Olsen et al. (1964) studied vibration induced segregation of steel, glass and copper spheres, of different sizes. Their approaches were more directed towards segregation kinetics than mixing kinetics. In their studies they observed an increase in the standard deviation of a "perfect" mixture to an equilibrium mixture due to vibration induced segregation. More recently, Bridgwater et al. (1969, 1971) and Masliyah et al. (1974) studied percolation (segregation) of small particles through beds of large particles where the ratio of small to large diameters always was less than 0.25.

In this part of the study reported here, mixing of granulations were carried out in a rotating cylinder mixer, where the particle

sizes of yellow to white granulations were of a wide range of ratios. Table III-2-1 details the experimental conditions used. Half of the load was a 20/30 mesh yellow granulation, and the other component, the white granulation, was used in a systematically varied particle size (mesh fraction). The coarsest white granulation was 6/10 mesh and the finest 60/80 mesh. This then allows a study of the effect of particle size on mixing kinetics and equilibrium variance.

It has been shown previously that mixing of granulations with identical particle sizes (of the two components) follows diffusion mixing theory. This does not seem to hold true for the case where mixing of two different particle sizes is carried out. It is surprising to note that for mixing of 20/30 mesh yellow and 30/40 mesh white granulations (i.e. components with a diameter ratio of 0.71) where the difference in particle size is obviously rather small, the diffusional equations do not hold. In the mixing of two different particle size components, the segregation of small particles into the mixing plane plays an important role. As mentioned earlier, in the rotating cylinder mixer with axial loading, mixing occurs primarily because of axial migration of particles in the mixing plane (or free surface). The behavior of these two particle sizes at the free surface is such that larger particles dominate the free surface and hinders the movement of the smaller particles (when the diameter ratio is reasonably high). However, it should be noted that axial movement of particles is not only due to migration from free surface but also due to migration in the cascading layer which is approximately a few layers thick. The movement here will be governed by the packing geometry

of the particles. For the case of cubic packing of a small particle between four larger particles touching in a square grid, as shown in Fig. IV-6, the ratio of small to large diameter is 0.41. Similarly for hexagonal packing (Fig. IV-6), where small particles can slip between three larger particles touching in a triangular grid, the ratio of small to large diameter is 0.15. The ratio of 0.71 for 30/40 mesh diameter to 20/30 mesh diameter is much too large for migration of particles due to percolation. The concentration versus time profile at 88.3 minutes and 833.3 minutes (Fig. IV-7) shows that there is very little migration of 20/30 mesh particles even after such a long time of mixing and this also is reflected in the results shown in Table III-3-14 and Fig. III-3-14, where the variance of the powder mixture does not change and has reached (a high) equilibrium value very rapidly. The theoretical random variance and the observed equilibrium variances will be compared at a later point. Similarly for the mixing of another set of two particle sizes (14/20 and 20/30, i.e. a diameter ratio of 0.59) gives a similar kinetic picture (Table III-3-13 and Fig. III-3-13). For convenience the ratio of small to large diameter (d/D) for the various mesh cuts used is shwon in Table IV-5-1.

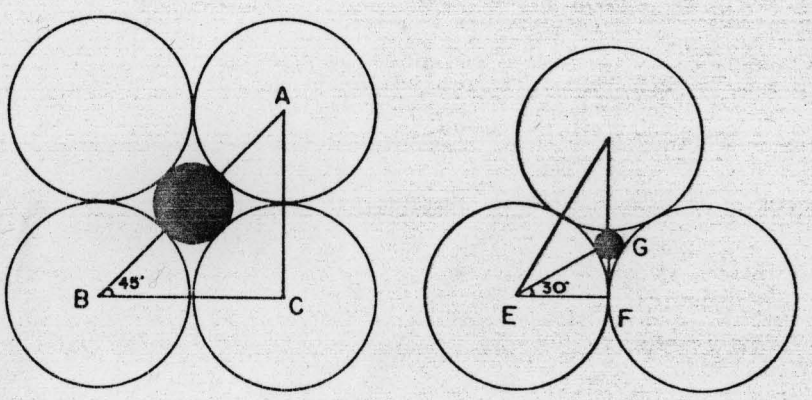

Fig. IV-6 Cubic and Hexagonal Packing Arrangement of Particles.

For Cubic Packing, AB = D + d, BC = D and Angle ABC = 45°.

Using the Relationship that $\cos 45^{\circ} = F/(D+d)$, $d/D = 0.41$.

Similarly for Hexagonal Packing, GE = $\frac{1}{2}(D+d)$ and EF = $D/2$.

$\cos 30^{\circ} = (D/2)/(\frac{1}{2}(D+d))$ and therefore $d/D = 0.15$.

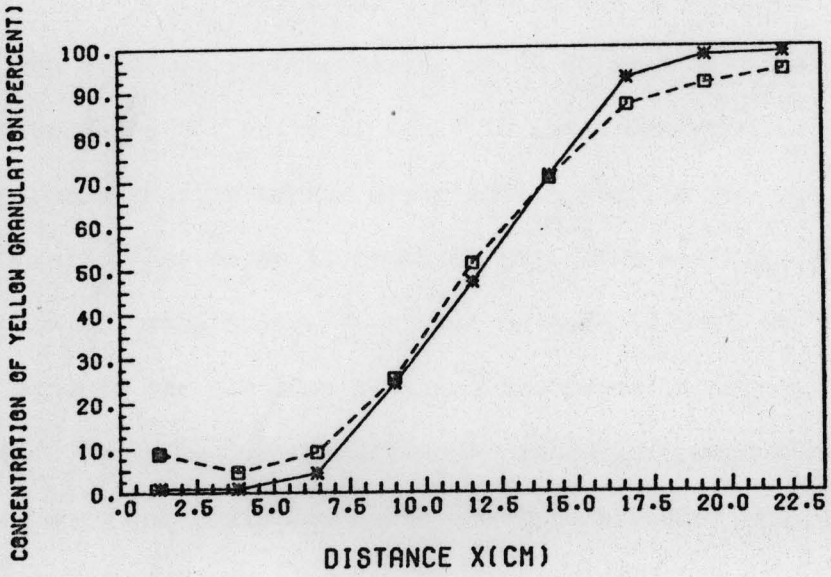

Fig. IV-7 Concentration Profile of Mixing of 20/30 Mesh Yellow and 30/40 Mesh White Granulation in 50:50 Ratio after 88.3 Minutes (✳) and 833 Minutes (⊡).

For the mixing of 20/30 with 6/10 mesh granulations it is seen (Fig. IV-8) that there is some mixing due to percolation. The diameter ratio (0.26) is, however, still such that there is a segregation effect, and therefore an equilibrium is reached between mixing and demixing (Table III-3-11) after a short period of mixing. Similar effects are observed for the mixing of 20/30 mesh with 40/60 mesh granulation where the ratio of small to large diameter is 0.30.

The concentration versus distribution profile for the last time point for all these cases is shown in Fig. IV-9 and Fig. IV-10 for the purpose of comparison. One point to note is that in Fig. IV-8 one can observe the tendency of large particles to segregate at the wall. This could be due to different reflection properties at the wall for large particles when they are in a mixture; this possibility has been raised earlier by Weidenbaum et al. (1955)

The ratio of 0.71 for 30/40 mesh diameter to 20/30 mesh diameter is much too large for migration of particles due to percolation. The concentration versus time profile at 88.3 minutes and 833.3 minutes in Fig. IV-7 shows that there is very little migration of 20/30 mesh particles even after such a long time of mixing and this also reflected in the fact apparent from Table III-3-14 and Fig. III-3-14 that the variance of the powder mixture does not change (i.e. equilibrium has been reached) very rapidly. The theoretical random variance and the observed equilibrium variances will be compared at a later point.

Findings similar to the above was made for the mixing of 20/30 with 14/20 and for 20/30 with 30/40 mesh size granulations.

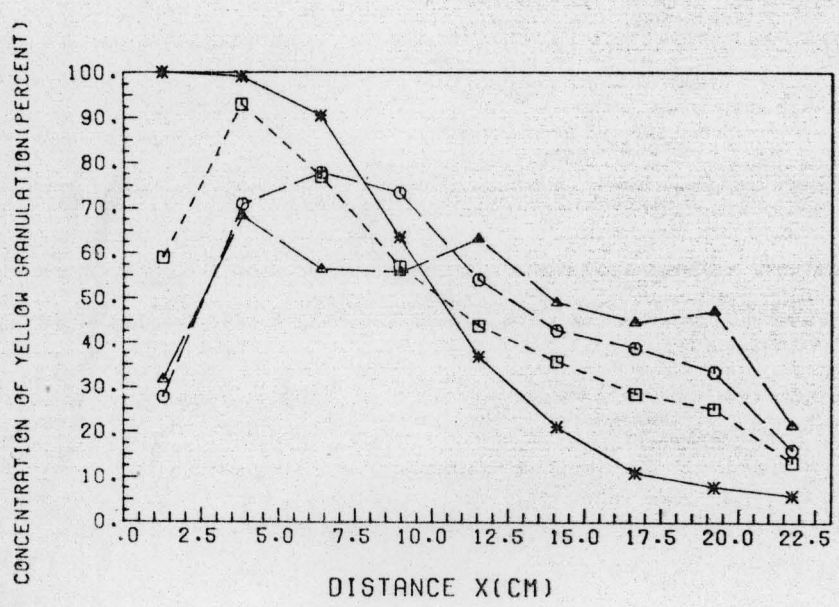

Fig. IV-8. Concentration versus Distance Profiles for Mixing of 6/10 versus 20/30 Mesh Granulation in a Rotating Cylinder at Different Time Periods. (✳) 8.3 min, (⊡) 41.7 min, (⊙) 100 min and (△) 233.3 min.

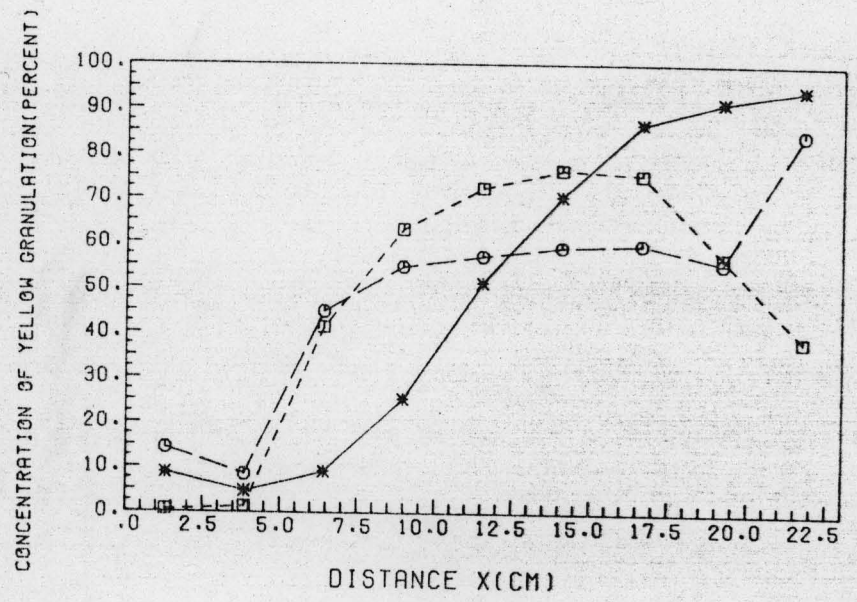

Fig. IV-9. Concentration versus Distance Profile at the End Point for Mixing of 20/30 Mesh Granulation with Various Mesh Fractions. (✳) 20/30 with 30/40 Mesh for 13.9 Hours. (⊡) 20/30 with 40/60 Mesh for 13.9 Hours. (⊙) 20/30 with 60/80 Mesh for 13.9 Hours.

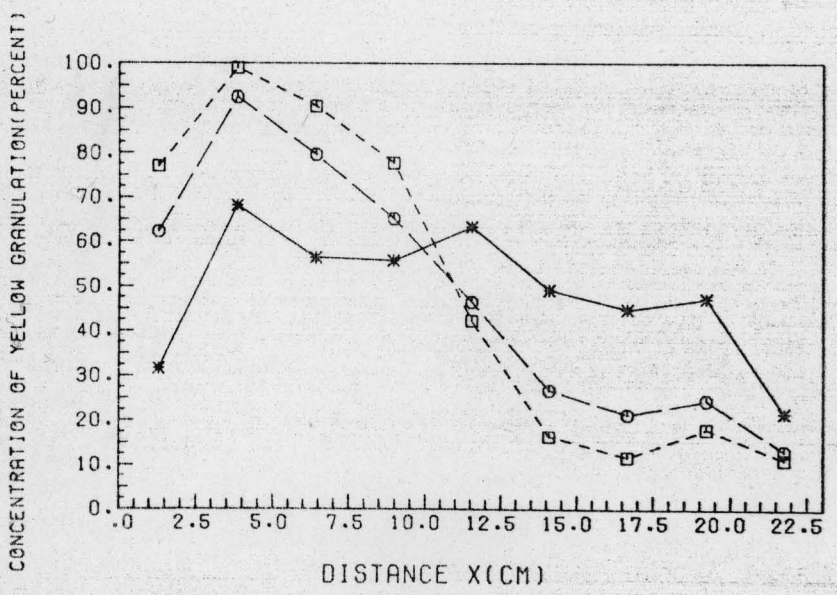

Fig. IV-10. Concentration versus Distance Profile at the End Point for Mixing of 20/30 Mesh Yellow Granulation with Various Mesh Fractions. (✳) 20/30 with 6/10 Mesh for 3.9 Hours (⊙) 20/30 with 10/14 Mesh for 8.9 Hours and (⊡) 20/30 with 14/20 Mesh for 13.9 Hours.

Table IV-5-1

Ratio of Small to Large Diameter for Mesh Sizes Indicated	d/D	Table	Fig.
$d_{20/30}/D_{6/10}$	0.26	III-3-11	III-3-11
$d_{20/30}/D_{10/14}$	0.40	III-3-12	III-3-12
$d_{20/30}/D_{14/20}$	0.59	III-3-13	III-3-13
$d_{20/30}/D_{20/30}$	1.0		
$d_{30/40}/D_{20/30}$	0.71	III-3-14	III-3-14
$d_{40/60}/D_{20/30}$	0.47	III-3-15	III-3-15
$d_{60/80}/D_{20/30}$	0.30		

There is some improvement for the case where mixing of 20/30 mesh is carried out with 10/14 mesh, i.e. in a case where the diameter ratio is 0.4.

The final equilibrium variance for the mixing of granulations of different particle sizes also reflects its dependence on interstitial geometry of the coarse fraction. When a granulation flows it will be loosely packed and assume an approximately cubic packing. The ratio of (a) the natural log of the experimentally determined variance at equilibrium to (b) the natural logarithm of the theoretical value of the variance of a random mixture was plotted versus the diameter ratio of the mesh fraction of the white granulation to the diameter of the 20/30 mesh yellow granulation. This plot is shown in Fig. IV-11. The figure indicates that (a) the mixing is efficient when the particle sizes of the two fraction are equal (i.e. when the ratio is 1.0), (b) that otherwise mixing is poor for diameter ratios between 0.4 and 2.5 and (c) that for ratios outside this range the mixing is better because of the ability of the smaller size granules to percolate.

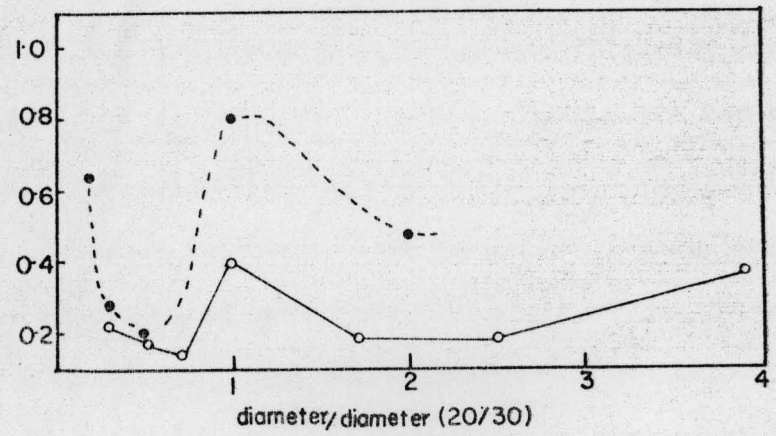

Fig. IV-11 Ratio of Natural Logarithm of Variance in an Equilibrium Mixture to the Natural Logarithm of the Theoretical Variance of a Random Mixture as a Function of Diameter Ratio. (●) V-Blender. (o) Horizontal Mixer.

IV-6 Mixing of Granulation in a V-Blender

The mathematical theories of the rate of mixing of solids at their present stage of development are applicable only to ideal systems. Since real systems differ from this ideal case, it is important to isolate and describe the principal mechanisms of mixing and to assess the contribution of each mechanism in any given mixing operation. The V-Blender or twin blender is widely used for mixing in the pharmaceutical industry. In this blender the bed of particles is split and redeposited during each cycle which leads to rapid mixing. This type of mixing is referred to as convective mixing because it involves movement of groups of particles from one position to another. For a high degree of mixedness, individual particles must diffuse across boundaries between regions rich in one component into regions rich in another. The purpose of this part of the study was to investigate the mechanism of mixing of granulations in the V-blender and to attempt to establish the relative contributions of convective and diffusional effects in the mixing process. As was seen in the case of mixing of equally sized granulations, diffusional mixing was followed when the geometry of the blender was symmetrical (e.g. cylindrical) and when the material was loaded side by side.

In earlier studies carried out by Carley-McCauly et al. (1962) sand was loaded side by side in a double cone blender and the mixing kinetics were interpreted via a diffusional mechanism (Eq. IV-10) because plots of the natural logarithm of the variance versus time were

linear. Their conclusion seems to be correct. The shape of a double cone blender is fairly symmetrical and for a side by side loading geometry for a two component system, mixing will be analogous to mixing in a horizontal rotating cylinder.

Initial studies using a V-blender were carried out by Yano et al. (1956). Their purpose was to study the effect of the following parameters in a V-blender: (a) rotational speed of the blender,(b) the charged volume, (c) the volume ratio of feed, and (c) the method of charging. Their system was sodium carbonate with polyvinyl chloride. Wiedenbaum et al. (1963) using equisized salt and sand studied the effect of sample size and the nature of the movement of the material in the blender when equal proportions and side by side loading was used. As shown in Fig. IV-12, exploratory work indicated that mixing starts at the center of the blender at the interface of the two components and spreads out symmetrically towards the sides and top. No further conclusions were drawn as far as kinetics of mixing was concerned. At a later point Cahn et al. (1965) analyzed the effect of blender geometry on mixing kinetics. They constructed various types of V-blenders where the two arms could be set at a variable number of degrees from one another so that the axis of one arm was not in the plane of the axis of the other arm and the axis of rotation. In a conventional V-blender all these three axes are in the same plane. The two extreme cases of this would be a conventional V-blender with zero degree angle and an inclined barrel mixer for 180°. In their study the standard deviation was plotted versus the natural logarithm of the number of revolutions. The analysis of the results showed that with increasing angle between two arms the amount of material transferred at each revolution is increased.

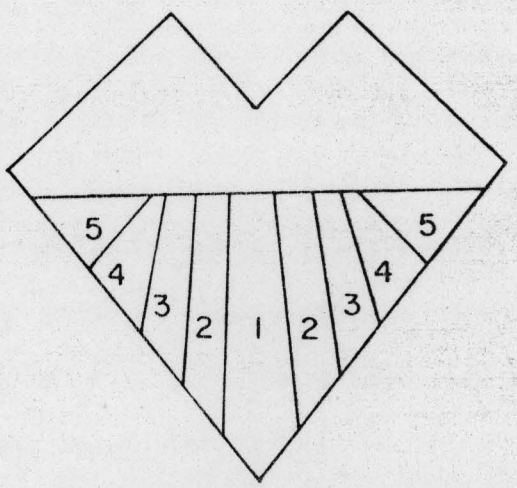

MIXING ZONES IN V-BLENDER

Fig. IV-12 Symmetrical Distribution of Material and Mixing Zones Showing How the Possible Mixing Proceeds from Zone 1 to Zone 5 with Time.

For a 0° angle little transfer occurs and for 180° all of the material is transferred between the arms each half cycle.

To analyze a situation of this kind for a conventional V-blender, a theoretical equation describing transfer of material between two arms has been derived here. Initial loading is assumed to be side by side loading of equal proportions of two components having properties that are identical except for a detectable property such as e.g. dye content. Prior to mixing all the colored material is kept in one arm and the other arm is filled with colorless material. In the mathematical derivation the assumption is made that equal fractions of the load of each arm is cross-transferred during every revolution.

At time zero or prior to mixing all the amount in the left arm is colored granulation, i.e. A = 100% yellow, and all the white granulation is in the right arm. The difference of concentration of yellow granulation between the right and left arm is denoted Δ. For simplicity, concentration is used in the derivation here, rather than amount. Initially Δ has the value of A percent yellow granulation. After the first revolution, a fraction, β, of yellow granulation from the left arm is transferred to the right arm and a fraction β of white granulation is transferred to the left arm. The constraint used here is that $0 < \beta < 0.5$ which is a reasonable assumption considering the geometry of the V-blender and that, under practical conditions of operation, from 30 to 70% of the capacity of the mixer is used for loading.

After the first revolution the concentration of yellow granulation in the left arm is $(1-\beta)A$ and the concentration of yellow granulation in the right arm is βA. It is noted that there is no change in the volume of material in each arm. The concentration of yellow granulation in each arm is the average concentration, and the difference of concentration

of yellow granulation between the two arms after the first revolution is A(1-2β). A similar argument can be carried out for subsequent revolutions and is shown in Table IV-6-1. The important assumption made here is that for each revolution the fraction of amount transferred, β, is the same and that the distribution of yellow and white granulations in each arm is such that the fraction of colored component transferred is also β. The concentration after N revolutions will hence be given by:

$$\Delta = A\,(1-2\beta)^{N} \qquad \text{(Eq. IV-26)}$$

This may be written:

$$\ln\Delta = \ln A + N \ln(1-2\beta) \qquad \text{(Eq. IV-27)}$$

For the V-blender used in this study the speed is 23 revolutions per minute, and hence N = 23t. When this is inserted in Eq. IV-27 the following relation results:

$$\ln\Delta = \ln A + 23t\ln(1-2\beta) \qquad \text{(Eq. IV-28)}$$

To check the validity of Eq. IV-28 three experiments were carried out using 20/40 mesh yellow and white granulation in the V-blender. The results of these experiments are shown in Tables IV-6-2 through 4 and in Fig. IV-13. The least squares fit equations are shown below each table along with the correlation coefficient and the calculated β-value. The results indicate that Eq. IV-28 is a fairly good model to describe the

Table IV-6-1

Δ-Values After Selected Numbers of Rotations.

Rotation Number	Percent Yellow Granulation in Left Arm	Right Arm	Difference Δ
0	A	0	A
1	$(1-\beta)A$	βA	$A(1-2\beta)^1$
2	$(1-\beta)A+\beta^2A-\beta(1-\beta)A$	$\beta A-\beta^2A+\beta(1-\beta)A$	$A(1-2\beta)^2$
N			$A(1-2\beta)^N$

Table IV-6-2

Mixing of Yellow and White Granulations of 20/40 Mesh in a V-Blender With 2 kg. Load.

Time (Min)	Percent Yellow Concentration* in Left Arm	Right Arm	Δ**	lnΔ
1	79.4	8.5	70.9	4.3
5	60.1	34.8	25.3	3.2
10	51.5	38.5	13.0	2.6
15	48.2	42.6	5.6	1.7
20	46.0	44.0	2.0	0.7

* Concentration of each Arm is Average Concentration

** Δ is Difference of Concentration Between Arms

Least Squares Fit Equation: $\ln\Delta = -0.18t + 4.40$

$\beta = 3.9\ 10^{-3}$

$R^2 = -0.994$

Table IV-6-3

Mixing of Yellow and White Granulation of 20/40 Mesh in a V-Blender with 4 kg. Load

Time (Min)	Percent Yellow Concentration in Left Arm	Right Arm.	Δ	lnΔ
5	85.7	16.0	69.7	4.2
10	80.9	36.3	44.6	3.8
15	70.4	31.9	38.5	3.7
30	61.6	47.5	14.1	2.6
45	56.2	48.6	7.6	2.0

Least Squares Fit Equation: $\ln\Delta = -0.056\ t + 4.43$

$\beta = 1.2\ 10^{-3}$

$R^2 = -0.993$

Table IV-6-4

Mixing of Yellow and White Granulations of 20/40 Mesh, Lubricated with One Percent Magnesium Stearate in a V-Blender at 2 kg. Load.

Time (Min)	Percent Yellow Granulation in Left Arm	Right Arm	Δ	lnΔ
1	84.1	10.1	74.0	4.3
5	65.2	32.6	32.6	3.5
10	56.0	41.4	14.6	2.7
15	51.8	45.3	6.5	1.9
20	48.0	49.1	-1.1	-

Least Squares Fit Equation: $\ln\Delta = -0.17\ t + 4.41$

$\beta = 3.7\ 10^{-3}$

$R^2 = -0.999.$

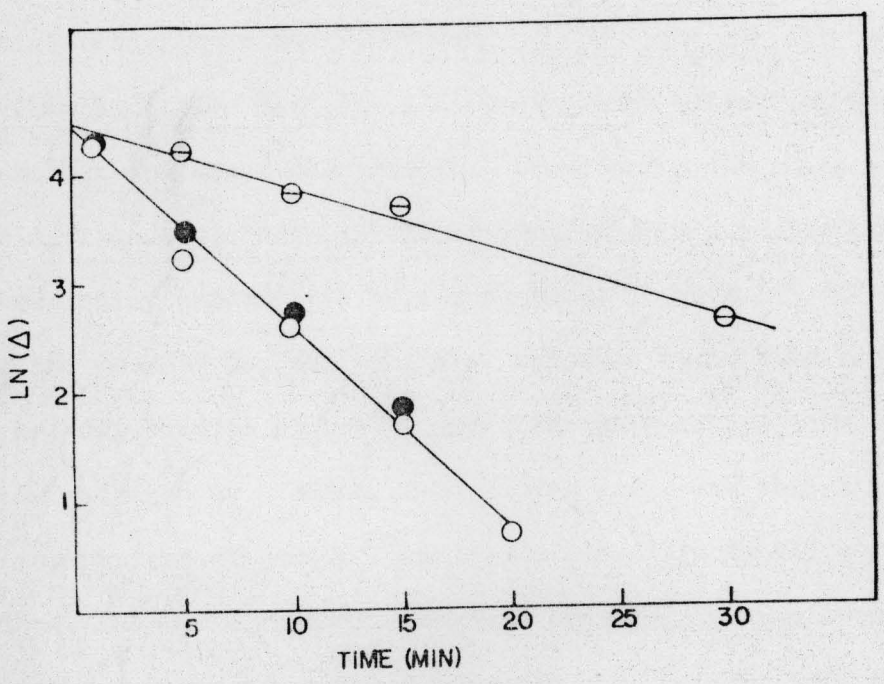

Fig. IV-13 Natural Logarithm of Concentration Difference Between the Two Arms versus Time for Mixing of 20/40 Mesh Yellow and White Granulation. (○) 2 kg. Load, (◍) 2 kg. Load Lubricated with 1 Percent Magnesium Stearate, (⊖) 4 kg. Load.

material transport in a V-blender under previously described conditions. In all three cases the predicted intercept values are close to the theoretical value of 4.6. The fraction of material transported after each revolution is 0.004 for a 2 kg load and decreases to 0.0012 for a 4 kg load which is consistent with the physics of the process of material transfer in the V-blender.

This indicates that for a V-blender both convection and diffusion are responsible for the mixing action. Considering the shape of the V-blender at this stage it is not possible to arrive at a suitable model which can mathematically explain the mixing kinetics in detail. In the present study the results for the rotating cylinder mixer have shown that for side by side loading of yellow and white granulation, the mixing kinetics can be described by a diffusional mixing model and that the mixing rates were independent of composition (ratio of yellow to white granulation). For the V-blender a similar series of experiments were carried out using 20/40 mesh yellow and white granulation with varying granulation contents of 50, 60, 70, 80 and 90 percent. In these experiments the total load was 2 kg. which occupied 24% of the V-blender volume. Two more studies were carred out where, in the first study, granulation was lubricated with 1% magnesium stearate and in the second study the load was doubled to 4 kg. which occupied 48% of the V-blender volume. Results of these experiments are shown in Tables III-2-1 to III-2-5, and in Fig. III-2-1 to III-2-5. To compare the results of the V-blender to the results of the rotating cylinder, the results of these sudies were analyzed using the diffusional mixing model in Eq. IV-10. The analysis of the results is shown in Table IV-6-5, and the results seem to follow the model fairly well. There is a good fit using Eq. IV-10 indicated

Table IV-6-5

Mixing Rates in V-Blender for Different Compositions of 20/40 Mesh Yellow and White Granulations, with Axial Loading and a 2 kg Load. Least Squares Parameters of $\ln\sigma^2$ Versus Time

Percent Yellow* Granulation	50	60	70	80	90	50**	50***
Slope (min^{-1})	-0.32	-0.33	-0.32	-0.35	-0.21	-0.083	-0.38
Intercept	-1.8	-1.89	-2.5	-3.0	-5.6	-1.84	-1.27
Theoretical Intercept	-1.6	-1.7	-2.0	-2.7	-4.0	-1.6	-1.6
Correlation Coefficient	-0.996	-0.998	-0.930	-0.991	-0.96	-0.99	-0.99

* Percent weight basis

** 4 kg initial load

*** 2 kg initial load lubricated with 1% magnesium stearate.

by the correlation coefficients. The experimentally observed intercepts are also close to the theoretically predicted values and, furthermore, the rates of mixing for 2 kg. loads are independent of composition. There seems to be no significant effect of the addition of 1 percent of magnesium stearate on the rate of mixing. The mixing kinetics in the V-blender can, therefore, be explained by the diffusional mixing equation (Eq. IV-10) developed for the horizontal rotating cylinder for long times of mixing. A detailed analysis is not possible, but a reasonable explanation could be that for side by side loading in equal proportions, the V-blender is at first upside down and filled with the yellow and white granulation in the separate arms. The first half revolution will cause material to flow downwards due to gravity. The important point to note is that both yellow and white granulations are now flowing towards the bottom of the V-shape and the direction of materials coming from the arms is approximately at 45^{o} compared to the plane normal to the axis of rotation which divides the V-blender into equal sections. As soon as contact is made at the interface of the plane between the left and right hand sides of the blender, there will be mixing (transfer of material between arms) due to the convective forces acting on the granulations. However, the convective forces acting on the granulations will not be totally dominant because opposing forces are created due to collisions between flow from both the directions. In mixing in a V-blender the blending only takes place in the region neighboring the imaginary plane. In a rotating cylinder mixing or movement of granulation is only in the axial direction and is limited to the cascading layer only. Compared to the rotating cylinder the mixing in the V-blender is not

limited to surface movement but here there will be mixing at the bulk interface bacause the material on both sides of the imaginary plane is flowing due to gravity flow.

After another half of a revolution, the granulation bed which is at the bottom of the cone has been split into two equal halves and transfered into each arm. During this type of motion, mixing in each individual arm will take place because of diffusion of particles within that arm. In a similar fashion for long times of mixing the picture will be somewhat as observed by Weidenbaum (1965); this view is presented pictorially in Fig. IV-12 and shows how mixing proceeds zone-wise.

To further probe the effect of convective forces, an experiment was carried out with equal proportions of yellow and white 20/40 mesh granulations, where a longitudinal loading geometry was used. Ususally the yellow and white granulations are kept separate in each arm which gives sided by side loading. In longitudinal loading the axis of rotation lies in the plane of the interface between yellow and white granulation. The transfer of material between the yellow and white granulation will be in the direction of the flow and mainly due to convection. The results of this experiment (Table III-2-13 and Fig. III-2-13) indicate that mixing is much more rapid than for the case of side by side loading, and that it does not follow a similar mechanism.

Hogg et al. (1972) and Inoue et al. (1970) have studied convective mixing effects in a horizontal rotating cylinder. To show the effect of rapid mixing due to convective forces in a horizontal rotating cylinder in

this study, experiments were carried out using yellow and white granulations of equal proportion. The loading geometry was front to back (longitudinal) so thet there was a concentration gradient in the direction of the flow of the material. This leads to very rapid mixing in the radial direction at the surface of the powder bed because of convection. The results are summarized in Table IV-6-6. The experiments were carried out for only one time period (1000 sec.). It is observed that compared to axial mixing it is very rapid. This also supports the assumption made in the derivation of the diffusional mixing equation (Eq. IV-1), that (for side by side loading) the rate limiting step is migration of particles in the axial direction and that mixing in radial direction is rapid and that, therefore, the limiting step in the mixing process is the axial movement of particles.

For further investigation of mixing mechanisms in a V-blender, experiments were carried out with mixing of equal volume proportions of granulations having different particle size, in an experimental design similar to that used in the horizontal rotating cylinder. The results are shown in Table III-2-7 to III-2-12. The results were analyzed using Eq. IV-10 (diffusional mixing model) and the plots are shown in Fig. III 2-7 to III-2-12. It is seen that (a) there is rapid initial mixing, and that equilibrium is attained in a short period of time, and (b) that the mixing kinetics do not follow diffusional mixing model. The general kinetic pattern is exemplified by the behavior of 20/30 mesh white granulation mixing with 10/20 mesh granulation (Table III-2-8 and Fig. III-2-8. Initially, for about 15 minutes, there is mixing, and linearity of $\ln\sigma^2$ with time prevails. There is then a period of demixing, followed by attainment of equilibrium.

Table IV-6-6

Comparison of Mixing Rates Obtained from Different Loading Geometries in a Rotating Cylinder. Comparison After 1000 Seconds of Mixing of a 50:50 Composition.

Mesh Size	Axial $\ln\sigma^2$	Longitudinal $\ln\sigma^2$
10/14	-2.5	-6.8
14/20	-1.6	-9.0
20/30	-1.6	-7.1
30/40	-1.5	-5.6
40/60	-1.5	-7.6

The final degree of mixedness, i.e. the final variance, is a function of the ratio of particle diameters. The findings, as shown in Fig. IV-11, are comparable to the findings in a horizontal blender: (a) for equal size diameters the blending is more rapid than (b) for sizes where the interstices between the large particles will not accomodate the smaller particles, i.e. in a range of d/D-values of 0.4 to 2.5 and (c) of the same order of magnitude as when the smaller particles will fit into the interstices between the larger ones (i.e. outside the range 0.4-2.5).

IV-7 Comparison of Final Experimental Variance and Predicted Theoretical Variance for Mixing of Granulation in a Horizontal Rotating Cylinder and a V-Blender.

The mixing of solid materials in the dry state is a purely mechanical operation but it has great practical importance. Its purpose is to produce homogeneous mixtures in which the compositions of the constituents are uniform throughout the whole mixture. In order to know the homogeneity of a mixture, some criteria of the degree of mixedness have to be defined. Because of the random nature of the mixing process, statistical analysis has become the approach most frequently used among investigators. The most frequently used units of measure are the standard deviation and the variance of the spot samples taken from a mixture.

The present discussion is limited to two component systems only. For multicomponent systems experimental variances for any particular component can be obtained by analyzing that component in spot samples and calculating the variance. It should be noted that for a two component system the variance for both the components will be identical regardless of their mean composition if variances due to sampling and analysis are not significant. (This is also true where the variances due to sampling and analysis are of the same magnitude for both the components).

There has been a great deal of theoretical and experimental work reported regarding the theoretical final variance of a mixture (the variance of a random mixture). Pioneering work in this area was done by Lacey (1943). Theoretical (binomial) random variances due only to mixing for a two component system of components that are identical except as regards a property used to distinguish between them was given by the following expression:

$$\sigma_R^2 = xy/N \qquad \text{(Eq. IV-29)}$$

where x is fractional composition of one component (e.g. a colored component), y = (1-x), and N is the number of particles in the sample.

An interesting point to note here is that for liquids it is possible to obtain perfect mixtures (essentially zero variance of mixing) because the particles in a fluid are of molecular size so that the smallest samples that can be taken in practice will contain

many millions of them and from Eq. IV-29 one can see that the mixing variance will be very small. It can be shown that the initial theoretical variance for a two component system, i.e. the variance prior to mixing is given by:

$$\sigma_o^2 = xy \qquad \text{(Eq. IV-30)}$$

Since, in actuality, components are not identical, Bulsik (1950) developed an expression for the theoretical random variance of a two component system where the two components differed only in particle size. Stange (1954) derived an expression giving random variance for a binary mixture of different particle sizes. Poole et al. (1964) modified Stange's expression so that it could be applied to a binary mixture of polydisperse powders, and it is given by the following expression:

$$\sigma_R^2 = xy\{y(\textstyle\sum fw)_x + x(\sum fw)_y\}/M \qquad \text{(Eq. IV-31)}$$

where M is the weight of the sample (g), w is the mean particle weight in a particular size range (g) and f is the fraction of the weight in that size range.

Similarly Kristensen (1973) derived an expression for random variance for a binary mixture with different particle size and density. His equation is:

$$\sigma_R^2 = xy\{\rho^4(xw_y+yw_x)\}/(M\rho_x^2\rho_y^2) \qquad \text{(Eq. IV-32)}$$

where ρ_x and ρ_y are particle densities of the component.

Before going into the analysis of the results of the present study as concerns experimentally observed final variance vis-a-vis the theoretical value, it should be noted that the experimentally observed final variance, σ_∞^2, is the sum of variances due to mixing (σ_m^2), sampling (σ_s^2) and assay (σ_A^2) (Ashton et al., 1966):

$$\sigma_\infty^2 = \sigma_m^2 + \sigma_s^2 + \sigma_A^2 \qquad \text{(Eq. IV-33).}$$

Sampling variance can be substantial (and has been so in some work reported in tha past). It is intuitively obvious that if ten 20 g samples were removed from a 1000 kg blend, then the sampling variance would be important. In the experiments reported here in the horizontal, rotating cylinder, the entire "batch" was sampled (and assayed) so that the sample variance can be neglected. As to the order of magnitude of the assay variance, a reasonable (actually generous) estimate is that the assay is ±5%, so that $3\sigma_A = 0.05$, i.e. $\sigma_A^2 = 0.0003$ which as shall be seen is orders of magnitude smaller than the observed final variances, in some cases.

It is seen in table IV-7 that the experimental values for blending in a horizontal,rotating cylinder of two fractions with equal size (the first 9 rows) is of the order of 10^{-3} to 10^{-2}. It cannot be stated with adequate statistical confidence that this differs from the assay

Table IV-7

Comparison Between Theoretical Random Variance (σ_R^2) and Final Experimental Variance (σ_∞^2) of the Mixtures in Rotating Cylinder Mixing Experiments.

Mesh	Percent Yellow	σ_o^2	$\ln\sigma_o^2$	σ_R^2	$\ln\sigma_R^2$	σ_∞^2	$\ln\sigma_\infty^2$	$\frac{\ln\sigma_\infty^2}{\ln\sigma_R^2}$
Tablets	50	0.25	-1.39	$1.3\ 10^{-3}$	-6.7	$3.8\ 10^{-3}$	-5.6	0.84
10/14	50	0.25	-1.39	$1.9\ 10^{-5}$	-10.9	$3.6\ 10^{-3}$	-5.6	0.51
14/20	50	0.25	-1.39	$5.9\ 10^{-6}$	-12.0	$1.0\ 10^{-2}$	-4.6	0.38
14/20	60	0.24	-1.43	$5.7\ 10^{-6}$	-12.1	$4.6\ 10^{-3}$	-5.4	0.45
14/20	70	0.21	-1.56	$5.0\ 10^{-6}$	-12.2	$2.1\ 10^{-3}$	-6.1	0.50
14/20	80	0.16	-1.83	$3.8\ 10^{-6}$	-12.5	$1.9\ 10^{-3}$	-6.3	0.50
20/30	50	0.25	-1.39	$1.4\ 10^{-6}$	-13.5	$1.1\ 10^{-2}$	-4.5	0.33
30/40	50	0.25	-1.39	$0.52\ 10^{-6}$	-14.5	$0.7\ 10^{-2}$	-4.9	0.34
40/60	50	0.25	-1.39	$1.5\ 10^{-7}$	-15.7	$3.8\ 10^{-3}$	-5.6	0.36
(6/10)+(20/30)*		0.25	-1.39	$3.8\ 10^{-5}$	-10.2	$2.5\ 10^{-3}$	-3.7	0.36**
(10/14)+(20/30)*		0.25	-1.39	$1.1\ 10^{-5}$	-11.4	$12\ 10^{-2}$	-2.1	0.18**
(14/20)+(20/30)*		0.25	-1.39	$3.7\ 10^{-6}$	-12.5	$9.7\ 10^{-2}$	-2.3	0.18**
(30/40)+(20/30)*		0.25	-1.39	$9.6\ 10^{-7}$	-13.9	$1.44\ 10^{-1}$	-1.9	0.14**
(40/60)+20/30)*		0.25	-1.39	$7.8\ 10^{-7}$	-14.1	$8.8\ 10^{-2}$	-2.4	0.17**
(60/80)+(20/30)*		0.25	-1.39	$7.2\ 10^{-7}$	-14.1	$5.6\ 10^{-2}$	-2.9	0.21**

*Contain 50% Yellow Granulation. ** Equilibrium Reached in < 10 Hours

variance, so the theoretical expression therefore may hold for blending in a horizontal rotating cylinder of rough, off-spherical particles as long as the diameter of the two fractions are identical.

If this is not the case, i.e. if d_1, the diameter of one of the monodisperse fractions, differs from that of the other, then, as seen in the last five rows of Table IV-7 the final variance are at least an order of magnitude higher than predicted, so that proposed equations of Stange (1954) and of Poole et al. (1964) do not apply to such a situation.

In the case of the V-blender (table IV-8), the sampling variance is greater, but it is obvious from the table that the same trend prevails. If the blending of equisized particles is estimated as presenting the order of magnitude of the sampling variance (i.e. $\sigma_s^2 = 10^{-5}$), then as seen in the last five rows (where σ_∞^2 is of the order of 10^{-3} to 10^{-1}) the final experimental variance is 2-4 orders of magnitude larger than the predicted variance, and the proposed theoretical equations of Stange (1954) and of Poole et al. (1964) do not apply.

Table IV-8 Comparison Between Theoretical Random Variance (σ_R^2) and Final Experimental Variance (σ_∞^2) of the Mixtures Studied in a V-Blender.

Mesh Size	Percent Yellow	σ_o^2	$\ln\sigma_o^2$	$10^6\sigma_R^2$	$\ln\sigma_R^2$	σ_∞^2	$\ln\sigma_\infty^2$	$(\ln\sigma_\infty^2)/(\ln\sigma_R^2)$
20/40	50	0.25	-1.39	2.0	-13.1	$6.4\ 10^{-5}$	-9.7	0.74
20/40	60	0.24	-1.43	1.9	-13.2	$2.0\ 10^{-5}$	-8.5	0.64
20/40	70	0.21	-1.56	1.7	-13.3	$1.2\ 10^{-5}$	-11.9	0.89
20/40	80	0.16	-1.83	1.3	-13.6	$1.9\ 10^{-5}$	-10.8	0.79
20/40	90	0.09	-2.41	0.7	-14.1	$2.5\ 10^{-5}$	-10.6	0.75
20/40	50*	0.25	-1.39	2.0	-13.1	$9.0\ 10^{-6}$	-11.6	0.89
20/40	50**	0.25	-1.39	2.0	-13.1	$1.6\ 10^{-5}$	-11.0	0.84
(10/20)+(20/30)	50	0.25	-1.39	11.0	-11.4	$4.6\ 10^{-3}$	-5.4	0.47
(40/60)+(20/30)	50	0.25	-1.39	1.2	-13.6	$6.8\ 10^{-2}$	-2.7	0.20
(60/80)+(20/30)	50	0.25	-1.39	1.1	-13.8	$2.3\ 10^{-2}$	-3.8	0.28
(80/100)+(20/30)	50	0.25	-1.39	1.0	-13.8	$1.4\ 10^{-4}$	-8.8	0.64
(40/60)+(20/30)	50*	0.25	-1.39	1.2	-13.6	$1.4\ 10^{-1}$	-2.0	0.15

* 4 kg Load **Granulation Lubricated with 1% Magnesium Stearate.

V. SUMMARY

Detailed studies using a horizontal rotating cylinder as a mixing apparatus for mixing of smooth non-spherical yellow and white tablets of equal size and proportion indicated that mixing kinetics of off--spherical,smooth particles follow diffusional mixing, with a final variance in the range of what is predicted by binomial theory.

Similarly off-spherical, non-smooth particles of identical size mix according to diffusional equations. The final variance could not be shown to differ significantly from the theoretically predicted final (random) variance. It was shown, by variation of particle size between experiments, that the diffusion coefficient decreases with decreasing particle size, but is independent of composition.

Mixing of off-spherical, non-smooth particles where the mean particle size of the two monodisperse fractions differs was shown not to follow diffusional equations and the final experimental variance differed at least two orders of magnitude from the theoretical random variance.

Mixing of off-spherical, non-smooth particles give rise to the same patterns when blended in a V-blender. The V-blender experiments provided a model allowing the calculation of mass transfer fractions between the arms of the V-blender.

VI. REFERENCES

Adams, J.F. and Baker, A.G., 1956, Trans.Inst.Chem.Eng.,34, 91

Ashton, M.D. and Valentin, F.H.H., 1966, Trans.Inst.Chem.Eng.,44,T166

Bourne, J.R., 1964, Chem.Eng., CE202

Bransby, P.L., Blair-Fish, P.M. and James, R.G., 1973, Powder Technol. 8, 197

Bridgwater, J., Sharpe, N.W. and Stocker, D.C., 1969, Trans.Inst.Chem. Eng., 47, T114

Bridgwater, J. and Ingram, N.D., 1971, Trans.Inst.Chem.Eng., 49, 163

Brown, R.L. and Hawksley, P.G.W., 1947, Fuel, 26, 159

Cahn, D.S., Healy, T.W. and Fuerstenau, D.W., 1965, Chem.Process Des.Dev., 4,318

Cahn,D.S., Fuerstenau, D.W., Healy, T.W. and Rose, H.E., 1966, Nature, 209, 494

Cahn, D.S. and Fuerstenau, D.W., 1967, Powder Technol., 1, 174

Cahn, D.S. and Fuerstenau, D.W., 1969, Powder Technol, 2, 215

Carley-Maccauly, K.W. and Donald, M.B., 1962, Chem.Eng.Sci., 17, 493

Carley-Maccauly, K.W. and Donald, M.B., 1964, Chem.Eng.Sci., 19, 191

Carstensen, J.T. and Chan P.C., 1976, Powder Technol., 15, 129

Cooke, C.H., Stephens, D.J. and Bridgwater, J., 1976, Powder Technol.15,1

Coulson, J.M. and Maitra, N.K., 1952, Ind.Chem., 26, 55

Crank, J., 1956, "The Mathematics of Diffusion", Oxford Univ. Press, London.

Cutress, J.O. and Pulfer, R.K., 1967, Powder Technol., 1, 293

Dankwerts, P.W., 1953, Research, 6, 355

Donald, M.B. and Roseman, B., 1962, Brit.Chem.Eng., 7, 749

Faiman, M.D. and Rippie, E.G., 1965, J.Pharm.Sci., 54, 719

Fan, L.T., Chen, S.J. and Watson, C.A., 1970, Ind.Eng.Chem., 62, 53

Fisher, R.K., 1961 "Rates of Diffusive Mixing of Particulate Solids" Ph.D. Thesis, Princeton University.

Gray, J.B., 1957, Chem.Eng.Progr., 53, 25

Harnby, N., 1967, Powder Technol., 1, 94

Hersey, J.A., 1975, Powder Technol., 11, 41

Hill, F.P., 1965, Trans.Inst.Chem.Eng., 43, T10

Hogg, R., Cahn, D.S. Healy, T.W. and Fuerstenau, D.W., 1966, Chem.Eng.Sci., 21, 102S

Hogg, R., Mempel, G. and Fuerstenau, D.W., 1968, Powder Technol., 2, 223

Hogg, R. and Fuerstenau, D.W., 1972, Powder Technol., 6, 139

Inoue, I, Yamaguchi, K. and Sato, K., 1970, Kagaku Kogaku, 34, 1323

Jenkin, C.F., 1931, Proc.Roy.Soc., A131, 53

Johnson, M.C.R., 1972, Pharm.Acta.Helv., 47, 446

Lacey, P.M.C., 1943, Trans.Inst.Chem.Eng., 21, 53

Lacey, P.M.C., 1954, J.Appl.Chem., 4, 257

Lloyd, P.J. and Yeung, P.C.M., 1967, Chem.Proc.Eng., 48, 57

Masliyah, J. and Bridgwater, J., 1974, Trans.Inst.Chem.Eng., 52, 31

Otake, T., Kitaoka, H. and Tone, S., 1961, Kagaku Kogaku, 25, 178

Olsen, J.L. and Rippie, E.G., 1964, J.Pharm.Sci., 53, 147

Poole, K.R., Taylor, R.F. and Wall, G.P., 1964, Trans.Inst.Chem.Engrs., 42, T305

Reynolds, O., 1885, Phil.Mag., 20, 469

Rippie, E.G., Olsen, J.L. and Faiman, M.D., 1964, J.Pharm.Sci., 53, 1360

Rippie, E.G., Faiman, M.D. and Pramoda, M.K., 1967, J.Pharm.Sci., 56,1523

Roseman, B., 1963, Ind.Chem., 39, 84

Rumpf, H. and Muller, W., 1962, Trans.Inst.Chem.Engrs., 42, 272

Scott, A.M. and Bridgwater, J., 1975, Ind.Eng.Chem.Fundam., 14,22

Scott, A.M. and Bridgwater, J., 1976, Powder Technol., 14, 177

Stange, K., 1953, Abh. Braunschw.Wiss., 5, 164

Stange, K., 1954, Chem.Ing.Tech., 26, 331

Stange, K., 1963, Chem.Ing.Tech., 35, 580

Stange, K., 1967, Chem.Ing.Tech., 39, 585

Steiner, G., Patel, M. and Carstensen, J.T., 1974, J.Pharm.Sci.,63, 1395

Train, D., 1960, J.Am.Pharm.Assoc., Sci.Ed., 49, 265

Weidenbaum, S.S. and Bonilla, C.F., 1955, Chem.Eng.Progr., 51, 27

Weidenbaum, S.S. 1958, "Solids Mixing"in"Advances in Chemical Engineering, II", Ed. Drew, T.B. and Hoopes, J.W.Jr., Academic Press N.Y.,

Weidenbaum, S.S., Carson, R.C. and Miller, D.P., 1963, Caramic Age, 79, 39

Yano, T., Kanise, I. and Tanaka, K., 1956, Kagaku Kogaku, 20, 20.

VII APPENDICES

APPENDIX I

Effects of Milling on Granulation Particle Size Distribution

by

G.Steiner, Mahendra Patel and J.T.Carstensen

APPENDIX II

Particle-Size Distributions of Milled Granulations and Powders.

by

J.T.Carstensen and Mahendra Patel

APPENDIX III

Nonsink Dissolution Rate Equations.

by

Mahendra Patel and Jens T. Carstensen

APPENDIX IV

Dissolution Patterns of Polydisperse Powders: Oxalic Acid Dihydrate.

by

J.T.Carstensen and Mahendra Patel.

APPENDIX V

Reduced Acid-Neutralizing Velocity of Spray-Dried Agglomerated Magnesium Carbonate

by

Mahendra Patel.

VITAE

MAHENDRA PATEL was born on September 20, 1949 in Nairobi, Kenya. He graduated from C.N.Vidyalaya (India) in 1967 (high school). He then attended Grujarat University from 1967 to 1971 when he received a Bachelor of Science Degree in chemistry. He was a Chemical Engineering student during 1972 to 1973 at the University of Wisconsin. He began his graduate study at the School of Pharmacy, University of Wisconsin in 1973 and was granted his Masters of Science degree in 1974.